

AXIALLY AND Laterally LOADED PILES IN LIQUEFIABLE SOIL

A
Dissertation
Submitted in Partial Fulfillment of the Requirements
for Award of the Degree of

**MASTER OF ENGINEERING
IN
STRUCTURAL ENGINEERING**

By
PANKAJ KUMAR JAIN
(Roll No. 8808)

Under the Guidance of
Prof. A. Trivedi
&
Mr. Amit kr.Srivastava



Department of Civil and Environmental Engineering
Delhi College of Engineering
Delhi University, Delhi-110042

JULY 2006

CANDIDATE'S DECLARATION

I hereby certify that the work presented in this dissertation entitled “**Axially and Laterally Loaded Piles in Liquefiable Soil**” in partial fulfillment of the requirements for the award of the degree of **MASTER OF ENGINEERING** in Civil Engineering, with specialization in **Structural Engineering**, submitted to the Department of Civil and Environmental Engineering, Delhi College of Engineering, Delhi is an authentic record of my own work, under the supervision of **Prof. A. Trivedi**, Professor, Department of Civil Engineering and **Mr. Amit Kr. Srivastava**, Lecturer, Department of Civil and Environmental Engineering, Delhi College of Engineering, Delhi

The matter embodied in this dissertation has not been submitted by me for the award of any other degree.

Date:

(**PANKAJKUMARJAIN**)

Place: Delhi

CERTIFICATE

This is to certify that the above statement made by the candidate is correct to the best of our knowledge.

(**Mr. Amit Kr. Srivastava**)
Lecturer,
Department of Civil & Environmental
Engg,
Delhi College of Engineering,
Delhi-110042, India.

(**Prof. A. Trivedi**)
Professor,
Department of Civil & Environmental
Engg,
Delhi College of Engineering,
Delhi-110042, India.

ACKNOWLEDGEMENT

I feel privileged in extending my earnest obligation, deep sense of gratitude, appreciation and honor to Prof. A. Trivedi, Department of Civil & Environmental Engineering, Delhi College of Engineering, Delhi and Mr. Amit Kr. Srivastava, Lecturer, Department of Civil & Environmental Engineering, Delhi College of Engineering, Delhi whose benevolent guidance, apt suggestions, unstinted help and constructive criticism have inspired me in successful completion of making of this dissertation report.

I also express my grateful thanks to Prof. P. R. Bose, Head of Department, Department of Civil & Environmental Engineering, Delhi College of Engineering, Delhi for their technical support, during the project.

I express my appreciation and thanks to all the faculty members of the Department of Civil & Environmental Engineering, Delhi College of Engineering, Delhi for free exchange of ideas and discussions which proved helpful.

I would like to thank my friends for their kind help extended to me carrying the work in preparing the report.

I also express my grateful thanks to Library and Computer Center staff for their technical support, during the project.

Finally, I am thankful and grateful to God the Almighty for ushering his blessings on all of us.

(Pankaj Kumar Jain)

ABSTRACT

Studies of seismic loading of substructure (e.g. piles) and liquefaction phenomenon are more than four decades old; however the combined problem of seismic behaviour of piles in liquefiable soil has received less attention. Most of the several experimental and analytical studies of this combined problem have been presented only in the last decade. Yet much has to be revealed especially the influence of flow characteristic on the behaviour of the system. Pile foundations may undergo substantial shaking while the soil is in a fully liquefied state and mass suffer severe cracking or even fracture. Therefore study on the performance of piles in liquefiable ground under earthquake loading is attempting here.

The dissertation report gives the salient features of soil-pile interaction in liquefiable soils using Winkler soil model. Because of versatility and simplicity in application the winkler model is preferred. These models can simulate most of phenomena involved in soil pile interaction: soil non-linearity, soil- pile gapping, and pile-soil-pile interaction in groups of piles,

The objective of this dissertation are study of pile-soil interaction and the response of pile in liquefiable soils for both the axial and lateral load using Winkler model in the time domain.

This dissertation describes the results of a study on the dynamic response of pile foundations in liquefiable soils during strong shaking. The research covers mainly study of the modeling of liquefaction phenomenon and a critical study of physical modeling of pile-soil interaction. The liquefaction modeling for determining the liquefaction analysis. The pile-soil interaction is quantified using Winkler model. Finally a computer code in C++ has been developed to predict the behaviour of pile in liquefiable soils.

CONTENTS

	Page No.
Candidate Declaration, Certificate	I
Acknowledgement.....	II
Abstract	III
List of Tables	IV
List of Figures	V
List of Flow Charts	VIII
Notations	IX
1. Introduction	1
1.1. General.....	1
1.2. Brief Literature Review	3
1.3. Objectives.....	3
1.4. Scope of Research.....	4
1.5. Organisation of Dissertation.....	4
2. Literature Review	6
2.1. General	6
2.2. Liquefaction.....	7
2.3. Soil-Pile Interaction	8
2.4. Piles in Liquefiable soils	17
2.5. Soil Liquefaction in Some Major Earthquakes	19
2.6. Case Histories of Liquefaction-Induced Pile Damage	19
3. Numerical Modeling of Pile in Liquefiable soil	27
3.1. Methodology.....	27
3.2. Numerical Modeling.....	27
3.3. Algorithm	35
3.4. Flow Charts for Pile-Soil Interaction in Liquefiable Soils	41

4. Verification of Model	45
4.1. General	45
4.2. Verification of Pile-Soil Interaction Model.....	45
4.3. Summary.....	49
	Page No.
5. Effect of Liquefaction on Pile-Soil Interaction	50
5.1. General	50
5.2. Liquefaction.....	50
5.3. Pore Pressure Generation and Change of Shear Modulus	52
5.4. Response of a Pile in Liquefiable Soils	54
5.5. Validation of the Results	66
6. Summary, Conclusions and Future Scope	67
6.1. Summary	67
6.2. Conclusions	67
6.3. Future Scope	68
7. References.....	70
8. Appendix 1: The pore pressure generation and change of shear modulus in different cycles	73
Appendix 2(A): C++ programme for checking the liquefaction potential.....	75
Appendix 2(B): C++ programme for liquefaction Model.....	78
Appendix 2(C): C++ programme for Pile-soil interaction Model in liquefiable Soil.....	81

LISTS OF TABLES

Table No.	Title	Page
2.1.	Typical cases of failure in liquefaction	20
2.2.	Case histories of liquefaction-induced pile damage.	23
3.1.	Equivalent number of significant stress cycles	38
3.2.	Relation between relative density and correction factor	38
3.3.	Guidelines for determining rate of uniform cyclic loading per unit time	40
4.1.	Inputs for verifications of the models	46
5.1.	Inputs for the analysis of liquefaction and pile-soil interaction	50

LISTS OF FIGURES

Fig. No.	Title	Page
2.1.	Cracking of road embankment	20
2.2.	Tilted buildings	20
2.3.	Failure of the Showa bridge	21
2.4.	Sand boil	21
2.5.	Fallen bridge deck	22
2.6.	Toppled building	22
3.1.	Soil- Pile system divided into horizontal slices	30
3.2.	One unit of soil model for axial pile shaft response	31
3.3.	Winkler soil model for lateral pile shaft response	33
3.4.	Range of r_d for different soil profiles in liquefaction analysis	37
3.5.	Stress causing liquefaction of sands in 10 cycles	37
3.6.	Stress causing liquefaction of sands in 30 cycles	38
3.7.	Relationship between cyclic stress ratio and number of cycles required to cause liquefaction for simple shear test for different relative density	39
4.1.	Soil-Pile system divided into horizontal slices	45
4.2.	Complex soil stiffness due to axial load	47
4.3.	Complex soil stiffness due to lateral load	47
4.4.	Pile Head Stiffness due to axial load	48
4.5.	Pile Head Stiffness due to lateral load for Poisson's ratio = 0.5	49
5.1.	Soil profile	51
5.2.	Liquefaction zone	52
5.3.	Rate of pore pressure generation	53
5.4.	Change of shear modulus with respect to N_L	53

Fig. No.	Title	Page
5.5.	Comparison of axial displacements in different frequencies (a_0) (a) Non-liquefied (b) liquefied	55
5.6.	Comparison of interacting forces in different frequencies (a_0) (a) Non-liquefied (b) liquefied	55
5.7.a	Axial displacement ($a_0 = 0.1$)	57
5.7.b	Axial displacement ($a_0 = 0.2$)	57
5.7.c	Axial displacement ($a_0 = 0.3$)	57
5.7.d	Axial displacement ($a_0 = 0.4$)	57
5.8.a	Interacting force ($a_0 = 0.1$)	58
5.8.b	Interacting force ($a_0 = 0.2$)	58
5.8.c	Interacting force ($a_0 = 0.3$)	58
5.8.d	Interacting force ($a_0 = 0.4$)	58
5.9.a	Lateral displacement	60
5.9.b	Bending moment	60
5.9.c	Rotational displacement	60
5.9.d	Interacting force	60
5.10.a	Axial displacement ($a_0 = 0.1$)	62
5.10.b	Axial displacement ($a_0 = 0.2$)	62
5.10.c	Axial displacement ($a_0 = 0.3$)	62
5.10.d	Axial displacement ($a_0 = 0.4$)	62
5.11.a	Interacting force ($a_0 = 0.1$)	63
5.11.b	Interacting force ($a_0 = 0.2$)	63
5.11.c	Interacting force ($a_0 = 0.3$)	63
5.11.d	Interacting force ($a_0 = 0.4$)	63
5.12.a	Lateral displacement	65
5.12.b	Bending moment	65
5.12.c	Rotational displacement.....	65

Fig. No.	Title	Page
5.12.d	Interacting force	65
5.13.	Validation of lateral displacement	66
5.14.	Validation of bending moment	66

LISTS OF FLOWCHARTS

FC. No.	Title	Page
3.1.	Flow chart for liquefaction potential	42
3.2.	Flow chart for liquefaction model	43
3.3.	Flow chart for pile soil interaction	44

NOTATIONS

Symbols	Descriptions
P	Soil resistance
y	Lateral displacement
$\frac{\partial N}{\partial t}$	Rate of application of shear stress cycles to the soil
σ'_{vo}	Initial effective overburden pressure
r_p	Pore pressure ratio
N_L	Number of uniform stress cycles required to produce a condition of initial liquefaction under undrained conditions.
N	Number of equivalent uniform cycles.
θ	A constant and value equal to 0.7 for best fit.
$\frac{\partial u}{\partial t}$	Excess pore water pressure developed in one dimensional formulation.
m_v	Tangent coefficient of volume compressibility
D_r	Relative density
A	Constant depending on relative density.
B	Constant depending on relative density.
m_{v_o}	Tangent coefficient of volume compressibility at low pressure
G_t	Shear modulus at time t
G_0	Shear modulus at time 0.
σ'_{ct}	Effective stress of soil at time t.
σ'_{c0}	Effective stress of soil at time 0.
n	Power exponent and generally equal to 0.5.
k_1, k_2, k_3	Spring constants of Winkler soil model
c_1, c_2, c_3	Dashpot constants of Winkler soil model

Symbols	Descriptions
G_s	Shear modulus
r_0	Radius of pile
V_s	Shear wave velocity.
w_i	Pile displacements both (axial and lateral)
P_i	Applied axial load
$\beta_1, \beta_2, \beta_3$ and β_4	Functions depending the heights of the layers
$[t]$	Functions of $\beta_1, \beta_2, \beta_3$ and β_4
$[q]$	Functions of $\beta_1, \beta_2, \beta_3$ and β_4
λ^2	Function depending on the dynamic stiffness.
γ_i	Quantity depending on the displacements , velocity and acceleration of previous time steps
\dot{w}	Velocity
\ddot{w}	Accelaration
m_p	Mnass per unit length of the pile
E_p	Young's modulus of pile
A	Cross sectional area of the pile
p_i	Interacting forces
k	Dynamic stiffness
d_i	Parameters used to determine interacting forces depending on the displacements and interacting forces of previous time steps.
m_s	Mass per unit length of the pile
ρ_s	Mass per unit volume
ξ_k	Parameters dependent on Poisson's ratio
$\bar{\xi}_k$	Parameters dependent on Poisson's ratio
θ_i	Rotational displacement respectively.
M_i	Bending moment
$E_p I$	Bending stiffness of pile shaft
$[T_n]$	Matrix depending on the layers of the soil.

Symbols	Descriptions
$\{Q_n\}$	A vector quantity depending on the number of layers.
λ^4	Function depending on the dynamic stiffness and bending stiffness of the pile
γ	Unit weight of sand.
h	Depth of the soil layer
a_{max}	Peak ground acceleration (PGA)
r_d	Depth factor.
τ_{av}	Average shear stress
N_c	Equivalent number of significant stress cycles
D_r	Relative density
C_r	Correction factor
τ	Stress causing liquefaction
σ'_0	Initial effective stress
σ_0	Initial stress
$\frac{\tau_{av}}{\sigma'_0}$	Cyclic stress ratio
N_L	Number of uniform stress cycles required to produce a condition of initial liquefaction
θ	A constant (the value is taken as 0.7 in this report)
r_p	Pore water pressure ratio.
N_{eq}	Number of equivalent stress cycles
K	Coefficient of permeability
G_0	Shear modulus at time 0.
G_t	Shear modulus at time t.
n	Power exponent- a constant.
$a_0 = r_0 \cdot \omega / V_s$	Dimensionless frequency.

Symbols

Descriptions

E_p	Modulus of elasticity of pile.
k_s	Soil stiffness.
E_s	Modulus of elasticity of Soil.
M	Magnitude of the earthquake.
D_{50}	It is a size of the sample which is 50 % finer than that size
γ_{sat}	Unit weight of saturated soil sample.
f_0	Natural frequency

Chapter-1

INTRODUCTION

1.1. GENERAL

Piles are long, firm, column-like members that are embedded in the soil to provide axial as well as lateral support of structures such as buildings, piers and bridges. Often, piles are installed near each other to create groups to optimize the support of the structure. Both a single pile and groups of piles rely significantly upon the conditions of the surrounding soil. Piles are often the first members of a structure to be installed. They are also some of the most expensive members. Therefore, it is very important to analyze piles under various loadings i.e. under axial and lateral loadings.

Loose cohesionless sands and non-plastic silts below the water table develop high pore water pressure and liquefy during strong earthquake shaking, leading to significant degradation of strength and stiffness. In such soil profiles, pile foundations may undergo substantial shaking while the soil is in a fully liquefied state and soil stiffness is at a minimum. During this shaking phase the pile is prone to suffering severe cracking or even fracture. After liquefaction, if the residual strength of the soil is less than the static shear stresses, significant lateral spreading or down slope displacements may occur. The moving soil can exert damaging pressures against the piles leading to failure. Such failures were prevalent during the 1964 Niigata and the 1995 Kobe earthquakes. Lateral spreading is particularly damaging, if a non-liquefied layer rides on top of the liquefied soil.

Dynamic pile-soil interaction analysis has become an important field in Civil Engineering over the last few decades. Several major earthquakes that caused damage to buildings, bridges, port facilities and other infrastructure have brought a lot of attention to how foundations behave under dynamic loading. The performance of piles in liquefiable ground under earthquake loading is a complex problem due to the effects of progressive build up of pore water pressure in the saturated soil.

Although studies of seismic loadings of piles and liquefaction phenomenon have been performed separately in the last four decades, the combined problem of seismic behavior of piles in liquefiable soil has received relatively less attention. Several experimental and analytical studies of this combined problem have been presented throughout the last decade. Yet much has to be revealed especially regarding all aspects of influence of flow characteristic on the behavior. The excess pore pressure generated during liquefaction alters the effective stresses in the soil and thereby change its mechanical behavior.

There are several approaches to study the combined problem of behavior of piles in liquefiable soils. There are many uncertainties in the mechanisms involved in pile-soil-structure interaction in liquefying soil, nevertheless the data recorded during the 1995 Kobe earthquake, shake table tests, and centrifuge tests provide an insight into the mechanism of pile-soil-structure interaction in liquefiable soils (Liyanapathirana and Poulos, 2005 a).

Available liquefaction models are based on either:

- 1) experimentally observed undrained stress paths during pore pressure build up,
- 2) a correlation between pore pressure response and volume change tendency of dry soils,
- 3) formulation of pore pressure response directly from observed data,
- 4) plasticity theory in which the plastic volume change is related to pore pressure build up and
- 5) treatment of the soil as a two phase medium.

The available models that formulate the pore pressure response directly from observed data on undrained tests require less effort to determine model parameters (Kagawa and Kraft, 1981)

Different experimental and analytical numerical models have been used to study the behavior of soil-pile interaction. In general, it is possible to classify the different analytical-numerical models according to three groups-(1) Continuum solution, (2) Finite

element Solution and (3) Discrete models such as Winkler models. Winkler model is preferred because of versatility and simplicity in its application (Miwa et al, 2005).

In this dissertation, the numerical formulation of modeling of liquefaction and pile-soil interaction are described. The available models that formulate the pore pressure response directly from observed data on undrained tests have been used to study the liquefaction phenomenon and Winkler model has been used to study the pile soil interaction. Finally combining these two models, the response of pile in liquefiable soils has been predicted. In general, the spring coefficients in the spring-dashpot model are degraded depending on the amount of development of pore pressure.

1.2 BRIEF LITERATURE REVIEW

The brief literature review of liquefaction, pile-soil interaction and piles in liquefiable soils are listed below.

In the liquefaction model developed by Seed et al. (1976), the pore pressure value is related to the ratio between the number of cycles of loading and the number of cycles required for liquefaction.

The module and shear strengths of the foundation soil were modified continuously to account for the effects of the changing seismic pore water pressure (Liyanapathirana and Poulos, 2002a, 2002b).

Novak (1974) was the first to use a Winkler model for representation of a laterally loaded pile in a visco-elastic material.

Nogami and Konagai (1986, 1988) suggested a simple mechanical model which may be used in time domain also.

Recently and Poulos (2005a) have studied the lateral response of pile in liquefiable soils and results obtained these authors have been in good agreement with those shown by Wilson et al. (1998).

1.3. OBJECTIVES

The objective of this dissertation can be divided broadly into two groups. They are (1) study of pile-soil interaction and (2) the response of pile in liquefiable soils for both the axial load and lateral load using Winkler model in the time domain.

1.4. SCOPE OF RESEARCH

This dissertation describes the results of a study on the dynamic response of pile foundations in liquefiable soils during strong shaking. The research covers mainly two aspects (1) Study of the modeling of liquefaction phenomenon. and (2) a critical study of physical modeling of pile-soil interaction.

The liquefaction modeling consists of three parts (1) Numerical modeling for pore pressure generation from ground response analysis (2) Pore pressure generation and redistribution from liquefaction analysis and (3) Effective stress response analysis with pore water pressure induced softening.

The pile-soil interaction is quantified using Winkler soil model. The study has been performed for only single pile for one dimensional case.

1.5. ORGANISATION OF DISSERTATION

This dissertation consists of six chapters. The brief contents have been described as follows:

Chapter 1: Introduction - includes a brief discussion on the pile-soil interaction in liquefiable soils, objectives and an organizational summary of the dissertation.

Chapter 2: Literature Review – Primarily focused on past works on pile-soil interaction and liquefaction separately. Further combined study of pile-soil interaction considering the effects of liquefaction is described. In pile-soil interaction, mainly Winkler model is discussed it. Moreover describes about soil liquefaction in some major earthquakes and also few case histories of liquefaction-induced pile damage are also discussed.

Chapter 3: Numerical Modelling of pile in liquefiable soil - Numerical modeling of liquefaction and soil-pile interaction is discussed. Finally the two models are combined. The algorithm and flow chart for the developed computer codes are described.

Chapter 4: Verification of Numerical Models - The verification of the numerical models and the algorithm developed is discussed.

Chapter 5: Effect of Liquefaction on Pile-Soil Interaction (results) – Provide details about the findings and the results.

Chapter 6: Summary, conclusions and future scope - Includes a summary of the studies, the conclusions have been drawn and the scope of the future work has been stated.

Chapter-2

LITERATURE REVIEW

2.1. GENERAL

Piles are primarily designed to carry axial loading, but in several situations they are subjected to lateral displacements as well as shear and moment applied at the pile head. The problem of piles under lateral loading is much more complex than that of axially loaded piles. Axially loaded piles may be designed using simple static methods, while laterally loaded piles require, sometimes, the solution of the fourth-order differential equation because of their non-linear behavior. The problem also can be solved as a beam on elastic foundation with nonlinear soil-pile interaction behavior.

Soil liquefaction has been a major cause of damage to earth structures, lifeline structures and foundations during past earthquakes, undoubtedly liquefaction, poses a significant threat to the integrity of structures and other facilities during future earthquakes. Evidence of the occurrence of liquefaction has been reported from a large number of earthquakes e.g. Assam (1897), Kanto (1923), Bihar (1934) Fukui (1948), Assam (1950) and Chile (1960). But the soil mechanics literature does not show much evidence of liquefaction studies before 1964 (Niigata and Alaska Earthquakes). However, the classical works of Casagrande (1936), as quoted by Seed (1976) and Terzaghi and Peck (1948) indicated that there was at least recognition that liquefaction could be induced by static loading (Taiebat, 1999). The enormous damage experienced in Alaska and Niigata earthquakes, where a number of buildings and apartment blocks tilted, played an important role in activating the earthquake geotechnical profession to study the liquefaction phenomenon induced in soil by earthquakes (Seed, 1976). The Niigata earthquake has been cited symbolically as the first event in the world where all kinds of modern infrastructure were destroyed by what came to be well known as soil liquefaction (Ishihara, 1993 and Arduino et al., 2002).

The behavior of pile foundations under earthquake loading is an important factor affecting the performance of many essential structures. The potential significance of liquefaction-related damage to piles was clearly demonstrated during the 1964 Alaskan earthquake (Youd and Bartlett, 1989) and during the 1995 Kobe earthquake. Observations of modern pile foundations during past earthquakes have shown that piles in firm soils generally perform well, while the performance of piles in soft or liquefied ground may be very poor. Predicting the behavior of pile foundations in soft clay or liquefied ground under earthquake loading is a complex problem involving consideration of design motions, free field site response, superstructure response and soil-pile-superstructure interaction (Wilson, 1998).

The literature has been reviewed under three headings namely (1) Pile-Soil interaction, (2) Liquefaction and (3) Piles in liquefiable soil.

Typical failure of structures due to liquefaction and a few case histories of pile damage in liquefaction have also been described.

2.2. LIQUEFACTION

The term liquefaction originally coined by Mogami and Kubu (1953) has historically been used in conjunction with variety of phenomenon that involves soil deformations caused by monotonic, transient or repeated disturbance of saturated cohesion less soils under undrained loading conditions. The generation of excess pore pressure under undrained loading conditions is a hallmark of all liquefaction phenomena. The tendency for dry cohesion less soils to densify under both static and cyclic loading is well known. When cohesion less soils are saturated, rapid loading occurs under undrained conditions, so the tendency for densification causes excess pore pressures to increase and effective stresses to decrease. Liquefaction phenomena that results from this process can be divided into two main groups i.e. (1) flow liquefaction and (2) cyclic mobility.

Generally flow liquefaction occurs much less frequently than cyclic mobility but its effects are usually far more severe. Cyclic mobility can occur under much boarder

range of soil and site conditions than flow liquefaction and its effects can range from insignificant to highly damaging (Kramer, 1996).

The soil-pile interaction in liquefiable soil is very much dependent on the geometry of the problem. If the geometry is not of level ground and horizontal phreatic surface liquefaction will usually result in a liquefaction related phenomena termed as lateral spreading. Because of lateral spreading the soil mass has displaced to several meters. Solution techniques for the lateral spreading loading of piles were suggested by Stewart and O'Rourke (1991) and Wang and Reese (1998). These techniques are based on applying static forces to the pile associated with the free field permanent displacement. The seminal work of Seed and Idriss (1971), Martin et al. (1975) and Martin and Seed (1979) established the basic understanding of the mechanism underlying the liquefaction of saturated sands. Their model is based on effective stresses concepts i.e. that the soil skeleton responds to changes in the effective stresses. Martin et al. (1975) showed that under drained conditions loose sand will compact due to shearing and that the incremental volumetric change is controlled by the cyclic shear strain amplitude and is independent of the vertical stress.

Finn et al. (1977) noted that the significant change in volume in drained shear corresponds to the unloading of shear strain. This model for pore pressure generation was much more fundamental than alternative popular models such as those of Seed et al. (1976) in which the pore pressure value was related to the ratio between the number of cycles of loading and the number of cycles required for liquefaction. Liyanapathirana and Poulos (2002a, 2002b) stated that module and shear strengths of the foundation soil were modified continuously to account for the effects of the changing seismic pore water pressure.

2.3. SOIL-PILE INTERACTION

2.3.1. General

The basic principle of dynamic soil-structure (soil-pile) interaction is explained as follows. Soil is a semi -infinite medium and a major problem in dynamic soil-structure

interaction is the modeling of the unbounded soil domain (Wolf, 1985). For dynamic loading, a structure always interacts with surrounding soil and it is not adequate to analyze the structure independently. If seismic loading is applied to the soil region around the structure, then one has to model this region along with the structure. In the case of a static loading a fictitious boundary can be included at a sufficient distance from the structure, where the response is diminished from a practical point of view. However, for dynamic loading this procedure can not be used. The fictitious boundary would reflect waves originating from the vibrating structure back into the discretized soil region, instead of letting them pass through and propagate through infinity. The fundamental objective of a soil-structure interaction analysis is modeling of this boundary.

2.3.2. Experimental Works

Experiments with seismic loading involve the fundamental problem of inability to perform full scale model test on site. The only large-scale shaking table tests of piles were so far conducted by Tao et al. (1998) and Tokimatsu et al. (2001). In Tao et al.'s tests, a 6m long pile was tested in a $3.1\text{m} \times 11.6\text{m} \times 5\text{m}$ laminar shear box filled with dry sand. The test results were compared with available numerical results, both for the free field and the pile response. It was concluded from the comparison that Ishibashi and Zhang (1993) stress strain relations are consistent with the test results and that the Winkler model of Kagawa and Kraft (1981) managed to predict the pile behavior quite well. Tokimatsu et al. (2001) conducted tests on saturated sand in order to examine the influence of liquefaction. Their laminar box dimensions are similar to those of Tao et al. (1998). They showed that once the soil liquefies the sub grade reaction becomes correlated with relative velocity rather than displacement. Similar observations were obtained by Kagawa et al. (1995) who tested smaller models ($2\text{m} \times 2\text{m} \times 1\text{m}$ laminar shear box) on a shaking table. Kagawa et al. (1995) also noted that excess pore pressures measured between the piles (in their pile group configuration) were different and in most cases higher than those in the free field at the same depth. Sakajo et al. (1995) in their shaking table test with a pile group of 36 piles showed that the existence of the pile group reduces excess pore pressure developed at any time compared with the free field value and may even prevent liquefaction. Although these two statements are contradictory to

each other but it was explained by Klar (2003) on the basis of the numerical parametric study. The results presented by Klar (2003) are consistent with the experimental results of both Kagawa et al. (1995) and Sakajo et al. (1995). The pore pressure value is greater than that of the free field at shallow depth, similar to the behavior observed in most of Kagawa et al.'s (1995) experiments in which measurement were all made at shallow depth. But at greater depth the pore pressures are in general smaller than those of the free field, similar to the behavior noted by Sakajo et al. (1995).

Two of the major factors controlling susceptibility to liquefaction, for soil with a given relative density and permeability, are the drainage conditions and the loading intensity. For an infinite pile group, pile spacing has opposing effects on each of these two factors. As spacing between the piles decreases, excess pore pressures dissipate more slowly and the potential for liquefaction is increased. However, as the distance between piles is decreased, each pile is subjected to less loading. Consequently, less pore pressure is generated and the potential for liquefaction is therefore reduced Klar (2003).

2.3.3. Numerical Methods

The numerical methods may be classified as follows:

- The finite element method (FEM)
- The finite difference method (FDM)
- The boundary element method (BEM)
- The discrete element method (DEM)

2.3.3.1. Finite Element Method

The finite element method is a numerical approach based on elastic continuum theory that can be used to model pile-soil-pile interaction by considering the soil as a three-dimensional, quasi-elastic continuum. Finite element techniques have been used to analyze complicated loading conditions on important projects and for research purposes. The salient features of this method have been discussed in the later sections.

2.3.3.2. Boundary Element Method

Significant advances have been made in the development of the boundary element method and as a consequence, this technique provides an alternative to the finite element method under certain circumstances, particularly for some problems in rock engineering (Beer and Watson, 1992). The main advantages and disadvantages can be summarized as follows.

Advantages

- Pre- and post-processing efforts are reduced by an order of magnitude (as a result of surface discretisation rather than volume discretisation).
- The surface discretisation leads to smaller equation systems and less disk storage requirements, thus computation time is generally decreased.
- Distinct structural features such as faults and interfaces located in arbitrary positions can be modeled very efficiently, and the nonlinear behavior of the fault can be readily included in the analysis (Beer, 1995).

Disadvantages

- Except for interfaces and discontinuities, only elastic material behavior can be considered with surface discretisation.
- In general, non-symmetric and often fully-populated equation systems are obtained.
- A detailed modeling of excavation sequences and support measures is practically impossible.
- The standard formulation is not suitable for highly jointed rocks when the joints are randomly distributed.
- The method has only been used for solving a limited class of problems, e.g., tunneling problems, and thus less experience is available than with finite element models.

2.3.3.3. Discrete Element Method

The methods described so far are based on continuum mechanics principles and are therefore restricted to problems where the mechanical behavior is not governed to a large extent by the effects of joints and cracks. If this is the case, discrete element methods are

much better suited for numerical solution. These methods may be characterized as follows:

- Finite deformations and rotations of discrete blocks (deformable or rigid) are calculated.
- Blocks that are originally connected may separate during the analysis.
- New contacts which develop between blocks due to displacements and rotations are detected automatically.

Due to the different nature of a discrete analysis, as compared to continuum techniques, a direct comparison seems to be not appropriate. The major strength of the discrete element method is certainly the fact that a large number of irregular joints can be taken into account in a physically rational way. The drawbacks associated with the technique are that establishing the model, taking into account all relevant construction stages, is still very time consuming, at least for 3-D analyses. In addition, a lot of experience is necessary in determining the most appropriate values of input parameters such as joint stiffness. These values are not always available from experiments and specification of inappropriate values for these parameters may lead to computational problems. In addition, runtimes for 3-D analyses are usually quite high.

2.3.3.4. Explicit Finite Difference Method

The finite difference method does not have a long-standing tradition in geotechnical engineering, perhaps with the exception of analyzing flow problems including those involving consolidation and contaminant transport. However, with the development of the finite difference code FLAC (Cundall and Board, 1988), which is based on an explicit time marching scheme using the full dynamic equations of motion, even for static problems, an attractive alternative to the finite element method was introduced. Any disturbance of equilibrium is propagated at a material dependent rate. This scheme is conditionally stable and small time steps must be used to prevent propagation of information beyond neighboring calculation points within one time step. Artificial nodal damping is introduced for solving static problems in FLAC. The method

is comparable to the finite element method (using constant strain triangles) and therefore some of the arguments listed above basically hold for the finite difference method as well. However, due to the explicit algorithm employed some additional advantages and disadvantages may be identified.

Advantages

- The explicit solution method avoids the solution of large sets of equations.
- Large strain plasticity, strain hardening and softening models and soil-structure interaction are generally easier to introduce than in finite elements.
- The model preparation for simple problems is very easy.

Disadvantages

- The method is less efficient for linear or moderately nonlinear problems.
- Until recently, model preparation for complex 3-D structures has not been particularly efficient because sophisticated pre-processing tools have not been as readily available, compared to finite element preprocessors.
- Because the method is based on Newton's law of motion no converged solution for static problems exists, as is the case in static finite element analysis.

2.3.5. Analytical Numerical Models

In general it is possible to classify the different analytical-numerical models according to three groups - (1) Continuum solution, (2) Finite element Solution and (3) Winkler models. This division into three groups is actually somewhat confusing as the methods are sometimes combined. For example there are many Winkler models in which the sub grade reaction is found from a closed form continuum solution.

Soil-pile interaction is rather a complicated phenomenon. This complexity is attributed mostly to the soil rather than to the pile and it involves phenomena such as soil nonlinearity, soil pile gapping, excess pore pressure development etc. Consequently the

classification presented above is quite general as there are many analytical models which consider these phenomena with varying levels of emphasis

2.3.6. Continuum Models

One of the most striking phenomena involved in soil-pile interaction is the radiation of energy to infinity i.e. radiation damping. Obviously the existence of such radiation is dependent both on soil, site and loading characteristics. The advantage of the continuum models over Winkler models and finite element models is that both the condition for radiation and the radiation itself are accurately modeled and are not artificially represented by other means. The disadvantage of the continuum models is that they are restricted to visco-elastic materials and any accommodation of nonlinearity is possible only by changing the material properties in space. In the continuum models the soil behavior is represented usually by closed form solutions (Green's functions) which correspond to a load pattern in space. The Green's function defines the displacement field due to the loading system associated with the pile-soil traction. (Klar, 2003).

Pak and Jennings (1987) solved the dynamic behavior of a pile embedded in an elastic half space by considering a uniform body force field in their Green's function (uniform along the cores section).

2.3.7. Finite Element Models

Finite element and finite difference methods appear to be the most powerful and promising tools both for analysis and solution of geotechnical problems in general and for soil-pile interaction in particular as they incorporate endless options of complexity. Taking advantage of symmetry and antisymmetry only one fourth of the actual model can be built, thus dramatically improving the efficiency of computation (Maheshwari et al., 2005).

Wu and Finn (1997a, 1997b) presented formulations for finite element analysis of piles in both frequency domain and time domain. The main item in their formulation is the computational efficiency achieved by reduction of degrees of freed

2.3.8. Winkler Models

Because of versatility and simplicity in its application the Winkler model is preferred. It includes models which simulate almost all the phenomena involved in soil-pile interaction: radiation damping, soil non-linearity, soil-pile gapping, development of excess pore pressure and even pile-soil-pile interaction in groups of piles. The calculation effort of these models is the smallest one compared to the other classes. However these are all based on an approximation of Winkler's assumption. The Winkler assumption is that each horizontal layer of the soil behaves independently of the others; i.e. the method entails complete disregard of the shear forces which may develop between soil layers (Klar, 2003).

Penzien et al. (1964) in an outstanding work used a Winkler model to analyse the seismic response of a bridge founded on piles. Their analysis was constructed of two stages: (1) the solution of the free field without any structure or piles (i.e. site response), and (2) application of the free field motion to the structure-pile system through a lumped parameter model (Winkler Model). Both the first and the second stages involved nonlinearity of the soil. The soil medium for the one-dimensional analysis of the site response was represented by a bi-linear hysteretic constitutive model. Penzien et al. (1964) conducted an excellent work in achieving and justifying their Winkler model. First they obtained a relation between the average displacements along the pile shaft to a force applied at the center of the pile cross section using Mindlin's solution. Then they went on and showed that this displacement decays very rapidly with vertical distance from the loaded region and that the displacement is not influenced greatly by the vertical position of loading in the half space (Badoni and Makris, 1996). From these two observations they advised on the use of the Winkler model. They then extended the work to consider a pile group where the average displacement is obtained by consideration of loading from all the piles. They constructed a Winkler model which has similar features

to that of the free field. They did not consider the possible radiation damping in the form of viscous dashpots. A convenient way of representing the soil behavior by a Winkler model is through the use of p - y curves. The p - y curve relates the soil resistance (p) to the pile lateral displacement (y). Although the p - y curves essentially represent Winkler models, most of the static or cyclic p - y curves used in practice is founded on full scale experiments which inherently capture the continuum aspects of the soil (Finn et al., 1999).

Novak (1974) was the first to use a Winkler model for representation of a laterally loaded pile in a visco-elastic material. In Novak's solution the soil is composed of horizontal layers that are homogenous, isotropic and linearly elastic. The soil reaction at any depth is that of an infinitely long rigid pile undergoing uniform harmonic vibration in an infinite medium. Novak and Aboul-Ella (1978) formulated an approach for calculating the pile behavior in layered soil using the assumption made by Novak (1974) for the soil resistance. EI Naggar and Novak (1996) calculated the stiffness of nonlinear spring for the inner field element with the assumption that plane conditions hold the inner field is homogeneous, isotropic, visco elastic medium, the pile is rigid and circular, there is no separation at the soil pile interface and the displacements are small. And in case of far field element the plane strain conditions are assumed to hold.

Nogami and Konagai (1986, 1988) suggested a simple mechanical model which approximates the frequency dependent behavior of Novak et al.'s (1978) plane strain Winkler model. The mechanical model which they suggested may be used in a time domain analysis and it was validated for wide range of frequencies (up to frequency is equal to 0.5). Nogami et al. (1988) and Nogami et al. (1992a) extended this Winkler model to account for the nonlinear behavior of the soil. This extension was obtained by regarding the elastic mechanical Winkler model as a far-field element and connecting to it in series a near field element which behave in nonlinear fashion. The near-field element consists of two masses and a nonlinear spring in between them. Nogami et al. (1992a) examined the behavior of this Winkler model through a comparison with finite element analysis of the plane strain problem which the Winkler model represents. It was found from their analysis that the location of the far field element (i.e. the radius, r_0 , which

should be introduced into the equation) i.e. the radius of the nonlinear area has little influence on the results and therefore there is no need to define it. They also found that at low frequencies of motion the nonlinearity increases the damping of the system whereas at high frequencies the damping is decreased compared with linear systems. This is due to the fact that at high frequencies the radiation damping is relatively high compared to the material damping and the nonlinearity significantly reduces it. This behavior cannot occur with nonlinear Winkler models in which the radiation damping is represented by a dashpot which is connected in parallel to the nonlinear element (e.g. Matlock et al., 1978; Kagawa and Kraft, 1980)

Nogami et al. (1992b) discussed the application of Winkler models to earthquake problems and concluded that Winkler models are capable of predicting the earthquake response of pile foundations reasonably well when the fundamental natural frequency of the structure foundation system is above that of the soil and when soil motion does not include significant components at the frequencies below the fundamental natural frequency of the soil. This conclusion was partly based on an analysis conducted by Takemiya and Yamada (1981) of a tall bridge pier with a deep pile group foundation using Novak-type (i.e. plane strain) model. To overcome the limitations of the Winkler models (i.e. the incapability to predict the response for all frequencies) Nogami et al. (1992b) suggested to couple the individual Winkler element by shear springs. They referred to this model as second order model and to the Winkler model as first order model. Kagawa (1992) extended the Kagawa and Kraft (1981) Winkler model to include redistribution of excess pore pressure. An axisymmetric finite-element consolidation model was used to simulate both the radial and the vertical flow of excess pore pressures. Kagawa (1992) applied both sinusoidal and earthquake excitations to his model. He showed that in cases where the development of excess pore pressure is disregarded there is almost a unique relation between the free field surface acceleration and the pile head acceleration. In cases where the development of excess pore pressure is taken into account the uniqueness is destroyed at high values of free field surface acceleration. It has been observed that damage of piles is sometimes associated with the presence of

discontinuities in strength and stiffness of the soil profile and it is not necessarily an outcome of inertia loadings or liquefaction.

EI Naggar and Novak (1995, 1996) proposed a Winkler model for nonlinear analysis of soil pile interaction. Similarly to Nogami et al. (1992a) they introduced a nonlinear near field element which is connected in series to a far field element. However the far field element consisted only of one spring and a dashpot instead of three spring and dashpots as used by Nogami et al. (1992a, 1992b). The spring and dashpot of the far field Kelvin Voigt element were calibrated by the value of Novak et al.'s (1978). The inner field element was represented by Novak and Sheta (1980) solution for their inner elastic cylindrical annulus zone. The nonlinearity was introduced to the inner field element through a modification of the elastic shear modulus in its closed form solution (Poisson's ratio was assumed to be constant).

Most of the Winkler's models are essentially different as some are formulated in the time domain while others in the frequency domain may produce similar results for linear elastic conditions. However it seems that when dealing with nonlinear dynamic behavior the combination of both regulation of nonlinear stiffness and the radiation damping causes some problems. Different conclusions regarding the effects of nonlinear behavior on the soil-pile system were found according to the arrangement of nonlinear springs and dashpots. The Winkler models were originated due to their simplicity and low computational costs.

2.4. PILES IN LIQUEFIABLE SOILS

The first measurements of dynamic p - y behavior for liquefying sand were presented by Wilson et al. (1998, 2000) based on back-analyses of dynamic centrifuge model tests (Katsuichiro et al. ,2004). Results showed that the p - y behavior has characteristics that are consistent with the stress-strain response of liquefying sand. Tokimatsu et al. (2001) observed that the lateral resistance at 1 m depth after liquefaction appeared to be more closely related to relative velocity than relative displacement. Ashford and Rollins (2002) also studied the p - y behavior in liquefied soil based on the blast induced liquefaction testing at Treasure Island. Boulanger et al. (2003) observed

that the subgrade reaction against a pile in liquefying soil is dependent on the excess pore pressures throughout the soil both near the pile and away from the pile i.e. near-field and far field.

Ramos et al. (1999) showed that lateral restraint on a pile head significantly affected the maximum bending moments and lateral pressure distribution on piles in centrifuge test. Dobry and Abdoun (2001) and Abdoun and Dobry (1998) found that maximum loads and bending moments occurred after liquefaction throughout the laterally spreading layer and subsequently decreased with increasing lateral spreading deformations (Jonathan et al., 2004) .

A seismic response analysis of soil–pile-structure interaction was conducted using a multi lumped mass model considering liquefaction proposed by Mori et al.(1992) whose basic concept is rather similar to the model proposed by Penzien et al. (1964) to evaluate the behavior of the piles during the earthquake as well as the causes and the processes of damage. One frame in the span direction was modeled for the analysis. The model consists of a structure-pile system, near-field system and free-field system. The piles were assumed to move identically to the near-field system in the horizontal direction. This system is connected to the free-field system by interaction springs at the corresponding masses. The free-field system is a model of layered ground composed of lumped masses and shear springs. The shear springs of the ground and interaction springs take into account nonlinearity depending not only on the shear strain but also on the changes in the effective confining pressure due to the build-up of the excess pore water pressure by liquefaction. The nonlinearity of soil depending on shear strain is modeled by a hyperbolic curve model in which the rigidity changes in proportion to the square root of the confining pressure and the strength changes in proportion to the confining pressure. The structure was modeled by a single-mass spring system and the piles and structure were modeled by linear beam elements in these analyses (Miwa et al., 2005).

Liyanapathirana and Poulos (2005a) have proposed a method which is based on Mindlin’s equation to determine the non linear spring constants of the Winkler model. Depending on the amount of pore pressure development, spring coefficients in the spring

dashpots model are degraded. A pseudo static approach has been adopted by Liyanapathirana and Poulos (2005b) which involves two main steps. First they carried out a nonlinear free field site response analysis to obtain the maximum ground displacements along the pile and the degraded soil modulus over the depth of the soil deposit and in the second step performed a static load analysis based on maximum ground surface acceleration. They observed that the location of peak values of bending moments and shear forces are same for both dynamic and pseudo static analyses.



2. 5. SOIL LIQUEFACTION IN SOME MAJOR EARTHQUAKES

All strong earthquakes are accompanied by the phenomena of soil liquefaction of some kind. Liquefaction can cause the failure of structures of any form in many modes. Some typical cases of structure failure and related phenomena caused by soil liquefaction in some major earthquakes e.g. the 1964 Alaska Earthquake, the 1964 Niigata Earthquake, the 1989 Loma Prieta Earthquake, the 1995 Kobe Earthquake and the 1999 Izmit Earthquake are summarized in Table 2.1 (Zuo, 2005).

2.6. CASE HISTORIES OF LIQUEFACTION-INDUCED PILE DAMAGE



The damaging effects of soil liquefaction on pile foundations and the structures they support have been observed in past earthquakes and reproduced in laboratory model tests. A brief review of some of these observations helps to illustrate the phenomena involved and to identify the important aspects of soil and foundation behavior that must be considered in a foundation analysis and design. Several cases showed that damage usually was found at the top and bottom of liquefied layer (Tokimatsu et al., 1997, Tokimatsu and Asaka, 1998, Ramos et al. 1999 and Boulanger et al., 2003.). Nine different types of case histories on response of pile foundations in Earthquakes are summarized in Table 2.2.

Table 2.1 Typical cases of failure in liquefaction

S. No.	The Earthquake	Effect due to liquefaction	Photographs	Reference and Fig. No.
1	The Alaska Earthquake, March 27, 1964 of Richter magnitude of 9.2.	Failure of a road embankment caused by soil liquefaction. The failure of the roadbed caused the embankment to spread to the two sides of the road, thereby tore the embankment apart.		www. ce. Washington. edu/ liquefaction /html /main.html Fig. 2.1 Cracking of road embankment
2	The Niigata Earthquake June 20, 1964 of Richter magnitude of 7.5.	The buildings remained relatively intact but rotated as whole structures because of the land-sliding under their foundations. The land-sliding was determined to have been caused by soil liquefaction		www. ce. Washington. edu/ liquefaction /html /main.html Fig. 2.2 Tilted buildings

Contd...

...Contd

S. No.	The Earthquake	Effect due to liquefaction	Photographs	Reference and Fig. No.
3	The Niigata Earthquake June 20, 1964 of Richter magnitude of 7.5.	Softening of pile foundations in liquefiable soils in combination with forces caused by soil movements has caused substantial damage to bridges.		www.eeri.org/Reconn/Turkey0899/Turkey0899.html Fig. 2.3 Failure of the Showa bridge
4	the Loma Prieta Earthquake, October 17, 1989 of Richter magnitude of 7.1	A sand boil at the Oakland International Airport.		www.ce.washington.edu/liquefaction/html/main.html Fig. 2.4 Sand boil

Contd...

...Contd.



S. No.	The Earthquake	Effect due to liquefaction	Photographs	Reference and Fig. No.
5	The Kobe Earthquake, January 17, 1995 of Richter magnitude of 6.9.	The Nishinomiya Bridge with one span of its deck fallen to the ground. The supports of the bridge were not damaged, but large ground deformation occurred.		www.ce.washington.edu/liquefaction/html/main.html Fig. 2.5 Fallen bridge deck
6	The Izmit Earthquake, August 17, 1999 of Richter magnitude of 7.4.	Failure of buildings is caused by soil liquefaction induced loss of bearing strength beneath shallow mat foundations.		www.eeri.org/Reconn/Turkey0899/Turkey0899.html Fig. 2.6 Toppled building

Table 2.2 Case histories of liquefaction-induced pile damage

S. No.	Site and Location	Type of foundation	Earthquake	Damage	Reference
1	Building in Niigata, Japan	Reinforced Concrete piles, 0.3 m diameter	1964 Niigata $M_L=7.5$	Cracking on piles throughout liquefied layer and into underlying dense layer. Some shear discontinuities about 3.5 meters below water table.	Matsui, 1993
2	NHK and NFCH buildings, Niigata, Japan	Reinforced concrete Piles, 0.35 m diameter.	1964 Niigata $M_L=7.5$	Severe concrete rupture at interfaces between liquefied and non liquefied soils.	Meyersohn et al., 1992
3	10-story Hotel east of State Highway 101, SF, U.S.A.	Prestressed concrete piles, 0.36 m square in size.	1989 Loma Prieta $M_L=7.1$	Piles performed well. No significant damage except one corner pile on which cracks on the pile head show possibility of a plastic hinge.	Adib et al. 1995.
4	Higashinada Gas Turbine Thermal Power Station, Kobe, Japan.	Prestressed concrete piles, 0.4 m diameter.	1995 Kobe, $M_L=6.9$	Cracks (horizontal and longitudinal) occurred to all piles. Some damaged only at the pile heads while others also damaged at depth.	Akiyama et al., 1997.

Contd...

...Contd

S. No.	Site and Location	Type of foundation	Earthquake	Damage	Reference
5	Building on reclaimed land in Higashinada-ku, Kobe, Japan.	Prestressed concrete piles of 0.4 m diameter embedded 0.1 m into pile caps.	1995 Kobe, $M_L = 6.9$	Large horizontal /diagonal cracks on seaside piles at three depth-near the pile head, in the middle of the liquefied layer and at the bottom of the liquefied layer. For piles on the mountainside of the building, cracks only near the pile heads and at the bottom of the liquefied layer.	Tokimatsu et al., 1997
6	Elevated highways and bridges in Kobe, Ashiya, Nishinomiya area, Japan.	Various Cast-in-places reinforced concrete piles of more than 1m diameter; precast concrete piles; steel pipe piles of 0.7 m diameter more than 1 m diameter.	1995 Kobe, $M_L=6.9$	Cast-in-place reinforced concrete piles-cracks near pile heads, some cracks at where reinforcement details changed and some cracks near interface of liquefied and non liquefied soil. Steel pipe piles-of large diameter (>1 m) not damaged even in lateral spreading, smaller diameter (0.7 m) indented at the bottom of the liquefied sand. Precast Concrete piles-cracking at pile heads and at depth. The degree of pile damage did not necessary correspond to that of the super and Substructures but instead corresponded to the subsurface conditions and occurrence of lateral spreading.	Matsui and Oda, 1996

Contd...

...Contd

S. No.	Site and Location	Type of foundation	Earthquake	Damage	Reference
7	Buildings on reclaimed land areas including Port and Rokko islands, Fukaehama, and Mikagehama, Japan.	Various- Prestressed concrete piles, prestressed high strength concrete piles, steel pipe piles and steel pipe reinforced concrete piles. Diameters of 0.35 to 0.6 m, typically. Cast-in-place reinforced concrete piles more than 1 m diameter.	1995 Kobe, $M_L = 6.9$	Pile failures concentrated at the interface between liquefied and non liquefied layer and near the pile heads. In the liquefied level ground severe damage to most reinforced concrete piles while less damage to steel or steel-shelled piles. In the waterfront with liquefaction induced lateral spreading damage to all types of piles and to pile caps and foundation beams.	Tokimatsu and Asaka, 1998.
8	Higashinada sewage treatment plant at a reclaimed area.	Prestressed concrete piles of diameter 0.35, 0.4, 0.5 and 0.6 m. Cast in place RC piles of diameters 1, 1.2 and 1.5 m	1995 Kobe, $M_L=6.9$	Cracks 2 or 3 m below the pile head and at the bottom of liquefiable layers with upper cracks larger than the lower ones. Some pile severed in areas of largest ground deformation.	Sasaki et al., 1997

Contd...

...Contd

S. No.	Site and Location	Type of foundation	Earthquake	Damage	Reference
9	Buildings on Port Island, Japan.	Building C: Pile of diameter 0.50 m. Building D: Pile of diameter 0.45 m.	1995 Kobe, $M_L = 6.9$	Building C: No damage. Building D: Severe damage near pile head and at liquefiable and non liquefiable interface.	Fujii et al., 1998.

Chapter-3

MODELLING OF PILE IN LIQUEFIABLE SOIL

3.1. METHODOLOGY

To analyze the pile-soil interaction in liquefiable soil, modeling has been done in two parts - one numerical modeling for liquefaction of soil and second modeling for pile-soil interaction. The interaction between pile and soil in liquefiable soil has been considered in one dimension only. The basic steps of analysis are as follows:

1. The numerical model for liquefaction considered in this study is as follows.
 - a) Numerical model for pore pressure generation from ground response analysis (Nath, Maheshwari, Ramasamy,2005)
 - b) Effective stress response analysis with pore pressure induced softening (Liyanapathirana and Poulos, 2002a).
2. Then in the second phase, soil and pile is modeled considering the effects of pore pressure generation (liquefaction effects) from the first phase of the modeling.
 - a) Numerical model for pile-soil interaction in axial and lateral direction (Nogami and Konagai, 1986 and 1988).
 - b) Incorporating the value of shear modulus considering liquefaction in to the model proposed above.
3. A computer code has been developed to analyze these numerical models in C++ and thus response of piles in liquefiable soil can be predicted.

3.2. NUMERICAL MODELING

The numerical modeling used in this dissertation report is divided into two groups. These are modeling for liquefaction of soil and modeling for pile-soil interaction. Finally combining these two models provides a new model for pile-soil interaction in liquefiable soils.

3.2.1. Modeling for Liquefaction of Soil

Step 1: Rate of pore pressure generation ($\frac{\partial u_g}{\partial t}$)

$$\frac{\partial u_g}{\partial t} = \frac{\partial u_g}{\partial N} \frac{\partial N}{\partial t} = \frac{\sigma'_{v0}}{\theta \pi N_L \sin^{2\theta-1}(\pi r_p / 2) \cos(\pi r_p / 2)} \frac{\partial N}{\partial t} \quad (3.1)$$

Here $\frac{\partial N}{\partial t}$ is the rate of application of shear stress cycles to the soil, σ'_{v0} is the initial effective overburden pressure, r_p is the pore pressure ratio that is ratio of excess pore water pressure to initial effective overburden pressure. The value of r_p is given by the following expressions.

$$r_p = \frac{u_g}{\sigma'_{v0}} \quad (3.2)$$

$$r_p = \frac{2}{\pi} \text{Sin}^{-1} \left(\frac{N}{N_L} \right)^{1/2\theta} \quad (3.3)$$

Here N_L is the number of uniform stress cycles required to produce a condition of initial liquefaction (Pore pressure = Effective confining Pressure) under undrained conditions (Seed et al., 1976), N is the number of equivalent uniform cycles and value of θ is 0.7 for best fit. u_g is the excess pore water pressure.

Step 2: Pore pressure redistribution and dissipation

$$\frac{\partial u}{\partial t} = \frac{1}{m_v \gamma_w} \frac{\partial}{\partial z} \left(k \frac{\partial u}{\partial z} \right) + \frac{\partial u_g}{\partial t} \quad (3.4)$$

Where

$\frac{\partial u}{\partial t}$ is the excess pore water pressure developed in one dimensional formulation.

m_v is the tangent coefficient of volume compressibility. The value of m_v is given by the following expression.

$$\frac{m_v}{m_{v_o}} = \frac{e^{ar_p^b}}{1 + ar_p^b + 0.5a^2r_p^{2b}} \quad (3.5)$$

The value of a and b is dependent of relative density of soil D_r and can be expressed as follows.

$$a = 5(1.5 - D_r) \quad (3.6 \text{ a})$$

$$b = \left(\frac{3}{2}\right)^{2D_r} \quad (3.6 \text{ b})$$

Here m_{v_o} is the tangent coefficient of volume compressibility at low pressure.

Step 3: Effective stress response analysis with pore water pressure induced (Liyanapathirana and Poulos, 2002a).

$$\frac{G_t}{G_0} = \left(\frac{\sigma'_{vt}}{\sigma'_{v0}}\right)^n \quad (3.7)$$

Here

G_t is the shear modulus at time t

G_0 is the initial shear modulus.

σ'_{vt} is the effective overburden stress at time t .

σ'_{v0} is the initial effective overburden stress.

n is the power exponent and generally equal to 0.5.

The average shear stress (τ_{av}) is calculated to analyze the liquefaction potential.

$$\tau_{av} = 0.65 \frac{a_{max}}{g} \sigma_{v0} r_d \quad (3.8)$$

Where

a_{max} is the peak ground acceleration (PGA).

σ_{v0} is the total overburden stress.

r_d is the depth factor.

The stress ratio causing liquefaction for a given soil at a relative density (D_r) can be estimated from the following equation (Prakash, 1981)

$$\left(\frac{\tau}{\sigma'_{v0}} \right)_{D_r} = \left(\frac{\sigma_{dc}}{2\sigma_a} \right)_{D_r=50} c_r \frac{D_r}{50} \quad (3.9)$$

Where

$\left(\frac{\sigma_{dc}}{2\sigma_a} \right)_{D_r=50}$ is the stress ratio causing liquefaction at relative density $D_r = 50$. This ratio is

based on the both triaxial compression test and simple shear test, which is shown in Figs. 3.5 and 3.6. In this report the value based on the triaxial test has been considered.

C_r is the correction factor based on relative density.

3.2.2. Modeling for Pile-Soil Interaction

The modeling of pile-soil interaction has been done for two different loadings namely axial load and lateral load using Winkler's hypothesis. The pile-soil system is divided into horizontal slices containing the pile segment and homogenous soil layer as shown in Fig. 3.1 below.

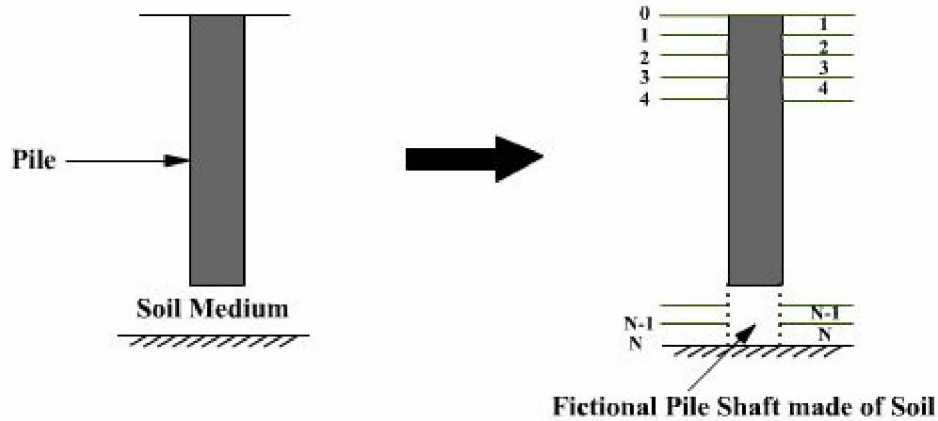


Fig. 3.1 Soil- pile system divided into horizontal slices (Nogami and Konagai, 1988)

The numerical models for axial load (Nogami and Konagai, 1986) and for lateral load (Nogami and Konagai, 1988) are described in details in the next section. Both are based on Winkler’s hypothesis i.e. the soil-pile interaction force is related to pile shaft displacements only at that depth where the interaction force is considered.

3.2.2.1. Pile- Soil-Interaction Model due to Axial Load

1. The Winkler soil model units are assumed to be uniformly distributed along the pile shaft for modeling the soil medium around the pile shaft. One model unit is shown in Fig. 3.2. The values of the model parameters are determined using the following expression for the axial load.

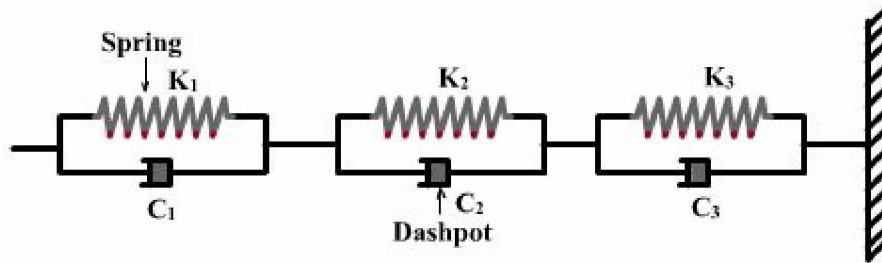


Fig. 3.2 One unit of Winkler soil model for axial pile shaft response (Nogami and Konagai, 1986)

$$(k_1, k_2, k_3) = G_s (3.518, 3.581, 5.529) \quad (3.10)$$

$$(c_1, c_2, c_3) = \frac{G_s r_0}{V_s} (113.0973, 25.133, 9.362) \quad (3.11)$$

Here G_s , r_0 and V_s are shear modulus, radius of pile and shear wave velocity of soil respectively. The value of G_s is considered G_0 and G_t for the analysis of pile-soil interaction in non-liquefiable soil and liquefiable soil respectively.

2. Applying the compatibility and equilibrium conditions at the boundary between two adjacent segments, the displacement and forces at the bottom of the n^{th} segment of the pile shaft or soil column can be expressed as below.

$$\begin{Bmatrix} w_i \\ P_i \end{Bmatrix}_n = [T_n] \begin{Bmatrix} w_i \\ P_i \end{Bmatrix}_0 + \{Q_n\} \quad (3.12)$$

Where

$$[T_1] = [t_1] \text{ and } \{Q_1\} = [q_1] \{\gamma_{i,1}\} \text{ for } n=1 \quad (3.12.1)$$

$$[T_n] = [t_n][T_{n-1}] \text{ and } \{Q_n\} = [t_n]\{Q_{n-1}\} + [q_n]\{\gamma_{i,n}\} \text{ for } n \geq 2 \quad (3.12.2)$$

Here w_i and P_i are axial pile displacement and applied axial load respectively and n indicates the number of layer. $[t]$ and $[q]$ can be expressed as follows.

$$[t] = \begin{bmatrix} \frac{\beta_1}{\beta_2} & -\frac{1}{\beta_2 E_p A} \\ E_p A \frac{\beta_2^2 - \beta_1^2}{\beta_2} & \frac{\beta_1}{\beta_2} \end{bmatrix} \quad (3.13)$$

and

$$[q] = \beta_4 \begin{bmatrix} \frac{2}{\beta_2} & \frac{1}{\beta_2} \\ -E_p A \left(1 + 2 \frac{\beta_1}{\beta_2}\right) & -E_p A \left(2 + \frac{\beta_1}{\beta_2}\right) \end{bmatrix} \quad (3.14)$$

Where $\beta_1, \beta_2, \beta_3$ and β_4 can be expressed as follows.

$$\beta_1 = \frac{1}{l} + \frac{\lambda^2 l}{3}, \beta_2 = \frac{1}{l} + \frac{\lambda^2 l}{3}, \beta_3 = \frac{1}{l} - \frac{\lambda^2 l}{6}, \beta_4 = \frac{l}{3} \text{ and } \beta_5 = \frac{l}{6} \quad (3.14.1)$$

Where l is the length of individual layer of pile-soil system.

The expression of λ^2 and γ_i are expressed as below.

$$\lambda^2 = \frac{m_p}{E_p A} \frac{(\alpha + 1)(\alpha + 2)}{\Delta t^2} + \frac{k}{E_p A} \quad (3.15)$$

$$\gamma_i = \frac{d_i}{E_p A} - \frac{m_p}{E_p A} \left[\frac{(\alpha + 1)(\alpha + 2)}{\Delta t^2} w_{i-1} + \frac{(\alpha + 1)(\alpha + 2)}{\Delta t} \dot{w}_{i-1} + \frac{\alpha(\alpha + 2)}{2} \ddot{w}_{i-1} \right] \quad (3.16)$$

The velocity (\dot{w}) and acceleration (\ddot{w}) can be expressed in terms of displacements. Here m_p, E_p and A are mass per unit length of the pile, Young's modulus of pile and cross sectional area of the pile respectively.

3. The interacting force p_i is as follows

$$p_i = k w_i + d_i \quad (3.17)$$

Where k and d_i can be defined as follows.

$$k = \left[\sum_{n=1}^3 \frac{1}{k_n} \left(1 - \frac{c_n}{k_n \Delta t} + \frac{c_n}{k_n \Delta t} e^{-\frac{k_n \Delta t}{c_n}} \right) \right]^{-1} \quad (3.18)$$

$$d_i = -k \sum_{n=1}^3 w_{i-1} e^{-\frac{\Delta t \cdot k_n}{c_n}} - k \cdot p_{i-1} \sum_{n=1}^3 \frac{1}{k_n} \left(-\frac{c_n}{\Delta t \cdot k_n} - \left(1 + \frac{c_n}{\Delta t \cdot k_n}\right) e^{-\frac{\Delta t \cdot k_n}{c_n}} \right) \quad (3.19)$$

3.2.2.2. Pile- Soil Interaction Model due to Lateral Load

1. The medium can be modeled by springs, dashpots and a mass as shown in Fig. 3.3.
The model parameters are as follows.

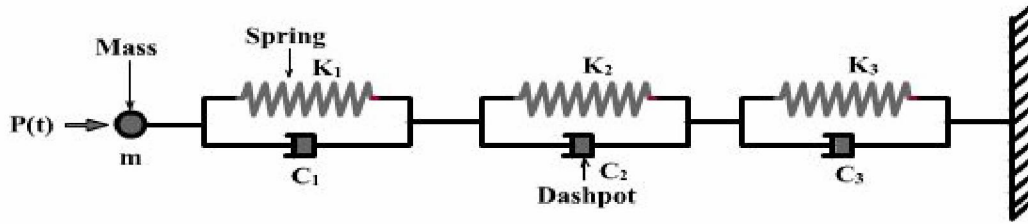


Fig. 3.3 Winkler soil model for lateral pile shaft response
(Nogami and Konagai, 1988)

$$m_s = \xi_m (\nu) \rho_s \pi r_0^2 \quad (3.20)$$

Where ρ_s is the mass per unit volume of the medium.

$$(k_1, k_2, k_3) = G_s \xi_k (\nu) (3.518, 3.581, 5.529) \quad (3.21)$$

$$(c_1, c_2, c_3) = \frac{G_s}{V_s} r_0 \xi_k (\nu) (113.0973, 25.133, 9.362) \quad (3.22)$$

Here G_s , ν and V_s are shear modulus, the Poisson's ratio and shear wave velocity of soil respectively and ξ_k and ξ_m are the dimensionless parameters dependent on Poisson's ratio and provided this values by Nogami and Konagai (1988).

2. Applying the compatibility and equilibrium conditions at the boundary between two adjacent segments, the displacement and forces at the bottom of the n^{th} segment of the pile shaft or soil column can be expressed as below.

$$\left(u_i, \theta_i, \frac{M_i}{E_p I}, \frac{P_i}{E_p I} \right)_n^T = [T_n] \left(u_i, \theta_i, \frac{M_i}{E_p I}, \frac{P_i}{E_p I} \right)_0^T + \{Q_n\} \quad (3.23)$$

Where u_i , θ_i , P_i , M_i , $E_p I$ are lateral displacement, rotational displacement, lateral load, bending moment and bending stiffness of pile shaft respectively. The $[T_n]$ and $\{Q_n\}$ are same as mentioned in the Eqs. 3.12.1 and 3.12.2 for different values of n . Further $[t]$ and $[q]$ can be expressed as follows.

$$[t] = \frac{1}{1 + \frac{l^2 \lambda^4}{120}} \begin{bmatrix} \left(1 - \frac{l^4 \lambda^4}{30} \right) & (-l) & \left(\frac{l^2}{2} \right) & \left(-\frac{l^3}{6} \right) \\ \left(\frac{l^4 \lambda^4}{6} - \frac{l^7 \lambda^8}{2880} \right) & \left(1 - \frac{l^4 \lambda^4}{30} \right) & \left(\frac{l^5 \lambda^4}{80} - l \right) & \left(\frac{l^2}{2} - \frac{l^6 \lambda^4}{360} \right) \\ \left(\frac{l^6 \lambda^8}{360} - \frac{l^2 \lambda^4}{2} \right) & \left(\frac{l^3 \lambda^4}{6} \right) & \left(1 - \frac{3l^4 \lambda^4}{40} \right) & \left(\frac{7l^5 \lambda^4}{360} - l \right) \\ \left(l \lambda^4 - \frac{l^5 \lambda^8}{80} \right) & \left(-\frac{l^2 \lambda^4}{2} \right) & \left(\frac{l^3 \lambda^4}{4} \right) & \left(1 - \frac{3l^4 \lambda^4}{40} \right) \end{bmatrix} \quad (3.24)$$

$$[q] = \begin{bmatrix} -\frac{l^4}{120} & -\frac{l^4}{30} \\ \frac{l^3}{24} & \left(\frac{l^3}{8} - \frac{l^7 \lambda^4}{2880} \right) \\ -\frac{l^2}{6} & \left(\frac{l^6 \lambda^4}{360} - \frac{l^2}{3} \right) \\ \frac{l}{2} & \left(\frac{l}{2} - \frac{l^5 \lambda^4}{80} \right) \end{bmatrix} \quad (3.25)$$

The term used above λ^4 and γ_i can be expressed as follows.

$$\lambda^4 = \frac{k}{E_p I} + \frac{m_p + m_s}{E_p I} \frac{(\alpha + 1)(\alpha + 2)}{\Delta t^2} \quad (3.26)$$

And

$$\gamma_i = \frac{d_i}{E_p I} - \frac{m_p + m_s}{E_p I} \left[\frac{(\alpha + 1)(\alpha + 2)}{\Delta t^2} u_{i-1} + \frac{(\alpha + 1)(\alpha + 2)}{\Delta t} \dot{u}_{i-1} + \frac{\alpha(\alpha + 3)}{2} \ddot{u}_{i-1} \right] \quad (3.27)$$

The velocity and acceleration can be expressed in terms of displacements. Here m_p , $E_p I$ and l are mass per unit length of the pile, bending stiffness of pile and length of layer of soil respectively.

3. The interacting force p_i is as follows

$$p_i = ku_i + d_i + m_s \ddot{w}_i \quad (3.28)$$

The expression of k and d_i are same as given in Eqs. 3.18 and 3.19.

3.2.3. Modeling for Pile in Liquefiable Soils

The liquefaction phenomenon can be studied by using the above formulation i.e. the Eqs. 3.1 to 3.9.

The pile-soil interaction phenomenon for both axial load as well as lateral load can be studied using the Eqs. 3.10 to 3.19 and 3.20 to 3.28 respectively.

Finally modeling of the pile-soil interaction in liquefiable soils has been developed to predict the response of pile in liquefiable soils by combining all the Eqs. 3.1 to 3.26.

3.3.ALGORITHM

In this report to predict the response of pile in liquefiable soil, a computer code has been developed in C++.

In the first phase the computer code has been developed to check whether the soil is liquefiable or not. If the soil is liquefiable then the rate of pore pressure generation has been determined. Thus the change of shear modulus of that particular soil has been calculated using the developed computer code. This changing value of shear modulus is incorporated in the next phase of computations to observe the behaviour of pile in liquefiable soils. The step by step procedure i.e. the algorithm for the development of the computer code has been described and finally details of the flowcharts is discussed.

3.3.1. Algorithm for Checking the Liquefaction Potential

1. Enter values of unit weight of sand (γ), depth (h), Peak Ground Acceleration (PGA) i.e. (a_{max}) and depth factor (r_d). The depth factor can be determined from Fig 3.4. In Fig. 3.4 the dotted line/ middle line indicates the average values whereas the thick lines show the range for different soil profiles.
2. Calculate the value of σ_{v0} and σ'_{v0} .
3. Determine the average shear stress (τ_{av}) in deposit using Eq.3.8.
4. Determine equivalent number of significant stress cycles (N) depending on earthquake magnitude from the Table 3.1.
5. Find D_{50} in mm.
6. Determine $\left(\frac{\sigma_{dc}}{2\sigma_a} \right)_{for D_{50}}$ from the Fig. 3.5 and 3.6 for 10 cycles and 30 cycles, respectively. For 20 cycles, the average value from Fig. 3.5 and 3.6 can be considered.
7. Enter the value of relative density (D_r) and calculate correction factor (C_r) from Table 3.2.
8. Determine stress causing liquefaction (τ) using Eq. 3.9.
9. Determine the interaction points of shear stress and stress causing liquefaction. That interaction points gives the depth of zone of liquefaction.

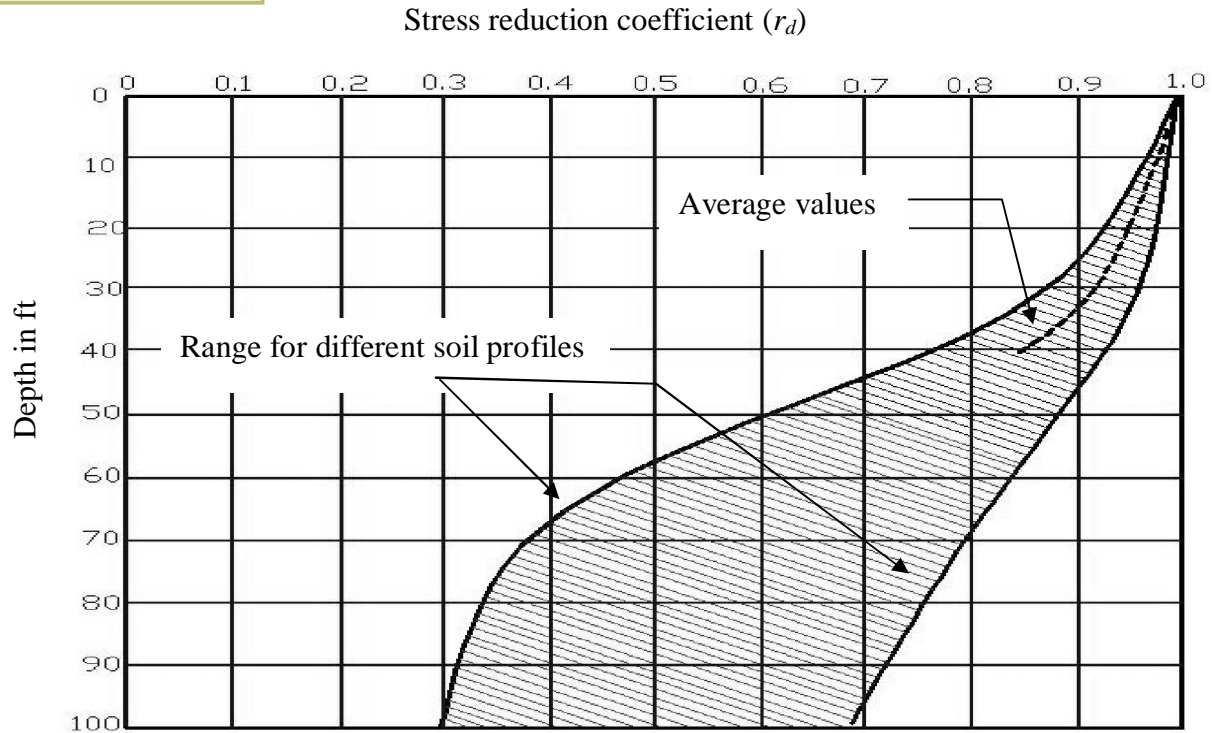


Fig. 3.4 Range of r_d for different soil profiles in liquefaction Analysis (Seed and Idriss, 1971)

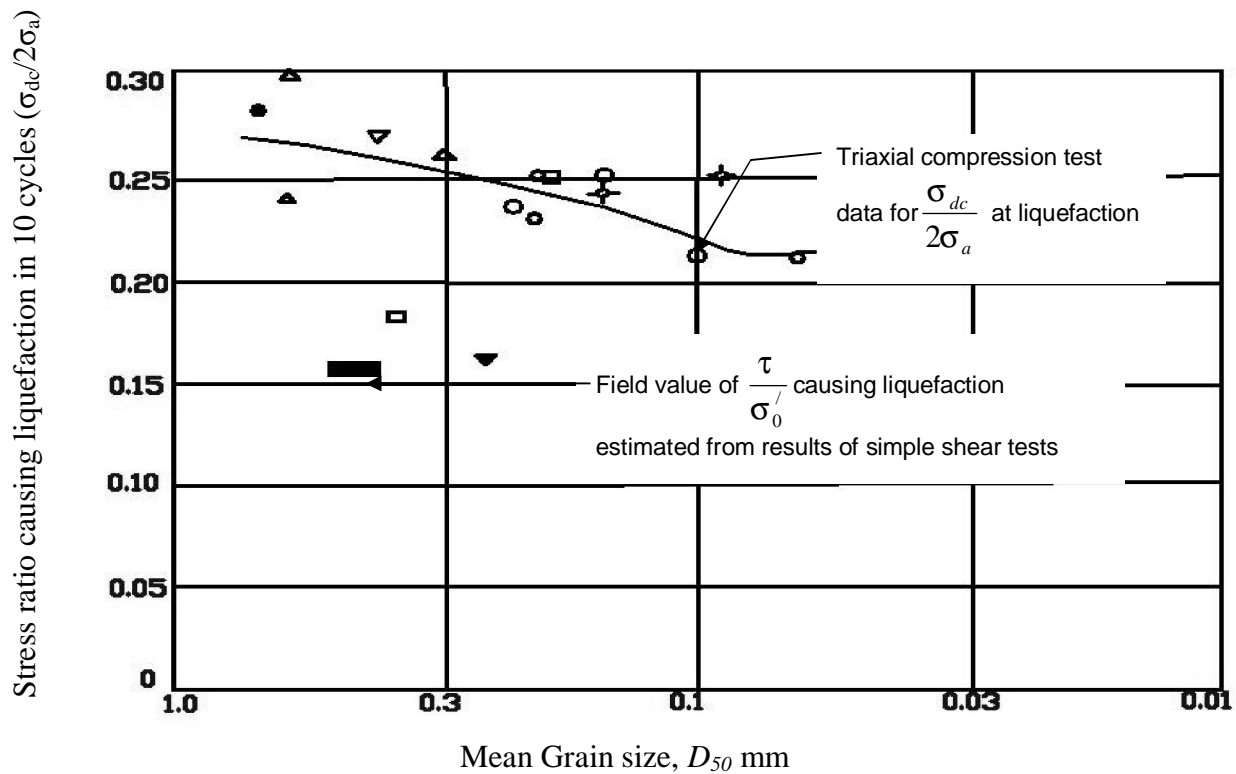


Fig.3.5 Stress causing liquefaction of sands in 10 cycles

(Seed and Idriss, 1971)

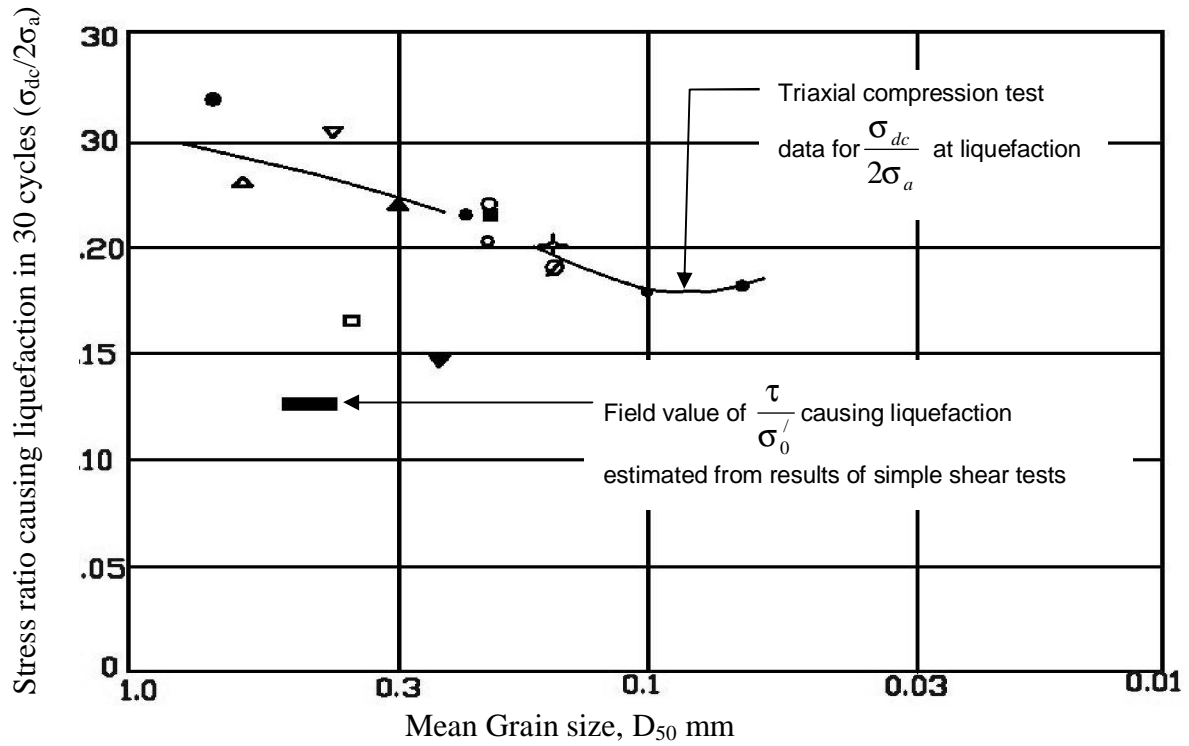


Fig.3.6 Stress causing liquefaction of sands in 30 cycles (Seed and Idriss, 1971)

Table 3.1 Equivalent number of significant stress cycles (Prakash, 1981)

Sr. No	Earthquake Magnitude	Number of significant stress cycles (N)
1	7.0	10
2	7.5	20
3	8.0	30

Table 3.2 Relation between relative density and correction factor (Prakash, 1981)

Relative Density (D_r) in percentage	Correction factor (C_r)
0-50	0.57
60	0.60
80	0.68

3.3.2. Algorithm for Liquefaction Model

1. Calculate effective overburden stress (σ'_{v0}), total overburden stress (σ_{v0}) and depth factor (r_d).
2. Enter PGA (a_{max})
3. Determine the Cyclic stress ratio ($\frac{\tau_{av}}{\sigma'_{v0}}$).
4. Determine number of uniform stress cycles required to produce a condition of initial liquefaction (N_L) from Fig. 3.7.

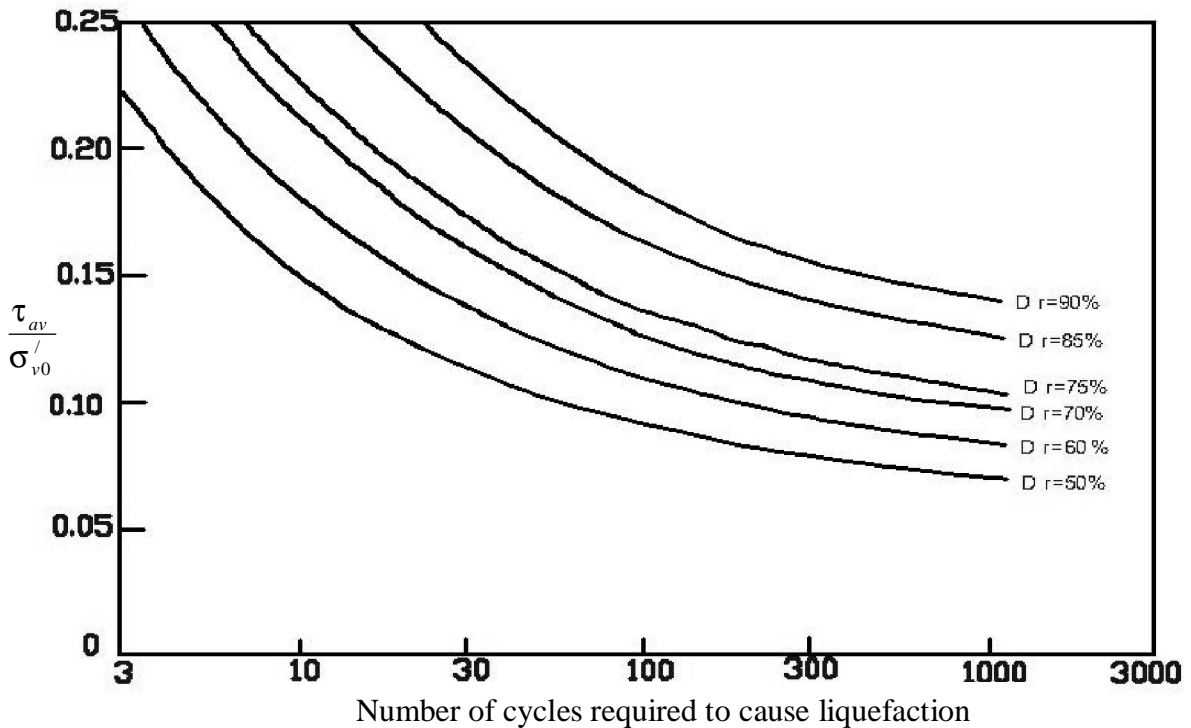


Fig. 3.7 Relationship between cyclic stress ratio and number of cycles required to cause liquefaction for simple shear test for different relative density

(Seed and Martin, 1976)

5. Enter the value of θ , which is given 0.7 by Martin and Seed (1979).
6. Calculate pore pressure ratio (r_p) from Eq. 3.3.
7. Enter the value of rate of uniform cycles per unit time ($\frac{\partial N}{\partial t}$) and it can be found from the Table 3.3.

Table 3.3 Guidelines for determining rate of uniform cyclic loading per unit time (Seed et al., 1976)

Earthquake magnitude	N_{eq}	Duration of strong shaking in seconds	$\frac{\partial N}{\partial t}$ in cycles per second
5.5 – 6	5	8	0.6
6.5	8	14	0.6
7	12	20	0.6
7.5	20	40	0.5
8	30	60	0.5

8. Calculate pore pressure generation from liquefaction analysis using the Eq. 3.4.
9. Calculate a and b for known value of relative density from Eqs.3.6 (a) and 3.6 (b) respectively.
10. Enter the value of tangent coefficient of volume compressibility at low pressure (m_{v_o}). The value of m_{v_o} may be taken as $26.1 \times 10^{-6} \text{ m}^2/\text{kN}$ and $41.8 \times 10^{-6} \text{ m}^2/\text{kN}$ for dense and loose soil respectively (Seed et al., 1976).
11. Enter the value of coefficient of permeability (k). According to Seed et al. (1976) k (in cm per sec) can be calculated from the following equation for average field value.

$$k = 77(D_{50})^{2.32} \text{ in which } D_{50} = \text{the } 50\% \text{ size in cm.}$$

12. Calculate pore pressure generation and redistribution from liquefaction analysis using equation 3.3., the term $\frac{\partial^2 u}{\partial z^2}$ in Eq. 3.4 has been expanded.
13. Enter the value of initial shear modulus (G_0) and value of n . Generally n value is equal to 0.5.
14. Calculate the effective stress response analysis with pore water pressure induced using Eq. 3.7.

3.3.3. Algorithm for Pile-Soil Interaction Model in Liquefiable Soils

1. Enter the initial value of shear modulus (G_s), mass density of soil (ρ_s), radius of pile (r_0) and applied load (P).
2. Calculate Shear wave velocity (V_s) using $\sqrt{\frac{G_s}{\rho}}$ and dimensionless frequency (a_0).

$$\text{Here } a_0 = \frac{\omega r_0}{V_s}$$

Where ω , r_0 and V_s are the angular frequency, radius of pile and shear wave velocity respectively.

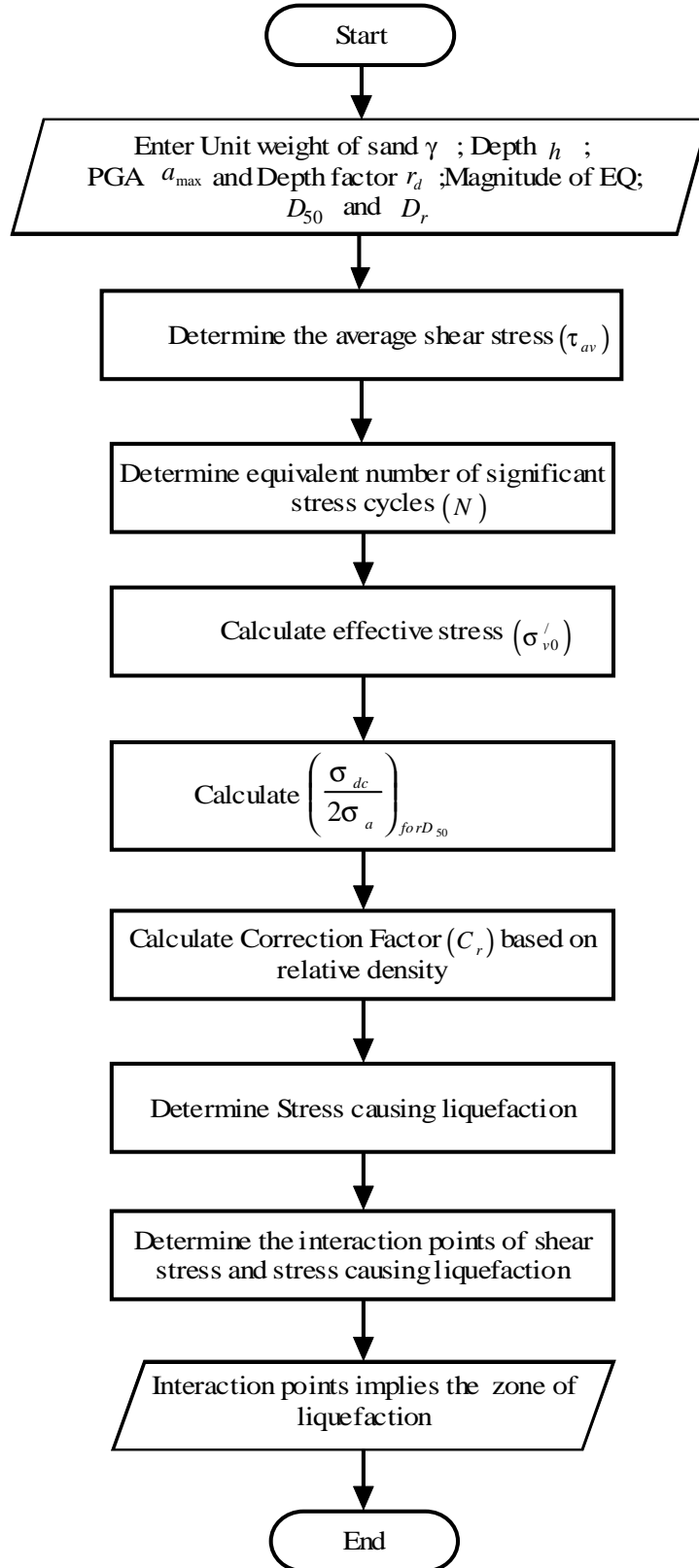
3. Calculate c_1, c_2, c_3 and k_1, k_2 and k_3 .
4. Calculate $\beta_1, \beta_2, \beta_3$ and β_4 .
5. Calculate $[t]$ and $[q]$.
6. Calculate λ^2, λ^4 and γ .
7. Calculate k and d_i
8. Calculate axial displacement and forces at different layers using Eq. 3.12.
9. Calculate lateral displacement, rotational displacement and bending moment at different layers using Eq. 3.23.
10. Calculate interacting force (π_i) using Eq.3.17 and Eq.3.28 for axial and lateral load respectively.

11. Enter the modified value of shear modulus via Eq. 3.7 due to liquefaction and repeat step 2 to step 8.

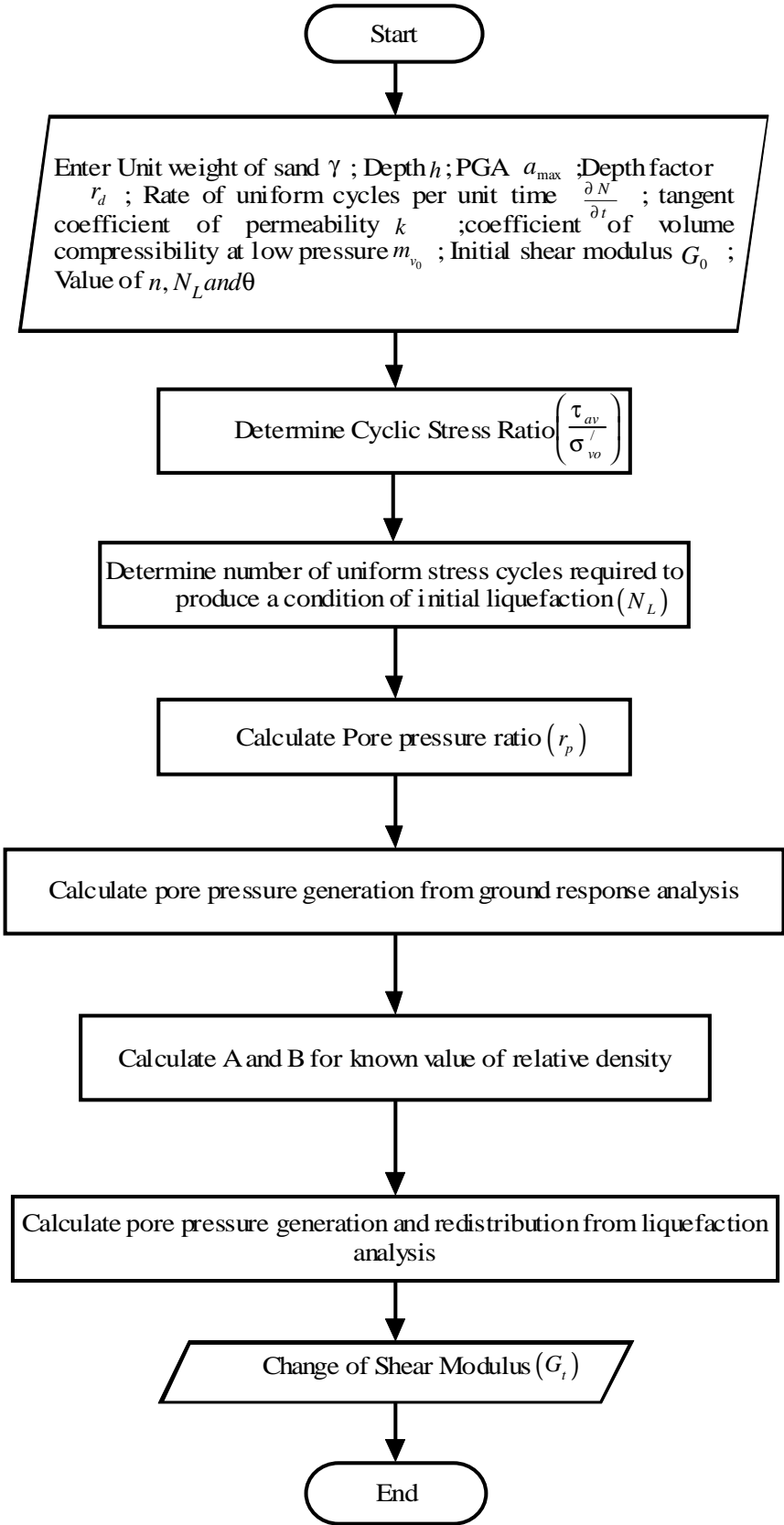
3.4. FLOW CHART FOR PILE-SOIL INTERACTION IN LIQUEFIABLE SOILS

The flow chart of the developed computer code is divided into three categories. These flowcharts are (1) for liquefaction potential, (2) for liquefaction model and (3) for pile-soil interaction with and without liquefaction.

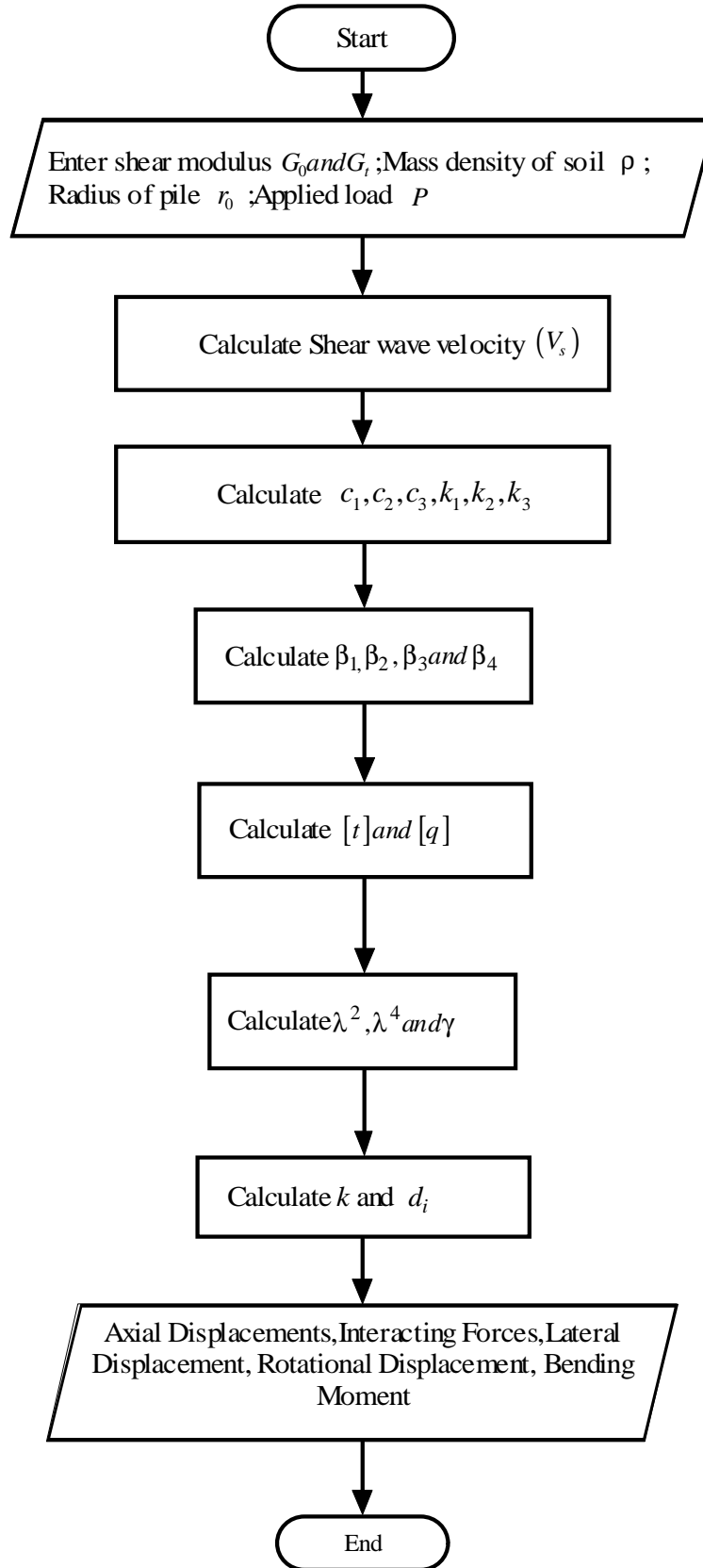
The details are described in flow charts 3.1 to 3.3. The flow chart 3.1 describes the liquefaction potential. Flow chart 3.2, deals the details about the liquefaction model. And finally the flow chart 3.3, describes the pile-soil interaction model in liquefiable soils



FC 3.1 Flow chart for liquefaction potential



FC 3.2 Flow chart for liquefaction model



FC 3.3 Flow chart for pile-soil interaction

Chapter-4

VERIFICATION OF MODEL

4.1 GENERAL

The numerical model for the pile-soil interaction and liquefaction are described in details in the chapter 3. As a rigorous approach is used, the verification of the models as well as the developed algorithm is one of the important issues before finding the dynamic response of pile in the liquefiable soils. All analysis and results presented in this dissertation are computed in the time domain.

4.2. VERIFICATION OF PILE-SOIL INTERACTION MODEL

The modeling of pile-soil interaction has been done for axial load and lateral load separately using Winkler's hypothesis. The pile-soil system is divided into four and five horizontal slices for axial and lateral load respectively as shown in Figs. 4.1. (a) and (b). The inputs for the verifications of the models are given in Table 4.1.

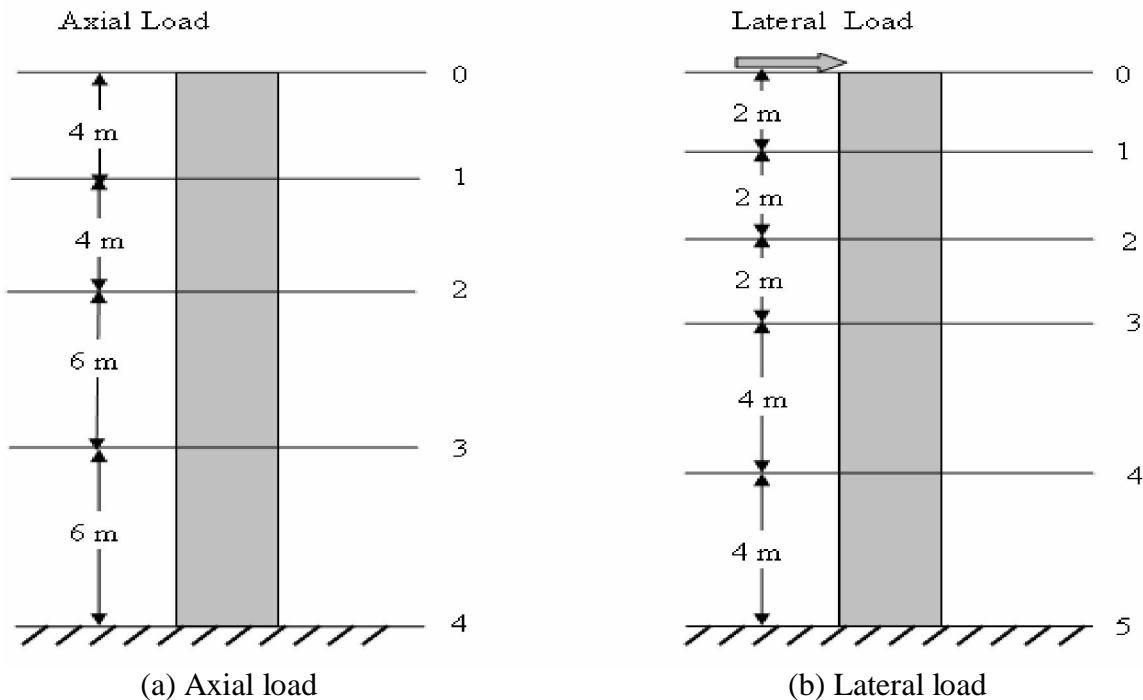


Fig. 4.1 Soil-pile system divided into horizontal slices

Table 4.1 Inputs for verification of the models

Sr. No	Items	Value
1	Shear modulus of soil (G_s)	$71.77 \times 10^3 \text{ kN/m}^2$
2	Pile diameter ($2r_0$)	1 m
3	Modulus of elasticity of pile (E_p)	$25 \times 10^6 \text{ kN/m}^2$
4	Mass density of soil (ρ_s)	1200 kg/m^3

4.2.1. Verification for Complex Soil Stiffness

The Fig. 4.2 shows the variation in complex soil stiffness (k_s) with respect to frequency for axial load. Both soil stiffness and frequency (a_0) are presented in dimensionless form. k_s is normalized with respect to G_s and $a_0 = \frac{r_0 \omega}{v_s} =$ dimensionless frequency. The results of Fig. 4.2 are in good agreement with those presented by Nogami and Konagai (1986).

The Fig. 4.3 shows the variation in dimensionless Complex soil stiffness with frequency for lateral load for the Poisson's ratio equal to 0.5. The trend of the result is similar to that presented by Nogami and Konagai (1988).

The real and imaginary part implies the spring stiffness and damping respectively. As the frequency increases the stiffness due to spring is almost constant, but stiffness due to damping increases linearly.

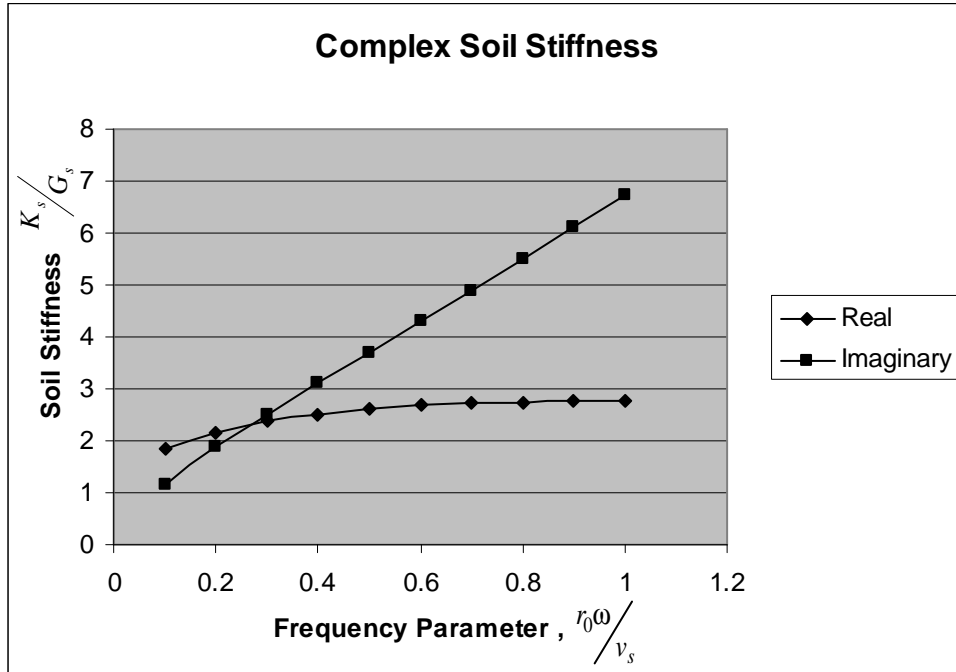


Fig. 4.2 Complex soil stiffness due to axial load

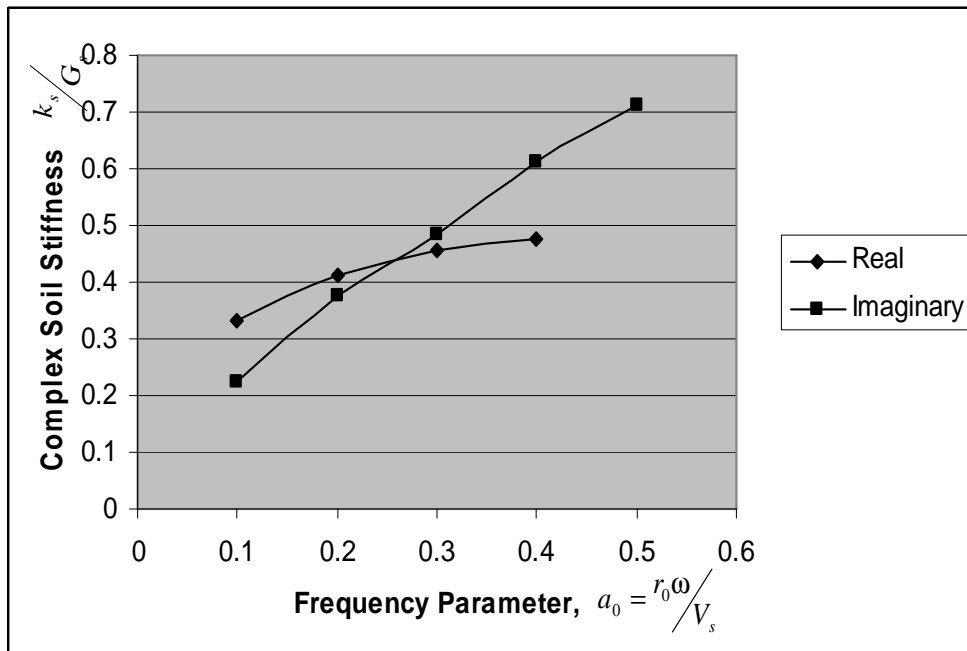


Fig.4.3 Complex soil stiffness due to lateral load

4.2.2. Verification for Pile Head Stiffness

The Fig. 4.4 shows the relationship between pile head stiffness k_s and dimensionless frequency (a_0) for axial load. The pile head stiffness is represented in dimensionless form by normalizing with respect to $E_s L$. The trend of the results shown in Fig. 4.4 are similar to the results that presented by Nogami and Konagai (1986)

The Fig. 4.5 shows the relationship between pile head stiffness and frequency for lateral load. Both pile head stiffness and frequency are dimensionless. It is shown for the Poisson's ratio equal to 0.5 only. Here the pile head stiffness is dimensionless with respect to E_p, I and L . The results of Fig. 4.5 are in good agreement with the results presented by Nogami and Konagai (1988).

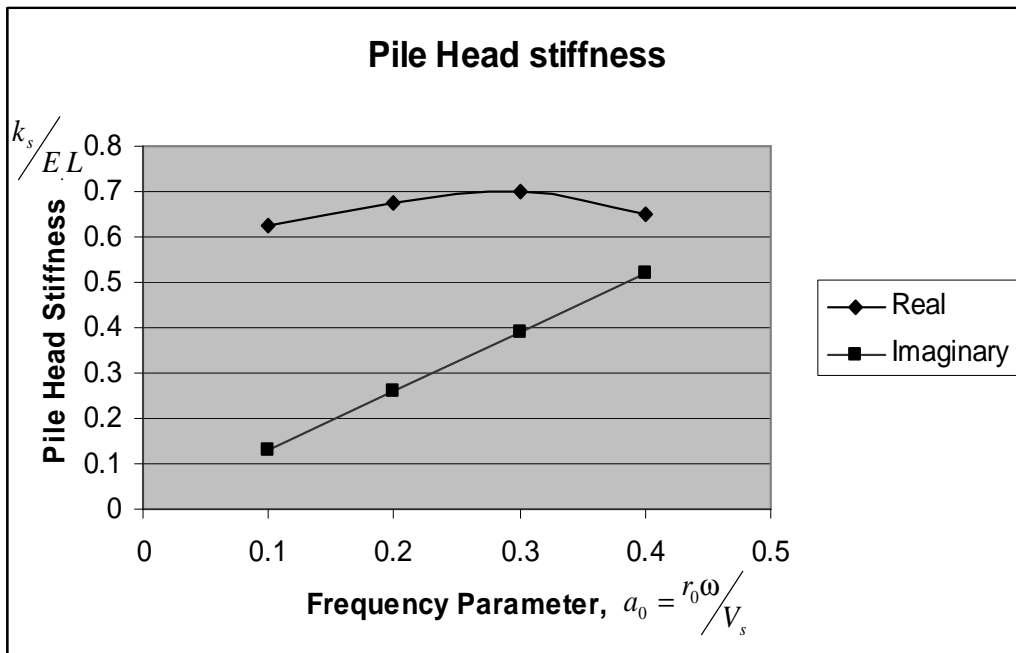


Fig 4.4 Pile head stiffness due to axial load

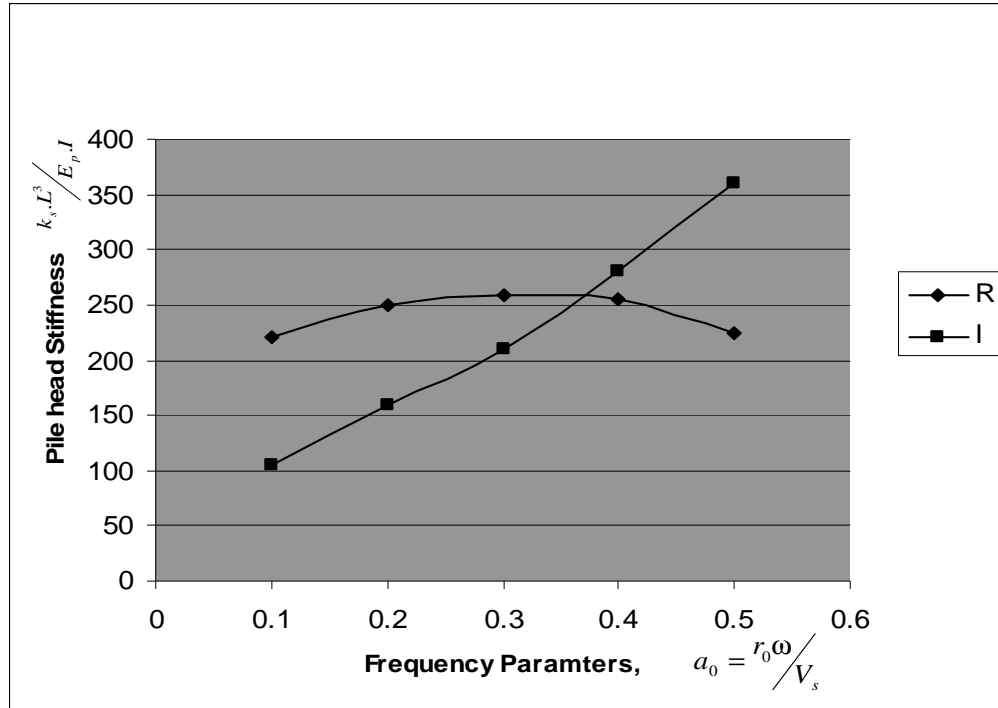


Fig. 4.5 Pile head stiffness due to lateral load for Poisson’s ratio = 0.5

4.3. SUMMARY

The pile-soil interactions model for both the axial and lateral load has been verified with the results available in the literature. The results found by combined model i.e. pile-soil interaction and liquefaction is verified/validated with the results from the literature in the chapter 5. The validation of the results is presented in Figs.5.13 and 5.14.

Thus it can be mentioned here that the developed combined model as well as algorithm is properly working to predict the response of pile in liquefiable soils.

Chapter-5

EFFECT OF LIQUEFACTION ON PILE-SOIL INTERACTION

5.1. GENERAL

First step in this problem is to find out the zone of liquefaction with known data of a particular soil. The rate of pore pressure generation is calculated and thus the variation of shear modulus of soil during the liquefaction is observed. This variation is used in the computer code developed to see the response of pile in liquefiable soil for axial and lateral load. Finally the results of pile-soil interaction are compared with and without liquefaction phenomenon for both axial load and lateral load separately with the developed computer code.

5.2. LIQUEFACTION

The soil profile is tested whether liquefaction will occur or not. The input data are shown in Table 5.1. The soil profile used in the analysis is shown in Fig. 5.1.

Table 5.1 Inputs for the analysis of liquefaction and pile-soil interaction.

Sr. No.	Items	Value
1	PGA(a_{max})	0.1 g
2	Magnitude of the earthquake (M)	7.5
3	D ₅₀ of Sand	0.2 mm
4	Relative Density (D_r)	40 %
5	Applied load (P)	100 kN

The Fig. 5.2 shows comparison of two sets of results i.e. average shear stress (τ_{av}) vs. depths and shear stress causing liquefaction (τ) vs. depths. It can be observed that both curves intersect at depths of 6 m and 12 m. As average shear stress exceeds the shear stress causing liquefaction in the zone of 6-12 m therefore the sand sample will be liquefiable for 0.1 g acceleration of earthquake in this zone.

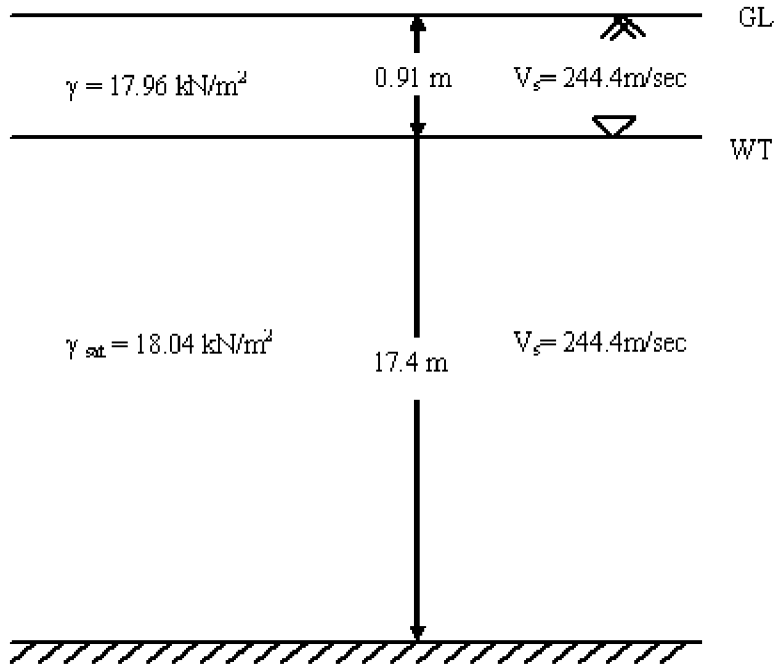


Fig. 5.1 Soil profile

The natural dimensionless frequency of the soil is equal to 0.1. The calculation of the natural dimensionless frequency of the soil is shown below.

The natural frequency of soil stratum $(f_0)_{natural} = \frac{V_s}{4h}$ (Hz)

But the dimensionless natural frequency, $a_0 = \frac{\omega r_0}{V_s}$

$$\begin{aligned}
 &= \frac{2\pi f_0 r_0}{V_s} \\
 &= \frac{2\pi}{V_s} \frac{V_s}{4h} r_0 \\
 &= \frac{\pi}{2h} r_0 \\
 &\cong 0.1
 \end{aligned}$$

Where h is the depth of the layer.

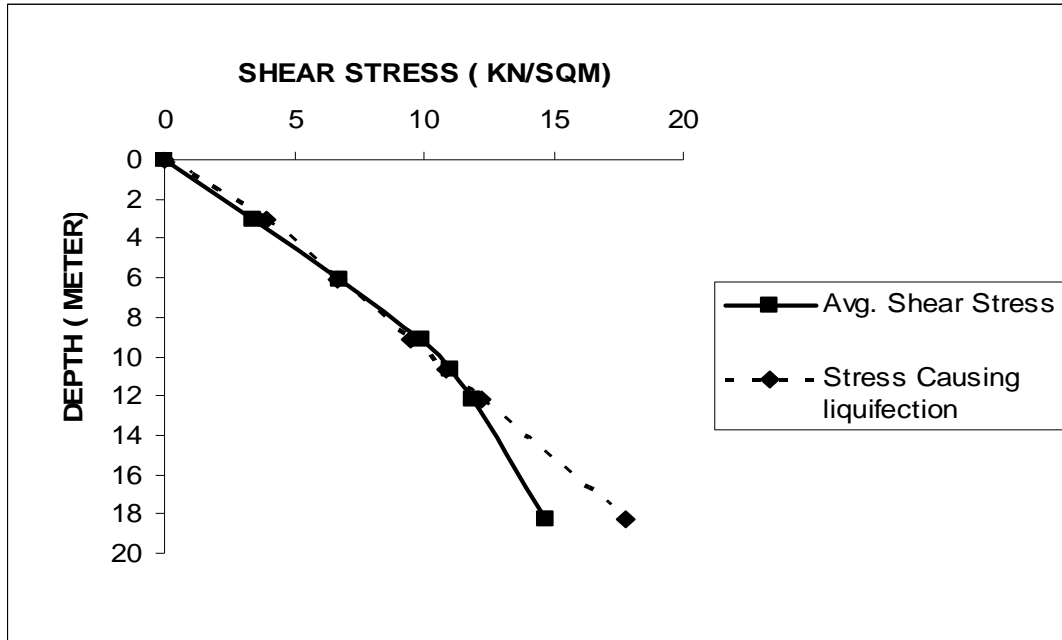


Fig. 5.2 Liquefaction zone

5.3. PORE PRESSURE GENERATION AND CHANGE OF SHEAR MODULUS

The Fig. 5.3 shows the rate of pore pressure generation vs. number of cycles. The rate of pore pressure generation has decreases gradually as number of cycles increases.

Fig. 5.4 presents the variation of dimensionless shear modulus of soil with respect to the number of cycles causing liquefaction (N_L). It was observed that the shear modulus of soil gradually decreases as number of cycles increases. It is obvious that the shear modulus of soil decreases as cumulative pore pressure increases. The pore pressure generation and change of shear modulus in different cycles are given in Table in Appendix A-1.

The calculated cyclic stress ratio $\left(\frac{\tau_{av}}{\sigma_{v0}} \right)$ is 0.12 and corresponding number of cycles required to cause liquefaction (N_L) is 59 as shown in Table 5.2.

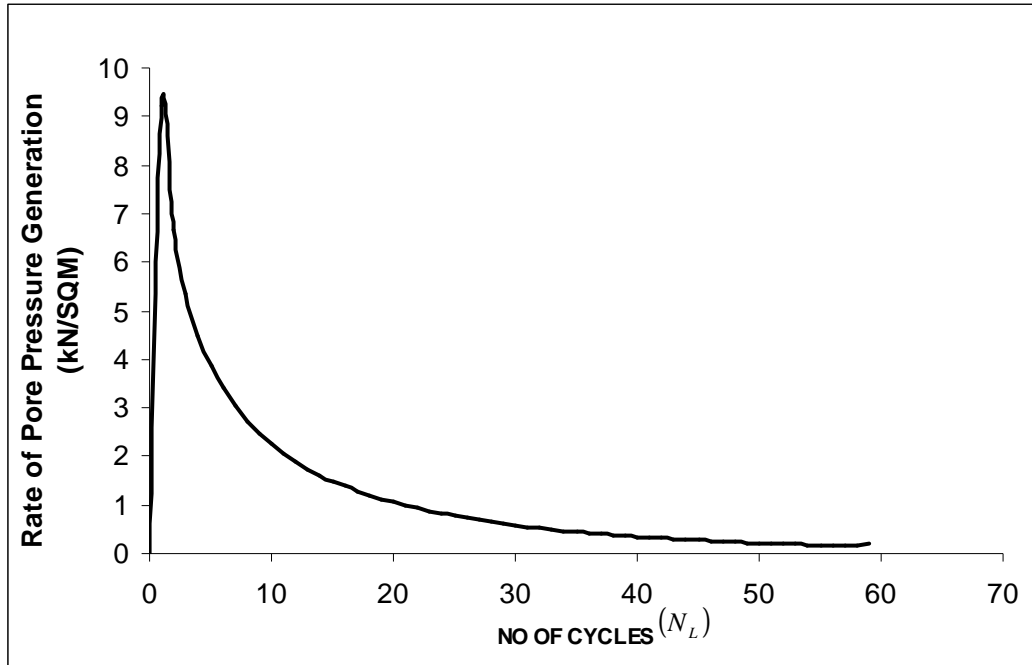


Fig.5.3 Rate of pore pressure generation

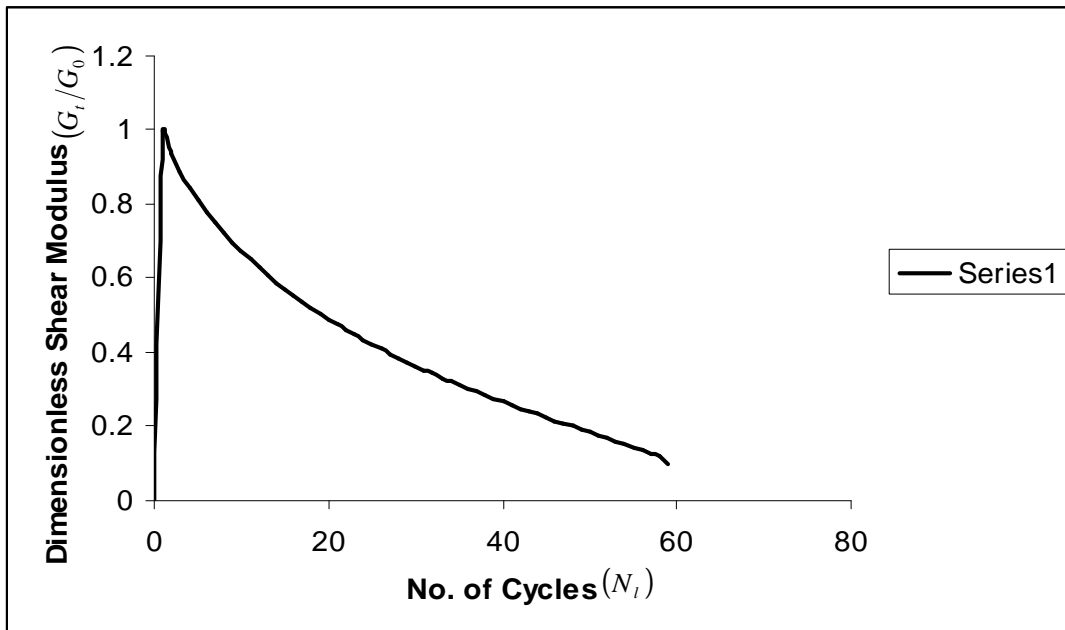


Fig.5.4 Change of shear modulus with respect to N_L

Table 5.2 Calculation of N_L at depth $h = 9$ m

Sr. No	Items	Value
1	Depth factor (From Fig. 3.4)	0.9
2	Initial effective stress(σ'_0)	81.22 kN/m ²
3	Initial total stress (σ_0)	160.588 kN/m ²
4	cyclic stress ratio $\left(\frac{\tau_{av}}{\sigma'_{v0}} \right)$	0.12
5	Initial shear modulus (G_s)	71.77×10^6 N/m ²
6	Value of N_L	59

5.4. RESPONSE OF A PILE IN LIQUEFIABLE SOILS

The behaviour of pile-soil interaction with and without liquefaction for harmonic loading is studied separately. This is analyzed for two type of loads i.e. axial and lateral load.

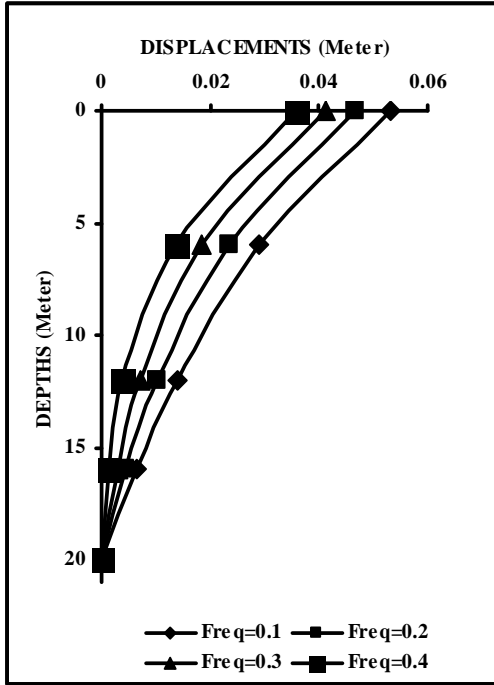
5.4.1. Axial Load

For axial load all the results are derived for the Poisson's ratio $\nu=0.4$

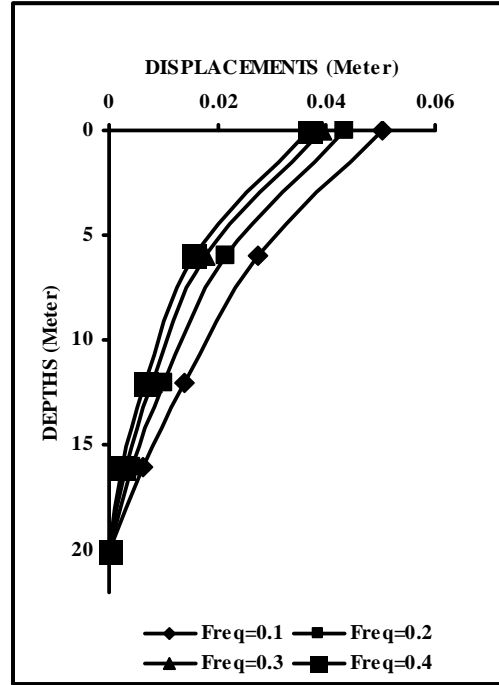
5.4.1.1. Effect of Frequency

The axial displacements developed due to pile-soil interaction for different frequency with and without liquefaction are compared in Figs. 5.5 (a) and 5.5 (b) respectively. Both figures show that displacements decreases as frequency increases from 0.1 to 0.4. Because the natural frequency of the soil stratum a_0 is about 0.1, therefore near frequency $a_0=0.1$, the displacements are maximum. Also it can be observed that effect of frequency is relatively smaller for liquefiable soil.

Figs. 5.6 (a) and 5.6 (b) represent the interacting forces with and without liquefaction respectively. The interacting forces increases with frequency in non-liquefiable soil. However effect of frequency is not significant on interacting force for liquefiable soil. It appears that the effect of liquefaction overshadows the effect of frequency.

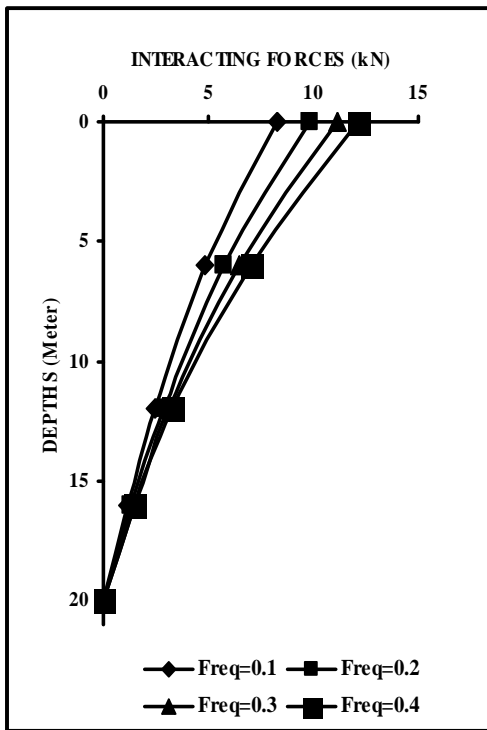


(a) Non-liquefied

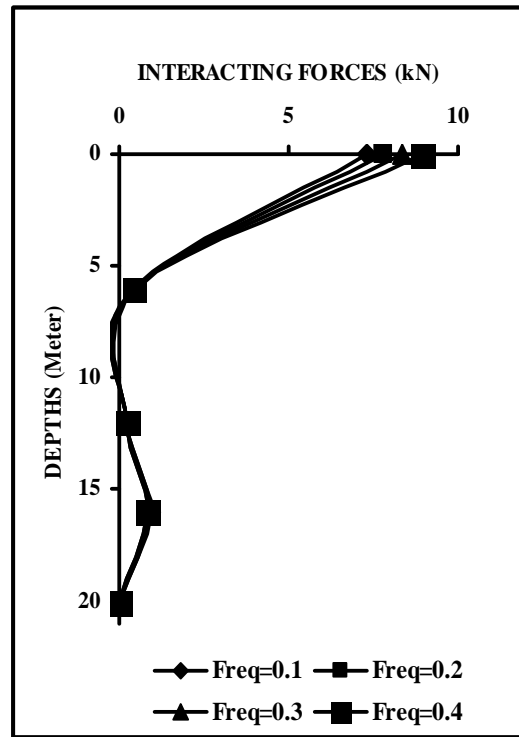


(b) liquefied

Fig. 5.5 Axial displacements at different frequencies (a_0)



(a) Non-liquefied



(b) liquefied

Fig. 5.6 Interacting forces at different frequencies (a_0)

5.4.1.2. Effect of Liquefaction on Displacements

The comparative results of axial displacement for different frequency for both liquefaction and non-liquefaction condition are graphically represented in Fig. 5.7 (a, b, c, d). At lower frequencies up to 0.3, the effect of liquefaction is not significant. However at higher frequencies the axial displacement at liquefaction zone is more than that of displacement without liquefaction. This is because of degradation of soil due to the liquefaction at higher frequencies.

5.4.1.3. Effect of Liquefaction on Interacting Forces

It was observed in section 5.4.1.1 that the amount of interacting forces increases as frequency increases. It has been observed in Fig. 5.8 (a, b, c, d) that in the liquefied zone the interacting forces are significantly reduced at all the frequencies. It is because; due to liquefaction there is a reduction in shear strength of soil that leads to lower interacting forces. This reduction can also be justified as k and d_i in Eqs. 3.18 and 3.19 reduce due to liquefaction. Thus reduction in shear strength leads to reduction in interacting forces in liquefiable zones.

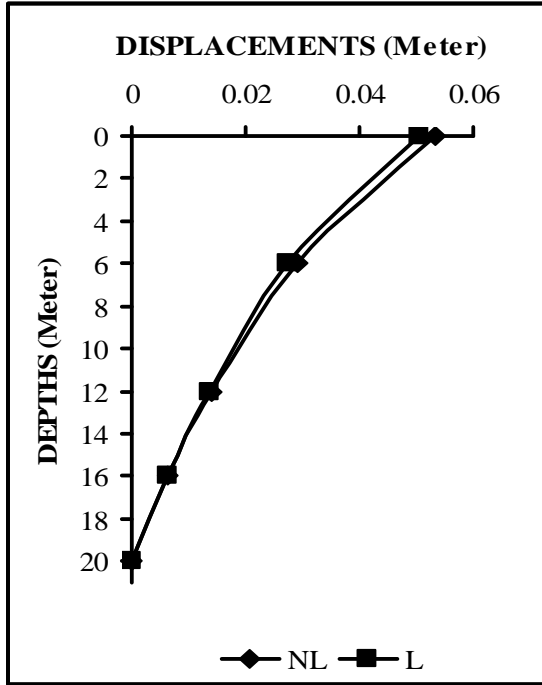


Fig. 5.7(a) Axial displacement ($a_0 = 0.1$)

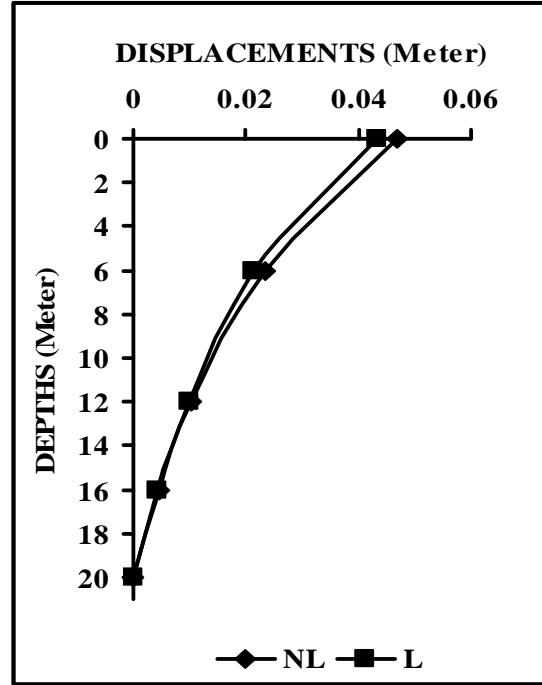


Fig. 5.7(b) Axial displacement ($a_0 = 0.2$)

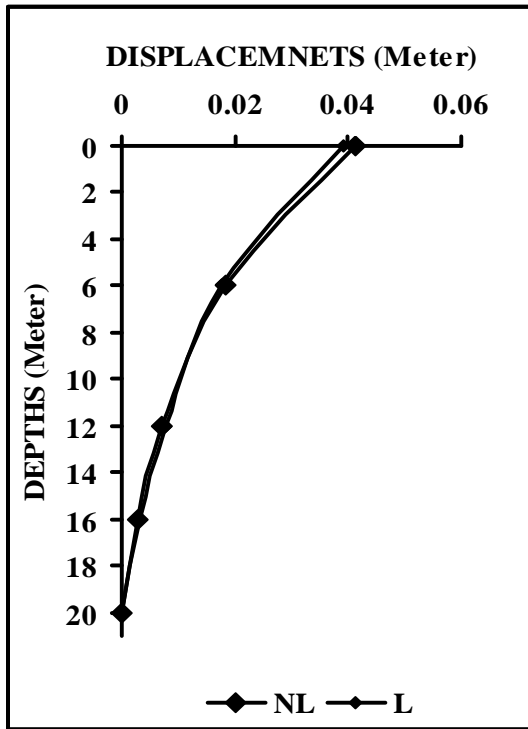


Fig. 5.7 (c) Axial displacement ($a_0 = 0.3$)

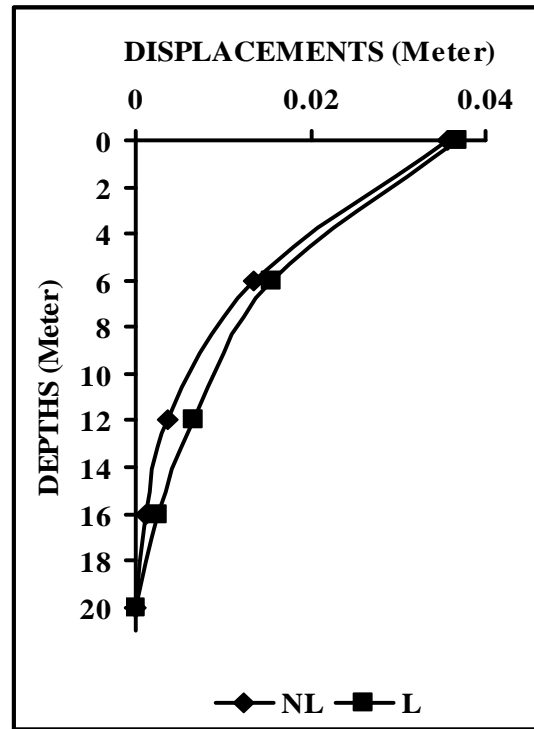


Fig. 5.7 (d) Axial displacement ($a_0 = 0.4$)

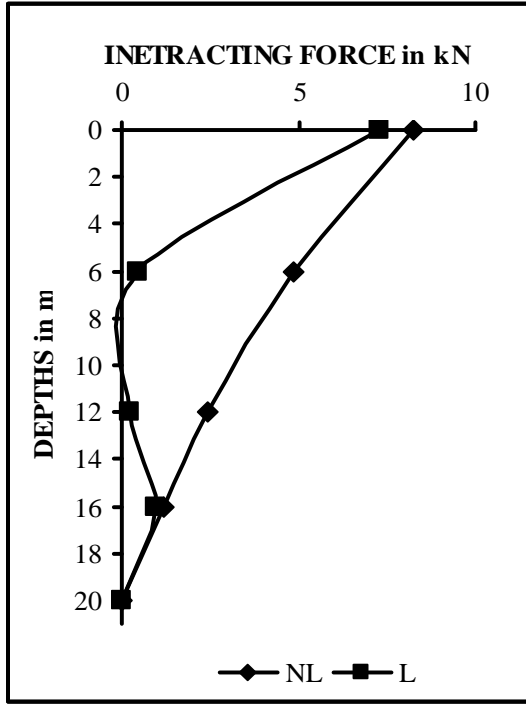


Fig. 5.8(a) Interacting force ($a_0 = 0.1$)

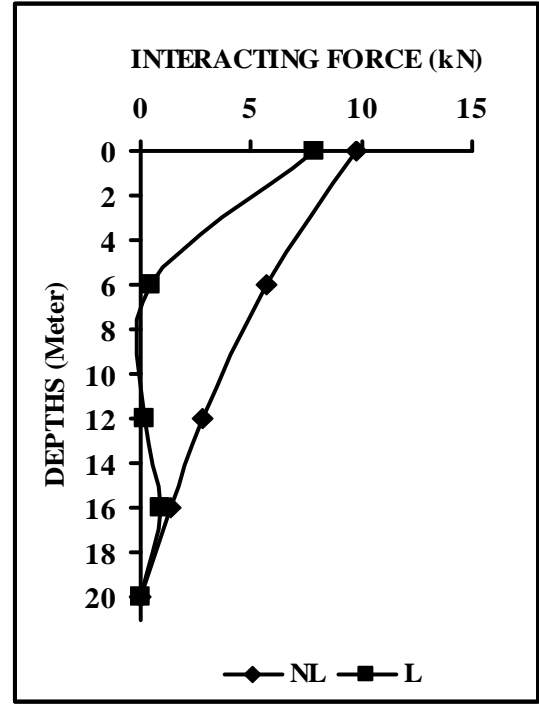


Fig. 5.8 (b) Interacting force ($a_0 = 0.2$)

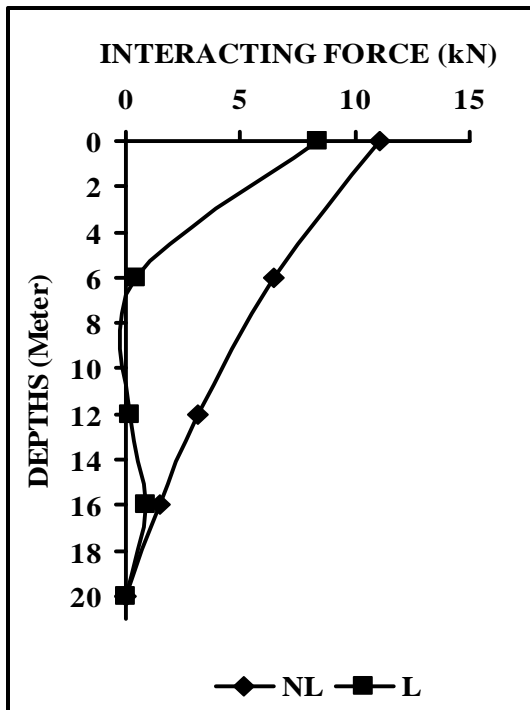


Fig. 5.8(c) Interacting force ($a_0 = 0.3$)

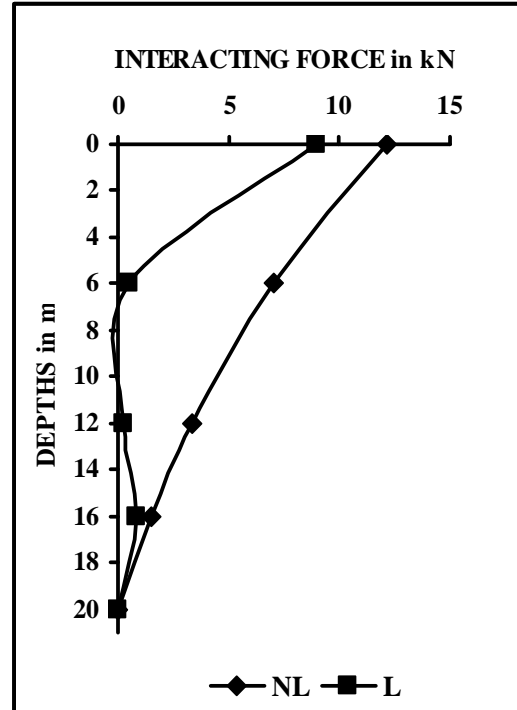


Fig. 5.8 (d) Interacting force ($a_0 = 0.4$)

5.4.2. Lateral Load

All the results for lateral load are derived at a frequency $a_0 = 0.1$ and the Poisson's ratio = 0.4.

5.4.2.1. Displacements

Fig. 5.9 (a) presents the comparison of lateral displacement with or without liquefaction. The diameter of the pile shaft is 1 m. Fig. 5.9 (a) shows that the lateral displacement at pile head is drastically increased due to liquefaction. The trend of the results is similar to that presented by Finn and Fujita (2002). Increased in the lateral displacement at pile head may be attributed to the reduction in shear modulus due to liquefaction.

5.4.2.2. Bending Moment

In Fig. 5.9 (b), bending moments are compared for non-liquefiable and liquefiable soils. Fig. 5.9 (b) shows that value of bending moment is significantly increased in case of liquefaction compare to non liquefiable soils. Similar trend of results was presented by Rollins et al. (2003). This is because of the deflection pattern creates a sharp curvature in the pile at the interface between the liquefiable and non-liquefiable zone, hence large amount of bending moments at the interface is developed.

5.4.2.3. Rotational Displacements

Fig. 5.9(c) presents the comparison of rotational displacement with or without liquefaction. It has been observed that the rotational displacement is significantly increased in the pile head in liquefiable soils. Fig. 5.9 (c) shows that the rotational displacements are drastically increased at pile head because of liquefaction. This is due to higher bending moment because of liquefaction.

5.4.2.4. Interacting Forces

Fig. 5.9 (d) shows the effect of liquefaction on interacting forces. It can be observed that there is not significant effect of liquefaction on interacting forces for lateral loading.

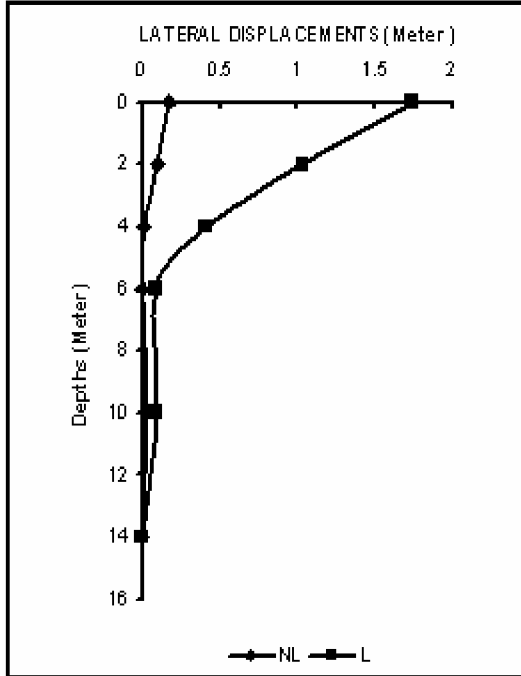


Fig. 5.9 (a) Lateral displacement

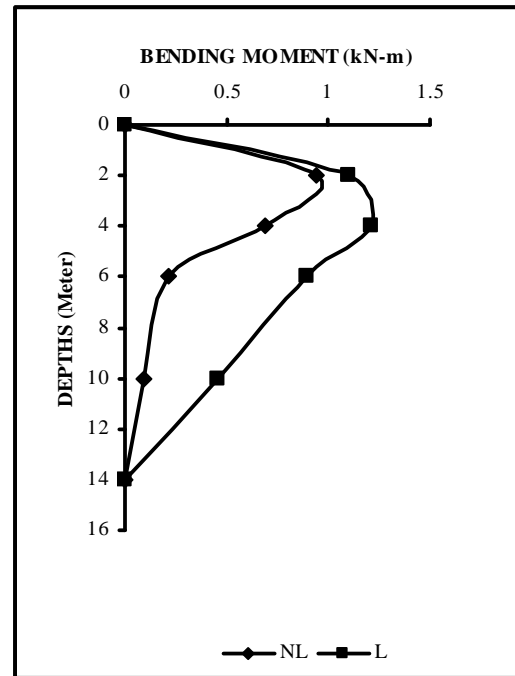


Fig. 5.9 (b) Bending moment

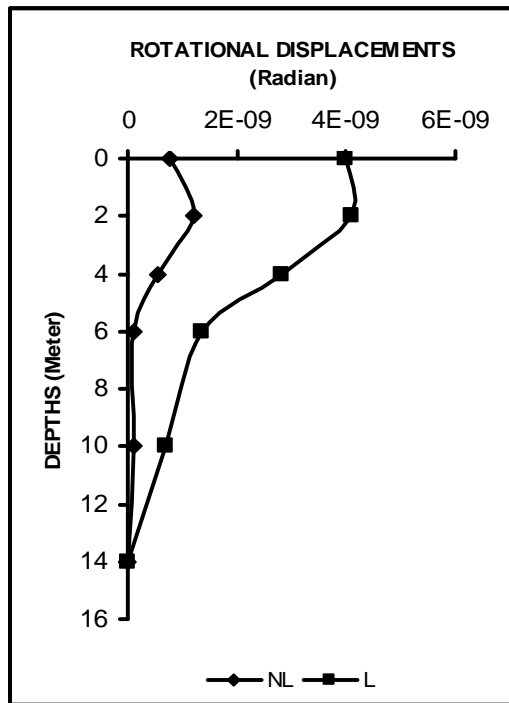


Fig. 5.9 (c) Rotational displacement

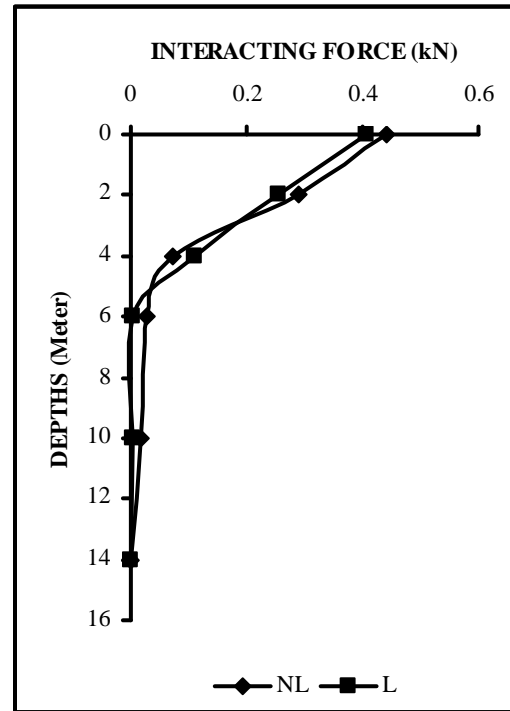


Fig. 5.9 (d) Interacting force

5.4.3. Parametric Study for Axial Load

In order to study the response of pile in the liquefiable soils a parametric study has been carried out by varying geometric property of the pile only. Fig. 5.10 (a, b, c, d) show the comparison of axial displacement for two diameters of pile at frequencies $a_0 = 0.1, 0.2, 0.3$ and 0.4 . The diameter of the pile considered for parametric study are $d = 0.5$ m and 1 m.

In case of $d = 0.5$ m the displacement is more compared to $d = 1$ m for all frequencies (a_0) from 0.1 to 0.4 . It is expected because in case of small diameter the displacements would be more. However the effect of diameter at lower depth increases with frequency of excitation.

The similar trend is observed in case of interacting forces. The variation is more or less same irrespective of its frequency (a_0). The comparative graphical representation of interacting forces is shown in Fig. 5.11 (a, b, c, d). Effect of reducing diameter of pile is more significant at higher frequencies.

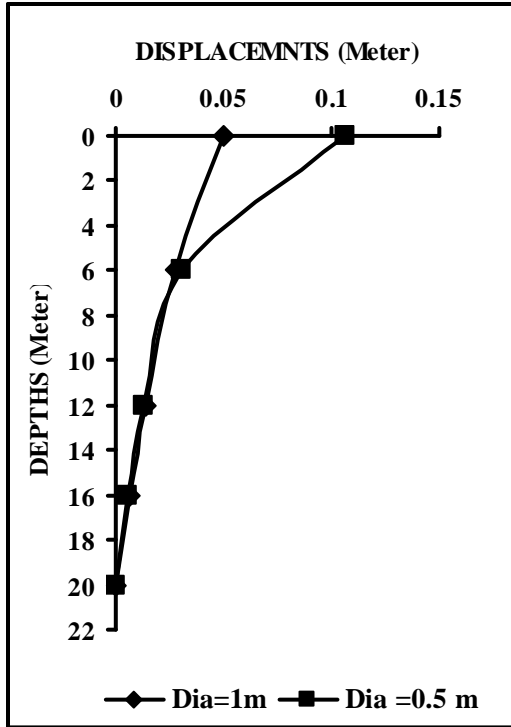


Fig. 5.10 (a) Axial displacement ($a_0 = 0.1$)

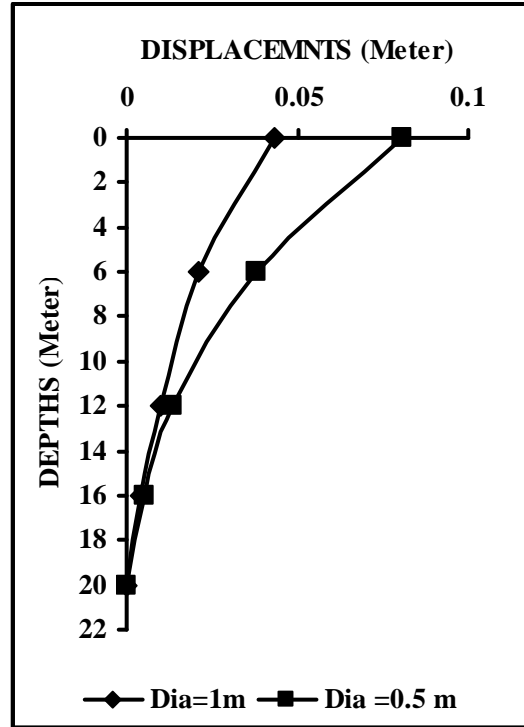


Fig. 5.10(b) Axial displacement ($a_0 = 0.2$)

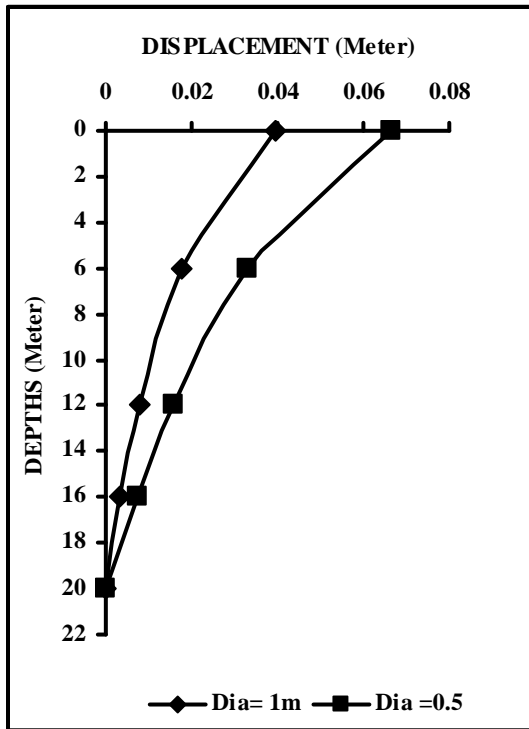


Fig. 5.10 (c) Axial displacement ($a_0 = 0.3$)

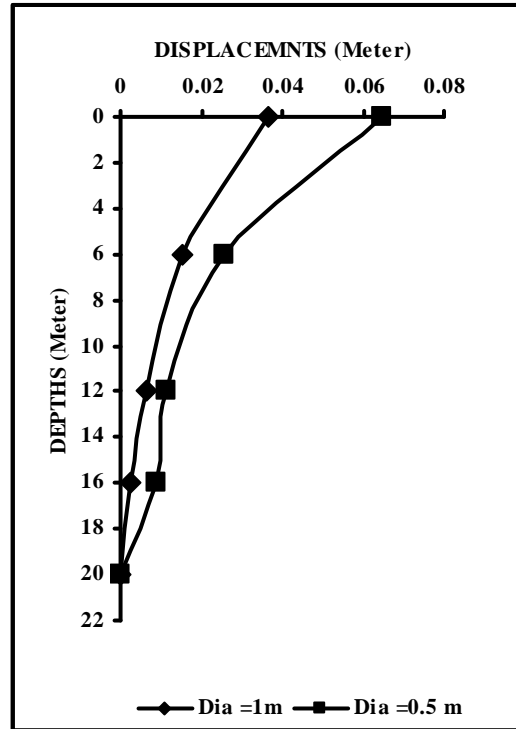


Fig. 5.10 (d) Axial displacement ($a_0 = 0.4$)

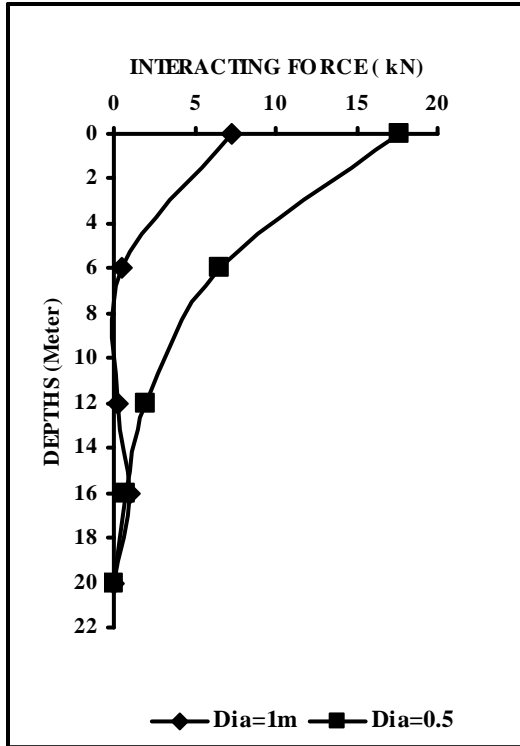


Fig. 5.11(a) Interacting force ($a_0=0.1$)

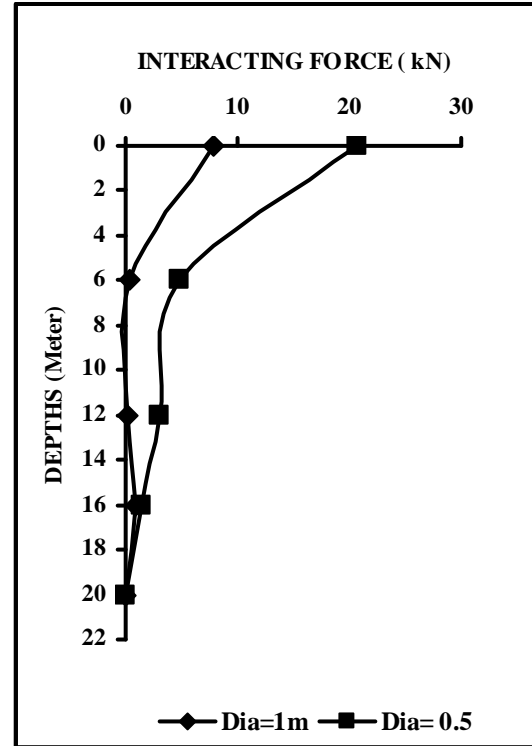


Fig. 5.11(b) Interacting force ($a_0=0.2$)

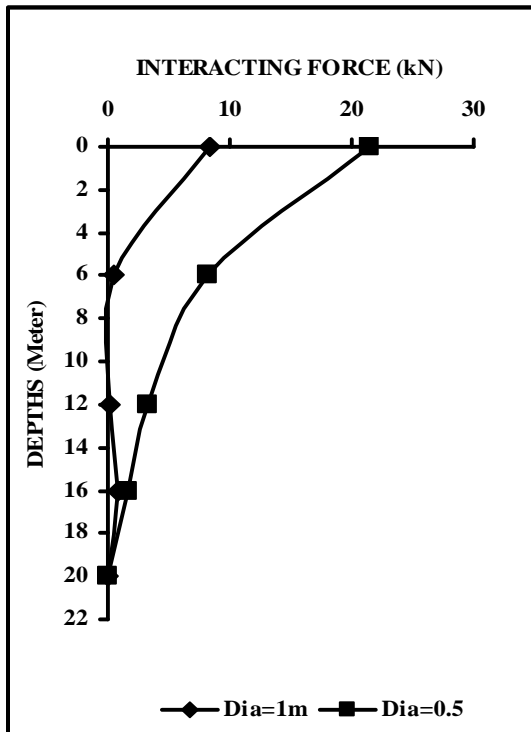


Fig. 5.11 (c) Interacting force ($a_0=0.3$)

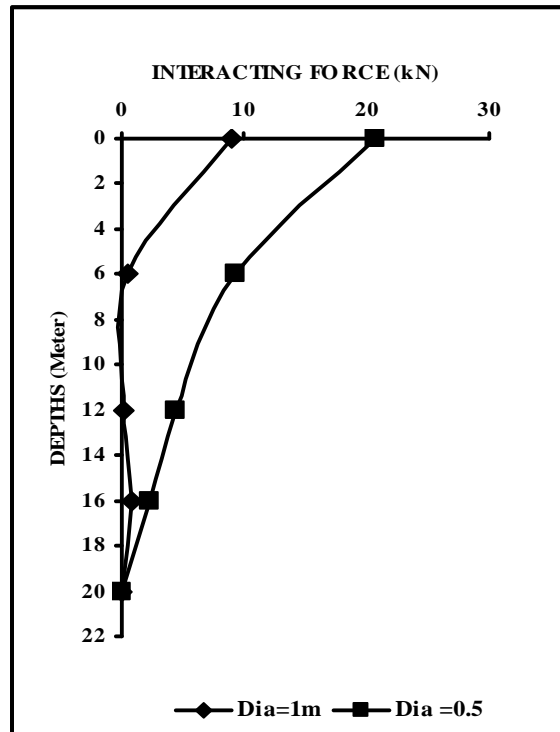


Fig. 5.11 (d) Interacting force ($a_0=0.4$)

5.4.4. Parametric Study for Lateral Load

The comparative studies have been carried out for two different diameters of the pile. The diameters of pile are $d = 0.5$ m and 1 m. Fig. 5.12 (a) shows the comparison of results for lateral displacements for different diameter in liquefaction. The lateral displacement at pile head for small diameter is more than the large diameter.

The bending moment is more for the larger diameter than that for small diameter, which is shown Fig. 5.12 (b). This may be attributed that more displacements developed at the interface of liquefiable and non-liquefiable zone.

Similar trend like lateral displacements is observed in case of rotational displacement. Fig. 5.12 (c) shows the comparison of rotational displacements for diameter of pile 0.5 m and 1 m.

The interacting forces for $d = 0.5$ m of the pile is more at the pile head. But the effect of variation of diameter of the pile is not significant in case of interacting forces. The comparison of interacting forces for different diameter of pile is presented in the Fig. 5.12 (d).

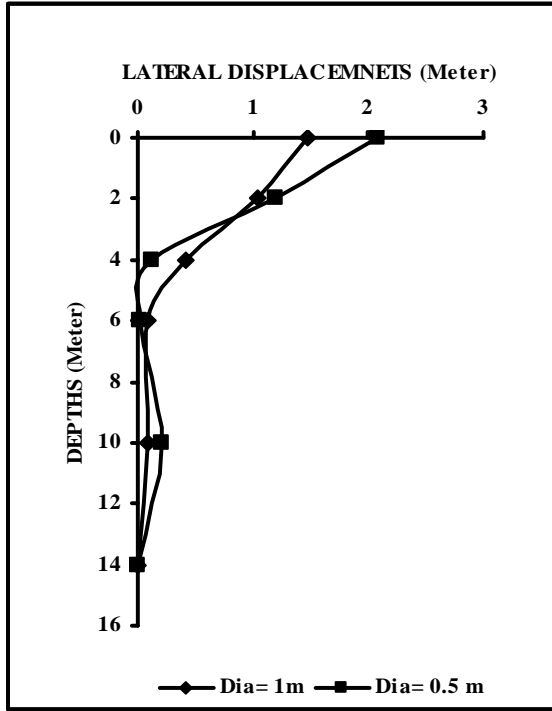


Fig. 5.12(a) Lateral displacement

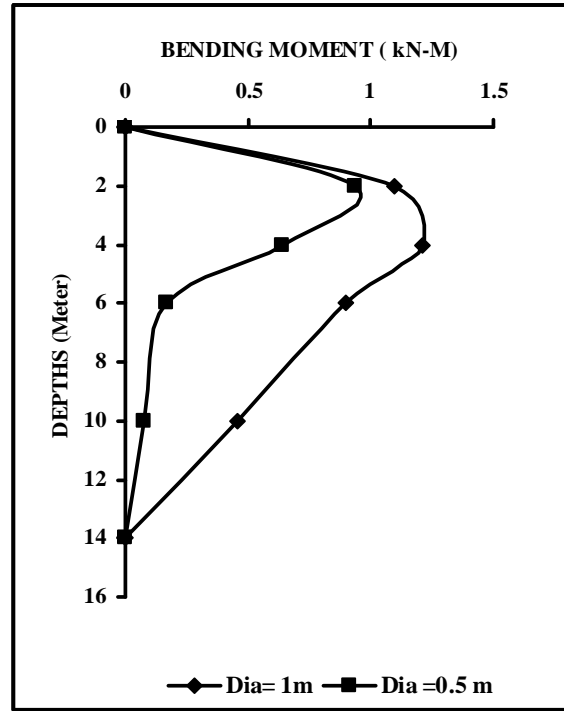


Fig. 5.12 (b) Bending moment

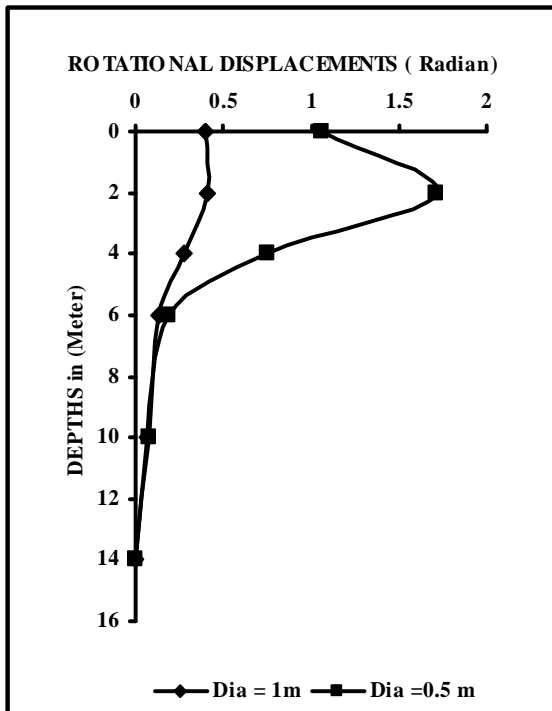


Fig. 5.12(c) Rotational displacement

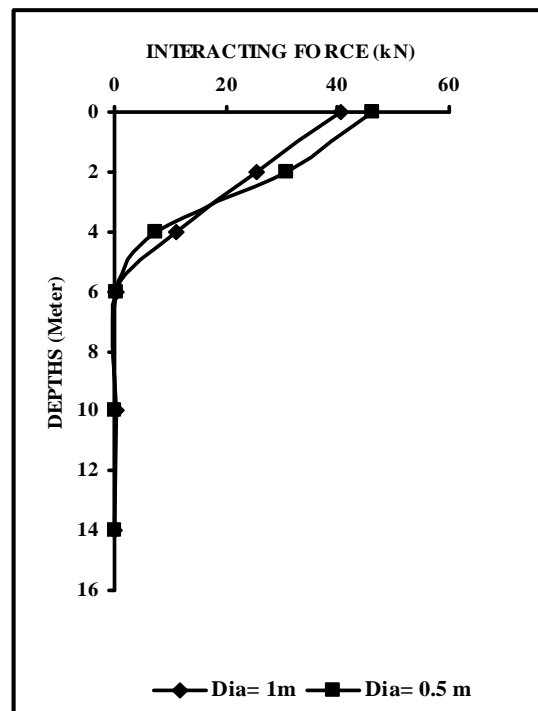


Fig. 5.12 (d) Interacting force

5.5. VALIDATION OF THE RESULTS

The Figs. 5.13 and 5.14 present comparison of present results with the results of Liyanapathirana and Poulos (2005) and Wilson et al. (1999). The variation of both displacements and bending moment are similar to the variation of the results presented by Liyanapathirana and Poulos (2005) and Wilson et al. (1999). But the values are different which may be due to the different inputs.

Still it can be mentioned that the trend of results computed with the developed code are in good agreement with the results presented by Liyanapathirana and Poulos (2005) and Wilson et al. (1999). Thus the response predicted by the developed computer code is in good agreement with the results reported in the literature.

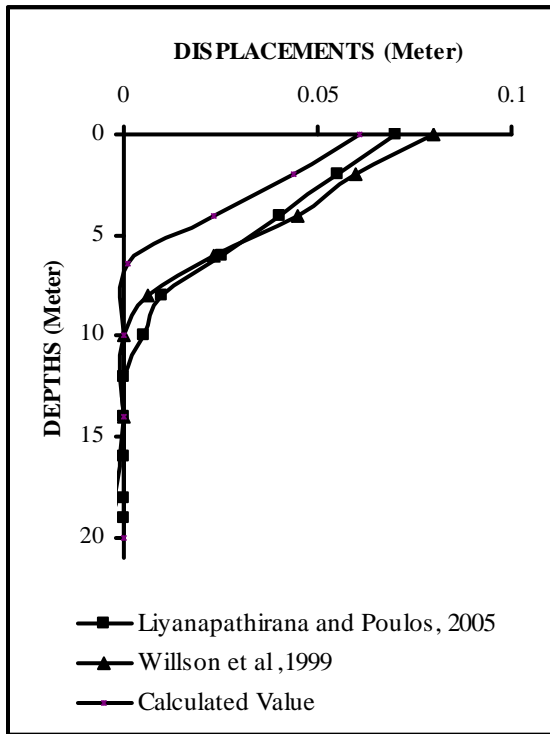


Fig.5.13 Validation of lateral displacement

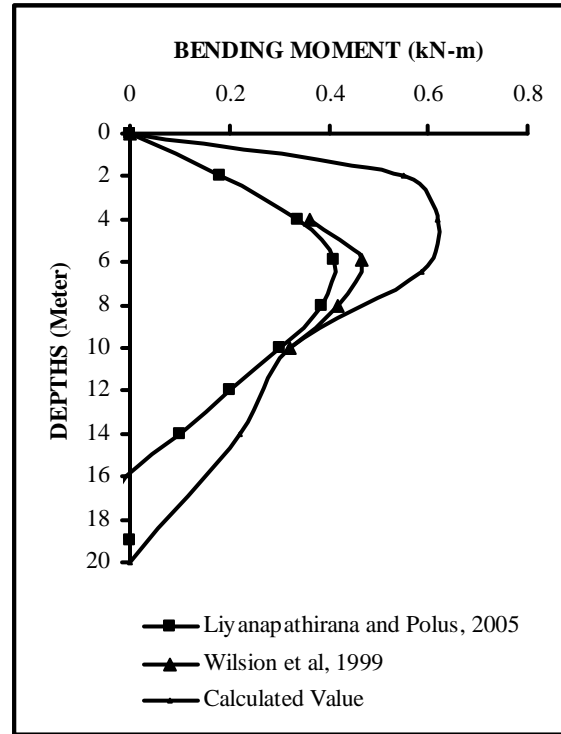


Fig. 5.14 Validation of bending moment

Chapter-6

SUMMARY, CONCLUSIONS AND FUTURE SCOPE

6.1. SUMMARY

The matter embodied in this report deals with the behaviour of single pile in liquefiable sand in the time domain. This was achieved through analytical approach using computer code in C++.

The objective of this research was to study the pile-soil interaction and the response of pile in liquefiable soils for both the axial load and lateral load.

To analyze the pile-soil interaction in liquefiable soil, modeling has been done in two parts – first numerical modeling for liquefaction of soil and second modeling for pile-soil interaction.

The numerical model for liquefaction used in this dissertation is broadly divided into three groups namely (1) Numerical model for pore pressure generation from ground response analysis, (2) Pore pressure generation and redistribution from liquefaction analysis and (3) Effective stress response analysis with pore pressure induced softening.

Next the pile-soil interaction is dealt using Winkler's hypothesis. Finally combining these two models, a formulation to predict the response of pile in liquefiable soils has been developed.

6.2. CONCLUSIONS

The following major conclusions may be drawn from this study.

For Axial Load

1. The axial displacements developed due to pile-soil are significant near the natural frequency of the soil stratum. Effect of frequency on displacement is relatively small for liquefiable soils.

2. The effect of frequency is not significant on interacting force for liquefiable soils. It appears that the effect of liquefaction is overshadowing the effect of frequency.
3. At lower frequencies (a_0) up to 0.3, the effect of liquefaction is not significant. However at higher frequencies the axial displacement in liquefaction zone is more than that without liquefaction.
4. The interacting forces are drastically reduced at all the frequencies due to liquefaction.
5. The effect of reducing the diameter of pile is to increase the displacement at lower depth and this effect is prominent at higher frequencies.

For Lateral Load

1. The displacement at pile head is drastically increased due to liquefaction.
2. Due to liquefaction bending moment increases significantly.
3. The rotational displacements are significantly increases due to liquefaction the pile head.
4. The change in interacting forces is not significant on liquefaction.
5. At lower depth, effect of diameter is more significant for displacement.
6. The rotational displacement shows similar trend as that of lateral displacement.
7. The variations in the interacting forces are not significant due to the variation in diameter of the pile.

6.3. FUTURE SCOPE

Determination of extent of liquefaction at a site during an earthquake is a complex problem. Also analysis of the pile-soil interaction itself is a very involving task in terms of computations. Combining these two problems resulted in a very complex task, requiring a lot of computation especially when considering nonlinearity of the soils.

The research presented here may be extended from following points.

1. Piles are rarely used a single pile, therefore present work may be extended for pile group.

2. The nonlinearity of soil can be incorporated using Winkler's method as mentioned by Nogami et al. (1992).
3. The present work is based on one dimensional analysis; however the study of pile-soil interaction in three dimensions can be carried out with the help of finite element methods.
4. Experimental studies on behaviour of piles in liquefiable soil are scarce. Therefore some small-scale experiment may be undertaken.

REFERENCES

1. Arduino, P., Kramer, S.L., Li, P., and Baska, D. A. (2002). "Dynamic stiffness of piles in liquefiable soils." *Research Report*, Prepared for Washington State Transportation Commission, Department of Transportation and in cooperation with U.S. Department of Transportation, Federal Highway Administration.
2. Badoni, D., and Makris, N. (1996). "Nonlinear response of single piles under lateral inertial and seismic loads." *Soil Dynamic and Earthquake Engineering* Vol. 15, pp. 29-43.
3. EI Naggar, M. H., and Novak, M. (1995). "Nonlinear lateral interaction in pile dynamics." *Soil Dynamics and Earthquake Engineering*, 14, pp. 141-157.
4. EI Naggar, M. H., and Novak, M. (1996). "Nonlinear analysis for dynamic lateral pile response." *Soil Dynamics and Earthquake Engineering*, 15, pp. 233-244.
5. Finn, W. D. L., and Fujita, N. (2002). "Piles in liquefiable soils: seismic analysis and design issues." *Soil Dynamics and Earthquake Engineering*, 22, pp. 731-742.
6. Kagawa, T. (1992). "Effect of liquefaction on lateral pile response." *Geotechnical Special Publication, ASCE*, No. 34, pp. 207-223.
7. Kagawa, T., and Kraft, L.M. (1980). "Lateral load-deflection relationship of piles subjected to dynamic loadings." *Soil and Foundation*, Vol.20 (4), pp.19-35.
8. Kagawa, T., and Kraft, L.M. (1981). "Lateral pile response during earthquakes." *Journal of Geotechnical Engineering*, Vol. 107(12), pp. 1713-1731.
9. Kagawa, T., and Kraft, L.M. (1981). "Modeling the liquefaction process." *Journal of Geotechnical Engineering*, Vol. 107(12), pp. 1593-1607.
10. Kagawa, T., Minowa, C., Abe, A., and Oda. S. (1995). "Shaking-table tests on and analyses of piles in liquefying sands." *Earthquake Geotechnical Engineering Proceedings of the first international conference*, IS-Tokyo, pp. 699-705.
11. Klar, A. (2003). "Model studies of seismic behavior of piles in sands." *Research Thesis Submitted in Partial Fulfillment of the Requirements for the Degree of Doctor of Philosophy*, Israel Institute of Technology. Haifa, Chapter 2 and Chapter 6.

12. Liyanapathirana, D. S., and Poulos, H.G. (2002a). "Numerical simulation of soil liquefaction due to earthquake loading." *Soil Dynamics and Earthquake Engineering*, 22, pp. 511-523.
13. Liyanapathirana, D. S., and Poulos, H.G. (2002b). "A numerical model for dynamic soil liquefaction analysis." *Soil Dynamics and Earthquake Engineering*, 22, pp. 1007-1015.
14. Liyanapathirana, D. S., and Poulos, H.G. (2005a). "Seismic lateral response of piles in liquefying soil." *Journal of Geotechnical and Geoenvironmental Engineering, ASCE*, Vol. 131, No. 12, pp. 1466-1479.
15. Liyanapathirana, D. S., and Poulos, H.G. (2005b). "Pseudostatic approach for seismic analysis of piles in liquefying soil." *Journal of Geotechnical and Geoenvironmental Engineering, ASCE*, Vol. 131, No. 12, pp. 1480-1487.
16. Maheshwari, B.K., Truman, K.Z., Gould, P, L., and El Naggar, M.H. (2005). "Three-dimensional nonlinear seismic analysis of single piles using finite element model: effects of plasticity of soil." *International Journal of Geomechanics, ASCE*, Vol. 5, No. 1, pp. 35-44.
17. Martin, P. P., and Seed, H. B. (1979). "Simplified procedure for effective stress analysis of ground response." *Journal of Geotechnical Engineering division*, Vol. 105, No. GT6, pp. 739-758.
18. Nogami, T., and Kubu, K. (1953). "The behavior of soil during vibration." *Proceedings, 3rd International Conference on Soil Mechanics and Foundation Engineering*, Zurich, Vol. 1, pp. 152-155.
19. Nogami, T., and Konagai, K. (1986). "Time domain axial response of dynamically loaded single piles." *Journal of Engineering Mechanics, ASCE*, Vol. 112 No. 11, pp.1512-1525.
20. Nogami, T., and Konagai, K. (1988). "Time domain flexural response of dynamically loaded single piles." *Journal of Engineering Mechanics, ASCE*, Vol. 114(9), pp.1512-1525.
21. Nogami, T., Konagai, K., and Otani, J. (1988). "Nonlinear pile foundation model for time-domain dynamic response analysis." *Proceedings of 9th World Conference on Earthquake Engineering*, Tokyo-Kyoto, Japan, Vol. 3, pp. 593-598.

22. Nogami, T., Otani, J., Konagai, K., and Chen, H.L. (1992a). "Nonlinear soil-pile interaction model for dynamic lateral motion." *Journal of Geotechnical Engineering*, Vol. 118(1), pp. 89-106.
23. Nogami, T., Zhu, J.X., and Ito, T. (1992b). "First and second order dynamic subgrade models for soil-pile interaction." *ASCE, Geotechnical Special Publication*, No. 34 Piles under Dynamic Loads, pp. 187-206.
24. Novak, M. (1974). "Dynamic stiffness and damping of piles." *Canadian Geotechnical Journal*, Vol. 11, pp. 574-598.
25. Novak, M., and Aboul-Ella, F. (1978). "Impedance function of piles in layered media." *Journal of Engineering Mechanics, ASCE*, Vol. 104(6), pp. 643-661.
26. Novak, M., Nogami, T., and Aboul-Ella, F. (1978). "Dynamic soil reaction for plane strain case." *Journal of Engineering Mechanics, ASCE*, Vol. 104(4), pp. 953-955.
27. Prakash, S. (1981). "Soil dynamics." *McGraw-Hill Book Company*, New York.
28. Seed, H. B., and Idriss, I.M. (1971). "Simplified procedure for evaluation soil liquefaction potential." *Journal of Soil Mechanics and Foundation Division, ASCE*, Vol. 97, No. SM 9, pp. 1249-1273.
29. Stewart H. E., and O'Rourke T.D. (1991). "The effects of liquefaction-induced lateral spreading on pile foundations." *Soil Dynamic and Earthquake Engineering*, Vol. 10(5), pp. 271- 279..
30. Trivedi, A. and Singh, S(2003) "Shear modulus approach in Geotechnical Engineering" *Journal Of Bridge & Structural Engineering*, Vol. 33, No. 2, pp. 9-21.
31. Wilson, D. W., Boulanger, R. W., and Kutter, B. L. (2000). "Seismic lateral resistance of liquefying sand." *Journal of Geotechnical & Geoenvironmental Engineering, ASCE*, Vol. 126, No.10, pp. 898-906.
32. Wolf, J. P. (1985). "Dynamics soil structure interaction." *Prentice Hall INC*, Englewood Cliffs N, J, 07632.

Appendix-1

The pore pressure generation and change of shear modulus in different cycles are given

No. of Cycles	Rate of Pore Pr. Generation in kN/m ²	Changing Shear modulus in kN/m ²	No. of Cycles	Rate of Pore Pr. Generation in kN/m ²	Changing Shear modulus in kN/m ²
0	0	0	23	0.872857	3.21*10 ⁷
1	9.21600	7.18*10 ⁷	24	0.821367	3.12*10 ⁷
2	6.65228	6.72*10 ⁷	25	0.773702	3.03*10 ⁷
3	5.34542	6.38*10 ⁷	26	0.729491	2.94*10 ⁷
4	4.49752	6.08*10 ⁷	27	0.688408	2.85*10 ⁷
5	3.88500	5.83*10 ⁷	28	0.650168	2.77*10 ⁷
6	3.41445	5.59*10 ⁷	29	0.614517	2.69*10 ⁷
7	3.03823	5.38*10 ⁷	30	0.581232	2.61*10 ⁷
8	2.72883	5.18*10 ⁷	31	0.550114	2.53*10 ⁷
9	2.46902	5.00*10 ⁷	32	0.520985	2.46*10 ⁷
10	2.24727	4.83*10 ⁷	33	0.493688	2.38*10 ⁷
11	2.05555	4.67*10 ⁷	34	0.468080	2.31*10 ⁷
12	1.88804	4.52*10 ⁷	35	0.444033	2.24*10 ⁷
13	1.74039	4.37*10 ⁷	36	0.421432	2.17*10 ⁷
14	1.60925	4.23*10 ⁷	37	0.400173	2.11*10 ⁷
15	1.49205	4.10*10 ⁷	38	0.380162	2.04*10 ⁷
16	1.38671	3.97*10 ⁷	39	0.361315	1.98*10 ⁷
17	1.29158	3.85*10 ⁷	40	0.343556	1.91*10 ⁷
18	1.20528	3.74*10 ⁷	41	0.326815	1.85*10 ⁷
19	1.12670	3.62*10 ⁷	42	0.311031	1.79*10 ⁷
20	1.05490	3.52*10 ⁷	43	0.296149	1.73*10 ⁷
21	0.98909	3.41*10 ⁷	44	0.282119	1.67*10 ⁷
22	0.92860	3.31*10 ⁷	45	0.268901	1.61*10 ⁷

No. of Cycles	Rate of Pore Pr. Generation in kN/m ²	Changing Shear modulus in kN/m ²	No. of Cycles	Rate of Pore Pr. Generation in kN/m ²	Changing Shear modulus in kN/m ²
46	0.256457	1.55*10 ⁷	53	0.1900310	1.15*10 ⁷
47	0.244760	1.49*10 ⁷	54	0.1839210	1.10*10 ⁷
48	0.227880	1.44*10 ⁷	55	0.1791450	1.04*10 ⁷
49	0.213993	1.38*10 ⁷	56	0.1762900	9.77*10 ⁶
50	0.213993	1.32*10 ⁷	57	0.1766580	9.13*10 ⁶
51	0.205192	1.27*10 ⁷	58	0.1838807	8.45*10 ⁶
52	0.213993	1.21*10 ⁷	59	0.2127690	7.67*10 ⁶

Appendix – 2 (A)

C++ programme for checking the liquefaction potential

```

#include <iostream.h>
#include <math.h>
#include <iomanip.h>
#include <fstream.h>
void main()
{
    ofstream outf("data.xls");
    int i,n;
    long double
d[100],wtabledepth,amaxbyg,rd[100],gamaH[100],tauv[100],gama,gamasasu,gamasub,cr,rden
sity;
    long double
stresratio,stresratio_20,effstress[100],tau[100],stresratio_10,stresratio_30,Nc;

    cout<<"\nEnter number of depth:"<<endl;
    cin>>n;

    cout<<"\nEnter gama of soil:"<<endl;
    cin>>gama;

    cout<<"\nEnter gamasaturated of soil:"<<endl;
    cin>>gamasasu;

    cout<<"\nEnter gamasubmerged of soil:"<<endl;
    cin>>gamasub;

    cout<<"\nEnter watertable depth:"<<endl;
    cin>>wtabledepth;

    cout<<"\nEnter Amax/g:"<<endl;
    cin>>amaxbyg;

    cout<<"\nEnter the " << n <<" differnt depth:"<<endl;

    for(i=0;i<n;i++)
    {
        cin>>d[i];
    }
    cout<<"\nEnter the corresponding " << n <<" depth factor:"<<endl;

```

```

for(i=0;i<n;i++)
{
cin>>rd[i];
}
cout<<"\nEnter value of Nc 10 , 20, 30 for EQ magnitude 7, 7.5 ,8:"<<endl;
cin>>Nc;

if(Nc==10)
{

cout<<"\n ENTER STRESS RATIO AVERAGE OF FROM FIG 8.17 FOR 10
CYCLES:"<<endl;
cin>>stresratio_10;

stresratio=stresratio_10;
}
else if(Nc==30)
{
cout<<"\n ENTER STRESS RATIO AVERAGE OF FROM FIG 8.18 FOR
30 CYCLES:"<<endl;
cin>>stresratio_30;

stresratio=stresratio_30;
}
else if (Nc==20)
{

cout<<"\n ENTER STRESS RATIO AVERAGE OF FROM FIG 8.17 FOR
10 CYCLES:"<<endl;
cin>>stresratio_10;

cout<<"\n ENTER STRESS RATIO AVERAGE OF FROM FIG 8.18 FOR
30 CYCLES:"<<endl;
cin>>stresratio_30;

stresratio_20= (stresratio_10+stresratio_30)/2;
stresratio=stresratio_20;
}

cout<<"\nEnter correction factor based on relative density:"<<endl;
cin>>cr;

cout<<"\nEnter Relative density:"<<endl;
cin>>rdensity;

```

```
outf<<"Depth"<<"\t"<<"tauv"<<"\t"<<"tau"<<endl;
outf<<"0"<<"\t"<<"0"<<"\t"<<"0"<<endl;
for(i=0;i<n;i++)
{

gamaH[i]=gama*wtabledepth+gamasasu*(d[i]-wtabledepth);

tauv[i]=0.65*gamaH[i]*amxbyg*rd[i];

effstress[i]=gama*wtabledepth+gamasub*(d[i]-wtabledepth);

tau[i]=effstress[i]*stresratio*cr*rdensity/50;

outf<<-d[i]<<"\t"<<tauv[i]<<"\t"<<tau[i]<<endl;
}

}
```

Appendix – 2 (B)

C++ programme for liquefaction Model

```
#include <iostream.h>
#include <math.h>
#include <iomanip.h>
#include <fstream.h>
void main()
{
    ofstream outf("PPGENERATION.xls");
    long double rp[100],alfa,rate_generation[100],NL,ini_eff_stress,eff_stress[100];
    long double
generation[100],final_generation[100],amaxbyg,d,rd,gama,wtab,gamasasu;
    long double
gamaw,ini_stress,dn_by_dt,stress[100],ratio_tauv_effstress,G[100],initialG;

    cout<<" Enter value of (amax/g):"<<endl;
    cin>>amaxbyg;

    cout<<"\nEnter value of depth:"<<endl;
    cin>>d;

    cout<<"\nEnter value of watertable depth:"<<endl;
    cin>>wtab;

    cout<<"\nEnter depth factor:"<<endl;
    cin>>rd;

    cout<<"\n Enter value of alfa:"<<endl;
    cin>>alfa;

    cout<<"\n Enter value of gama of soil:"<<endl;
    cin>>gama;

    cout<<" \nEnter value of gama sasurated:"<<endl;
    cin>>gamasasu;

    cout<<"\n Enter value of gama of water:"<<endl;
    cin>>gamaw;
```



```

ini_eff_stress = gama*wtab+gamasasu*(d-wtab)-gamaw*(d-wtab);

ini_stress = gama*wtab +gamasasu*(d-wtab);

ratio_tauv_effstress=(0.65*amaxbyg*ini_stress*rd)/ini_eff_stress;

cout<<"\nRATIO OF TAUV and EFFECTIVE
STRESS:"<<ratio_tauv_effstress<<endl;

cout<<"\n Enter value of NL:"<<endl;
cin>>NL;

cout<<"\n Enter value of rate of uniform cycles per second-TABLE-1_MARTIN,
1979:"<<endl;
cin>>dn_by_dt;

eff_stress[0]=ini_eff_stress;

stress[0]=ini_stress;

cout<<"\nEnter the initial values of Shear Modulus of Soil:"<<endl;
cin>>initialG;

rp[0]=(2/3.141592)*(asin(pow((0/NL),(0.5/alfa))));

rate_generation[0]=0;//(eff_stress[0]*dn_by_dt)/(alfa*3.141592*NL*(pow((sin(3.141
592*rp[0]*0.5)),(2*alfa-1)))*(cos(3.141592*rp[0]*0.5)));

G[0]=initialG*(pow((eff_stress[0]/ini_eff_stress),0.5));

outf<<"No of Cycles"<<"\t"<<"pore pressure"<<"\t"<<"rate of
generation"<<"\t"<<"eff_stress"<<"\t"<<"pore pr
generation"<<"\t"<<"final_generation"<<"\t"<<"Shear Modulus"<<endl;

outf<<"0"<<"\t"<<rp[0]<<"\t"<<rate_generation[0]<<"\t"<<eff_stress[0]<<"\t"<<"0"
<<"\t"<<"0"<<"\t"<<endl;

generation[0]=0;

final_generation[0]=0;

for (int i=1;i<NL;i++)

```

```

    {
        {
            eff_stress[i]=eff_stress[i-1]-(rate_generation[i-
1]);//eff_stress[i]=eff_stress[i-1]-(rate_generation[i-1]*1/(dnby dt))( if multiplied by 1by
dn/dt abnormal results come)

            rp[i]=(2/3.141592)*(asin(pow((i/NL),(0.5/alfa))));

            rate_generation[i]=(eff_stress[i]*dn_by_dt)/(alfa*3.141592*NL*(pow((sin(3.141592
*rp[i]*0.5)),(2*alfa-1)))*(cos(3.141592*rp[i]*0.5)));

            generation[i]=rate_generation[i]/dn_by_dt;

            final_generation[i]=generation[i]+final_generation[i-1];

            G[i]=initialG*(pow((eff_stress[i]/ini_eff_stress),0.5));

        }

        outf<<i<<"\t"<<rp[i]<<"\t"<<rate_generation[i]<<"\t"<<eff_stress[i]<<"\t"<<generati
on[i]<<"\t"<<final_generation[i]<<"\t"<<G[i]<<endl;

    }
}

```

Appendix – 2 (C)

C++ programme for Pile-soil interaction Model in Liquefiable Soils

```
#include<iostream.h>
#include<math.h>
#include<fstream.h>
#include <conio.h>
#define M 400

class complex
{
    double real,img;

    public:

        complex()
        {
            //real=0;img=0;
        }

        complex (double a,double b)
        {
            real=a;img=b;
        }
        complex(complex &c)
        {
            real=c.real;img=c.img;
        }

        complex operator +(complex c)
        {
            complex temp;
            temp.real = real + c.real;
            temp.img = img + c.img;
            return(temp);
        }

        complex operator -(complex c)
        {
            complex temp;
            temp.real = real-c.real;
            temp.img = img - c.img;
            return(temp);
        }
}
```

```
    }  
    complex operator /(complex c)  
    {  
        complex temp;  
        temp.real = (real*c.real + img*c.img)/(c.real*c.real + c.img*c.img);  
        temp.img = (real*c.img - img*c.real)/(c.real*c.real + c.img*c.img);  
        return(temp);  
    }  
  
    complex operator *(double x)  
    {  
        complex temp;  
        temp.real = real*x;  
        temp.img = img*x;  
        return(temp);  
    }  
  
    complex operator /(double x)  
    {  
        complex temp;  
        temp.real = real/x;  
        temp.img = img/x;  
        return(temp);  
    }  
  
    void get(double x,double y)  
    {  
        real = x;img = y;  
    }  
  
    void show()  
    {  
        cout << real << " +i " << img;  
    }  
    double mag()  
    {  
        double temp,x;  
        x = (real*real) + (img*img);  
        temp = sqrt(x);  
        return(temp);  
    }  
    double rshow()  
    {  
        return(real);  
    }  
}
```

```

        double ishow()
        {
            return(img);
        }
};

void main()
{
    ofstream outf("test4.xls");
    int n;
    long double Gs,r0,vs,c[5],k[5],cL[5],kL[5],pi;
    long double freq,wemga,P,delta_t;
    long double In,Hn,I1,I2,I3,H1,H2,H3,K,t[1500],lemda_square,mp,Ep,A,alfa;
    long double InL,HnL,I1L,I2L,I3L,H1L,H2L,H3L,KL,lemda_squareL;

    long double
A2,B2,C2,D2,A3,B3,C3,D3,A4,B4,C4,D4,M2,X2,Y2,Z2,M31,Y31,X31,Z31,M32,X32,Y32,
Z32;
    long double M41,X41,Z41,Y41,M42,X42,Z42,Y42,M43,X43,Z43,Y43;
    long double
betaone1,betatwo1,betafour1,betaone2,betatwo2,betafour2,betaone3,betatwo3,betafour3;

    long double
I1,I2,T11,T21,T31,T41,Q11,Q21,Q31,Q41,T12,T22,T32,T42,Q12,Q22,Q32,Q42;
    long double I3,T13,T23,T33,T43,Q13,Q23,Q33,Q43;
    long double
I4,T14,T24,T34,T44,Q14,Q24,Q34,Q44,betaone4,betatwo4,betafour4,w_mag_0[M];

    long double GL;

    complex dis_1[M],dis_2[M],dis_3[M],p_1[M],p_2[M],p_3[M],p_0[M];
    complex
text1[M],text2[M],text3[M],text30[M],text40[M],text4[M],text5[M],text6[M],text7[M],text8
[M],text11[M],text12[M],text13[M],text14[M],text21[M],text22[M],text23[M],text24[M];
    complex
text31[M],text32[M],text33[M],text34[M],text41[M],text42[M],text43[M],text44[M],text110
[M],text120[M],text130[M],text140[M],text150[M],text160[M],text170[M],text180[M],text1
110[M],text1120[M],text1130[M],text1140[M];
    complex
text1150[M],text1160[M],text1170[M],text111[M],text121[M],text131[M],text141[M],text1
111[M],text1121[M],text1131[M],text1141[M],text1151[M],text1161[M],text1171[M],text1
12[M],text113[M],text114[M],text115[M],text116[M];
    complex
text117[M],text1112[M],text1122[M],text1132[M],text1142[M],text1152[M],text1162[M],te

```

```

xt1172[M],text1003[M],text1023[M],text1033[M],text1043[M],text1053[M],text1063[M],te
xt1073[M],text1083[M],text1113[M],text1123[M],text1133[M];
    complex text1143[M],text1153[M],text1163[M],text1173[M];
    complex
p_real_0[M],w_real_0[M],d_real_0[M],w1_real_0[M],w2_real_0[M],w3_real_0[M];
    complex vel_real_0[M],acc_real_0[M],P_real_0[M];
    complex gama_real_0[M],gama_real_1[M],P_real_1[M];
    complex P_real_4[M],P_real_2[M],P_real_3[M];
    complex
vel_real_1[M],vel_real_2[M],vel_real_3[M],vel_real_4[M],acc_real_1[M],acc_real_2[M],ac
c_real_3[M],acc_real_4[M];
    complex p_real_1[M],p_real_2[500],p_real_3[M],p_real_4[M];
    complex d_real_1[M],d_real_2[500],d_real_3[M],gama_real_2[M],gama_real_3[M];
    complex w1_real_1[M],w1_real_2[M],w1_real_3[M];
    complex w2_real_1[M],w2_real_2[M],w2_real_3[M];
    complex w3_real_1[M],w3_real_2[M],w3_real_3[M],w_0[M];
    complex
w_real_1[M],w_real_2[M],w_real_3[M],gama_real_4[M],text45[M],text15[M],text25[M],te
xt35[M];
    complex fact[M];

    pi=3.141592654;

```

```

cout<<endl;
cout<<"Enter the value of Gs in SI unit in NON LIQUEFIABLE ZONES:"<<endl;
cin>>Gs;
cout<<"Enter the value of Gs in SI unit in LIQUEFIABLE ZONES:"<<endl;
cin>>GL;
cout<<endl;
cout<<"Enter the value of r0 in SI unit:"<<endl;
cin>>r0;
cout<<endl;
cout<<"Enter the value of vs in SI unit:"<<endl;
cin>>vs;

```

```

c[1]=(Gs*r0/vs)*113.097;    c[2]=(Gs*r0/vs)*25.133;
c[3]=(Gs*r0/vs)*9.362;

```

```

k[1]=Gs*3.518;                k[2]=Gs*3.581;
k[3]=Gs*5.529;

```

```

cL[1]=(GL*r0/vs)*113.097;    cL[2]=(GL*r0/vs)*25.133;
cL[3]=(GL*r0/vs)*9.362;

```

```

kL[1]=GL*3.518;          kL[2]=GL*3.581;
kL[3]=GL*5.529;

cout<<"\nEnter Frequency:"<<endl;
cin>>freq;

wemga=(freq*vs)/r0;

delta_t=pi/(10*wemga);

In=0;  Hn=0; InL=0; HnL=0;

for(n=1;n<=3;n++)
{
    In+=(1/k[n])*((1-c[n]/( k[n]*delta_t))+c[n]/(k[n]*delta_t))*exp(-
(kL[n]*delta_t)/c[n]));
    Hn+=(1/k[n])*((c[n]/(k[n]*delta_t)-(1+c[n]/(k[n]*delta_t))*exp(-
(kL[n]*delta_t)/c[n]));

    InL+=(1/kL[n])*((1-cL[n]/( kL[n]*delta_t))+cL[n]/(kL[n]*delta_t))*exp(-
(kL[n]*delta_t)/cL[n]));
    HnL+=(1/kL[n])*((cL[n]/(kL[n]*delta_t)-(1+cL[n]/(kL[n]*delta_t))*exp(-
(kL[n]*delta_t)/cL[n]));
}

K=1.0/In;    KL=1.0/InL;

I1=(1/k[1])*((1-c[1]/( k[1]*delta_t))+c[1]/(k[1]*delta_t))*exp(-(k[1]*delta_t)/c[1]));
I2=(1/k[2])*((1-c[2]/( k[2]*delta_t))+c[2]/(k[2]*delta_t))*exp(-(k[2]*delta_t)/c[2]));
I3=(1/k[3])*((1-c[3]/( k[3]*delta_t))+c[3]/(k[3]*delta_t))*exp(-(k[3]*delta_t)/c[3]));

H1=(1/k[1])*((c[1]/(k[1]*delta_t)-(1+c[1]/(k[1]*delta_t))*exp(-(k[1]*delta_t)/c[1]));
H2=(1/k[2])*((c[2]/(k[2]*delta_t)-(1+c[2]/(k[2]*delta_t))*exp(-(k[2]*delta_t)/c[2]));
H3=(1/k[3])*((c[3]/(k[3]*delta_t)-(1+c[3]/(k[3]*delta_t))*exp(-(k[3]*delta_t)/c[3]));

I1L=(1/kL[1])*((1-cL[1]/( kL[1]*delta_t))+cL[1]/(kL[1]*delta_t))*exp(-
(kL[1]*delta_t)/cL[1]));
I2L=(1/kL[2])*((1-cL[2]/( kL[2]*delta_t))+cL[2]/(kL[2]*delta_t))*exp(-
(kL[2]*delta_t)/cL[2]));
I3L=(1/kL[3])*((1-cL[3]/( kL[3]*delta_t))+cL[3]/(kL[3]*delta_t))*exp(-
(kL[3]*delta_t)/cL[3]));

```

```

H1L=(1/kL[1])*((cL[1]/(kL[1]*delta_t)-(1+cL[1]/(kL[1]*delta_t))*exp(-
(kL[1]*delta_t)/cL[1]));H2L=(1/kL[2])*((cL[2]/(kL[2]*delta_t)-
(1+cL[2]/(kL[2]*delta_t))*exp(-(kL[2]*delta_t)/cL[2]));
H3L=(1/kL[3])*((cL[3]/(kL[3]*delta_t)-(1+cL[3]/(kL[3]*delta_t))*exp(-
(kL[3]*delta_t)/cL[3]));

cout<<"\nApplied Load in Newton:"<<endl;
cin>>P;

cout<<"\nEnter mass (2496.3):"<<endl;
cin>>mp;

cout<<"\nEnter Ep (25e9):"<<endl;
cin>>Ep;

cout<<"\nEnter alfa:"<<endl;
cin>>alfa;

A=pi*r0*r0;

lemda_square=(mp/(Ep*A))*(((alfa+1)*(alfa+2))/(delta_t*delta_t))+K/(Ep*A);

lemda_squareL=(mp/(Ep*A))*(((alfa+1)*(alfa+2))/(delta_t*delta_t))+KL/(Ep*A);

t[0]=0;

cout<<"\nEnter 1st layer height:"<<endl;
cin>>l1;

cout<<"\nEnter 2ND layer height:"<<endl;
cin>>l2;

cout<<"\nEnter 3rd layer height:"<<endl;
cin>>l3;

cout<<"\nEnter 4th layer height:"<<endl;
cin>>l4;

betaone1=1/l1+(lemda_square*l1)/3; betatwo1=1/l1-(lemda_square*l1)/6;
betafour1=l1/6;

T11=betaone1/betatwo1;    T21=-1/(Ep*A*betatwo1);
T31=(Ep*A*(betatwo1*betatwo1-betaone1*betaone1))/betatwo1; T41=T11;

Q11=(2*betafour1)/betatwo1; Q21=Q11/2;  Q31=-betafour1*Ep*A*(1+2*T11);
Q41=-betafour1*Ep*A*(2+T11);

```


//SECOND LAYER ASSUME AS LIQUEFIED LAYER

$$\text{betaone2} = 1/12 + (\text{lemda_squareL} * 12) / 3; \quad \text{betatwo2} = 1/12 - (\text{lemda_squareL} * 12) / 6;$$

$$\text{betafour2} = 12/6;$$

$$\text{T12} = \text{betaone2} / \text{betatwo2}; \quad \text{T22} = -1 / (\text{Ep} * \text{A} * \text{betatwo2});$$

$$\text{T32} = (\text{Ep} * \text{A} * (\text{betatwo2} * \text{betatwo2} - \text{betaone2} * \text{betaone2})) / \text{betatwo2}; \quad \text{T42} = \text{T12};$$

$$\text{Q12} = (2 * \text{betafour2}) / \text{betatwo2}; \quad \text{Q22} = \text{Q12} / 2; \quad \text{Q32} = -$$

$$\text{betafour2} * \text{Ep} * \text{A} * (1 + 2 * \text{T12}); \quad \text{Q42} = -\text{betafour2} * \text{Ep} * \text{A} * (2 + \text{T12});$$

$$\text{betaone3} = 1/13 + (\text{lemda_square} * 13) / 3; \quad \text{betatwo3} = 1/13 - (\text{lemda_square} * 13) / 6;$$

$$\text{betafour3} = 13/6;$$

$$\text{T13} = \text{betaone3} / \text{betatwo3}; \quad \text{T23} = -1 / (\text{Ep} * \text{A} * \text{betatwo3});$$

$$\text{T33} = (\text{Ep} * \text{A} * (\text{betatwo3} * \text{betatwo3} - \text{betaone3} * \text{betaone3})) / \text{betatwo3}; \quad \text{T43} = \text{T13};$$

$$\text{Q13} = (2 * \text{betafour3}) / \text{betatwo3}; \quad \text{Q23} = \text{Q13} / 2; \quad \text{Q33} = -$$

$$\text{betafour3} * \text{Ep} * \text{A} * (1 + 2 * \text{T13}); \quad \text{Q43} = -\text{betafour3} * \text{Ep} * \text{A} * (2 + \text{T13});$$

$$\text{betaone4} = 1/14 + (\text{lemda_square} * 14) / 3; \quad \text{betatwo4} = 1/14 - (\text{lemda_square} * 14) / 6;$$

$$\text{betafour4} = 14/6;$$

$$\text{T14} = \text{betaone4} / \text{betatwo4}; \quad \text{T24} = -1 / (\text{Ep} * \text{A} * \text{betatwo4});$$

$$\text{T34} = (\text{Ep} * \text{A} * (\text{betatwo4} * \text{betatwo4} - \text{betaone4} * \text{betaone4})) / \text{betatwo4}; \quad \text{T44} = \text{T14};$$

$$\text{Q14} = (2 * \text{betafour4}) / \text{betatwo4}; \quad \text{Q24} = \text{Q14} / 2; \quad \text{Q34} = -$$

$$\text{betafour4} * \text{Ep} * \text{A} * (1 + 2 * \text{T14}); \quad \text{Q44} = -\text{betafour4} * \text{Ep} * \text{A} * (2 + \text{T14});$$

$$\text{A2} = \text{T12} * \text{T11} + \text{T22} * \text{T31}; \quad \text{B2} = \text{T12} * \text{T21} + \text{T22} * \text{T41};$$

$$\text{C2} = \text{T32} * \text{T11} + \text{T42} * \text{T31}; \quad \text{D2} = \text{T32} * \text{T21} + \text{T42} * \text{T41};$$

$$\text{A3} = \text{T13} * \text{A2} + \text{T23} * \text{C2}; \quad \text{B3} = \text{T13} * \text{B2} + \text{T23} * \text{D2};$$

$$\text{C3} = \text{T33} * \text{A2} + \text{T43} * \text{C2}; \quad \text{D3} = \text{T33} * \text{B2} + \text{T43} * \text{D2};$$

$$\text{A4} = \text{T14} * \text{A3} + \text{T24} * \text{C3}; \quad \text{B4} = \text{T14} * \text{B3} + \text{T24} * \text{D3};$$

$$\text{C4} = \text{T34} * \text{A3} + \text{T44} * \text{C3}; \quad \text{D4} = \text{T34} * \text{B3} + \text{T44} * \text{D3};$$

$$\text{M2} = \text{T12} * \text{Q11} + \text{T22} * \text{Q31}; \quad \text{X2} = \text{T12} * \text{Q21} + \text{T22} * \text{Q41};$$

$$\text{Y2} = \text{T32} * \text{Q11} + \text{T42} * \text{Q31}; \quad \text{Z2} = \text{T32} * \text{Q21} + \text{T42} * \text{Q41};$$

$$\text{M31} = \text{T13} * \text{M2} + \text{T23} * \text{Y2}; \quad \text{X31} = \text{T13} * \text{X2} + \text{T23} * \text{Z2};$$

$$\text{Y31} = \text{T33} * \text{M2} + \text{T43} * \text{Y2}; \quad \text{Z31} = \text{T33} * \text{X2} + \text{T43} * \text{Z2};$$

$M_{32}=T_{13}*Q_{12}+T_{23}*Q_{32};$ $X_{32}=T_{13}*Q_{22}+T_{23}*Q_{42};$
 $Y_{32}=T_{33}*Q_{12}+T_{43}*Q_{32};$ $Z_{32}=T_{33}*Q_{22}+T_{43}*Q_{42};$

$M_{41}=T_{14}*M_{31}+T_{24}*Y_{31};$ $X_{41}=T_{14}*X_{31}+T_{24}*Z_{31};$
 $Y_{41}=T_{34}*M_{31}+T_{44}*Y_{31};$ $Z_{41}=T_{34}*X_{31}+T_{44}*Z_{31};$

$M_{42}=T_{14}*M_{32}+T_{24}*Y_{32};$ $X_{42}=T_{14}*X_{32}+T_{24}*Z_{32};$
 $Y_{42}=T_{34}*M_{32}+T_{44}*Y_{32};$ $Z_{42}=T_{34}*X_{32}+T_{44}*Z_{32};$

$M_{43}=T_{14}*Q_{13}+T_{24}*Q_{33};$ $X_{43}=T_{14}*Q_{23}+T_{24}*Q_{43};$
 $Y_{43}=T_{34}*Q_{13}+T_{44}*Q_{33};$ $Z_{43}=T_{34}*Q_{23}+T_{44}*Q_{43};$

$P_real_0[0].get(0,0);$ $w_real_0[0].get(0,0);$ $p_real_0[0].get(0,0);$

$gama_real_0[0].get(0,0);$ $gama_real_1[0].get(0,0);$ $gama_real_2[0].get(0,0);$

$gama_real_3[0].get(0,0);$ $gama_real_4[0].get(0,0);$

$P_real_4[0].get(0,0);$

$w1_real_0[0].get(0,0);$ $w2_real_0[0].get(0,0);$ $w3_real_0[0].get(0,0);$

$w_real_1[0].get(0,0);$ $w_real_2[0].get(0,0);$ $w_real_3[0].get(0,0);$

$w1_real_1[0].get(0,0);$ $w2_real_1[0].get(0,0);$ $w3_real_1[0].get(0,0);$

$w1_real_2[0].get(0,0);$ $w2_real_2[0].get(0,0);$ $w3_real_2[0].get(0,0);$

$w1_real_3[0].get(0,0);$ $w2_real_3[0].get(0,0);$ $w3_real_3[0].get(0,0);$

$vel_real_0[0].get(0,0);$ $acc_real_0[0].get(0,0);$ $vel_real_1[0].get(0,0);$

$acc_real_1[0].get(0,0);$ $vel_real_2[0].get(0,0);$ $acc_real_2[0].get(0,0);$

$vel_real_3[0].get(0,0);$ $acc_real_3[0].get(0,0);$ $vel_real_4[0].get(0,0);$

$acc_real_4[0].get(0,0);$ $p_real_1[0].get(0,0);$ $p_real_2[0].get(0,0);$

$p_real_3[0].get(0,0);$ $p_real_4[0].get(0,0);$ $d_real_0[1].get(0,0);$

$d_real_1[1].get(0,0);$ $d_real_2[1].get(0,0);$ $d_real_3[1].get(0,0);$

$gama_real_0[1].get(0,0);$ $gama_real_1[1].get(0,0);$ $gama_real_2[1].get(0,0);$

$gama_real_3[1].get(0,0);$ $gama_real_4[1].get(0,0);$

```

outf<<"Time"<<"\t"<<"wmag
"<<"\t"<<"ForceR_0"<<"\t"<<"ForceI_0"<<"\t"<<"DissR_0"<<"\t"<<"DissI_0"<<"\t"<<"IF
R_0"<<"\t"<<"IFI_0"<<"\t"<<"DissR_1"<<"\t"<<"DissI_1"<<"\t"<<"IFR_1"<<"\t"<<"IFI_1
"<<"\t"<<"DissR_2"<<"\t"<<"DissI_2"<<"\t"<<"IFR_2"<<"\t"<<"IFI_2"<<"\t"<<"DissR_3"
<<"\t"<<"DissI_3"<<"\t"<<"IFR_3"<<"\t"<<"IFI_3"<<endl;
outf<<"0"<<"\t"<<"0"<<"\t"<<"P"<<"\t"<<"0"<<"\t"<<"0"<<"\t"<<"0"<<"\t"<<"0"<<"\t"<<"0"<<"\t"<<"0"
"<<"\t"<<"0"<<"\t"<<"0"<<"\t"<<"0"<<"\t"<<"0"<<"\t"<<"0"<<"\t"<<"0"<<"\t"<<"0"<<"\t"<<"0"<<"\t"
"<<"0"<<"\t"<<"0"<<"\t"<<"0"<<"\t"<<"0"<<"\t"<<"0"<<"\t"<<"0"<<endl;

```

```

for (int i=1;i<=200;i++)
{
    t[i]=i*delta_t;
    P_real_0[i].get((P*cos(3.141592654*i/10)),(P*sin(3.141592654*i/10)));
    fact[i].get((cos(3.141592654*i/10)),(sin(3.141592654*i/10)));

    {

        text1[i]=w1_real_0[i-1]*((-1)*K*(exp(-(k[1]*delta_t)/c[1]))) + w2_real_0[i-1]*((-
1*K)*exp(-(k[2]*delta_t)/c[2]));

        text2[i]=w3_real_0[i-1]*(-1*K*exp(-(k[3]*delta_t)/c[3]));

        text3[i]=p_real_0[i-1]*(-1*K*Hn);

        text4[i]=text1[i]+text2[i];

        d_real_0[i]=text4[i]+text3[i];

        text11[i]=w_real_0[i-1]*(((-1)*mp*(alfa+1)*(alfa+2))/(Ep*A*delta_t*delta_t));

        text12[i]=vel_real_0[i-1]*(((-1)*mp*(alfa+1)*(alfa+2))/(Ep*A*delta_t));

        text13[i]=acc_real_0[i-1]*(((-1)*mp*alfa*(alfa+3))/(Ep*A*2));

        text14[i]=text11[i]+text12[i];

        text15[i]=text14[i]+text13[i];

```

```

gama_real_0[i]=d_real_0[i]/(Ep*A)+text15[i];

}

{

//SECOND LAYER
text30[i]=w1_real_1[i-1]*(-1*KL*exp(-(kL[1]*delta_t)/cL[1]))+w2_real_1[i-1]*(-
1*KL*exp(-(kL[2]*delta_t)/cL[2]));
text40[i]=w3_real_1[i-1]*(-1*KL*exp(-(kL[3]*delta_t)/cL[3]))+p_real_1[i-1]*(-
1*KL*HnL);
d_real_1[i]=text30[i]+text40[i];

text21[i]=w_real_1[i-1]*(((-1)*mp*(alfa+1)*(alfa+2))/(Ep*A*delta_t*delta_t));
text22[i]=vel_real_1[i-1]*(((-1)*mp*(alfa+1)*(alfa+2))/(Ep*A*delta_t));
text23[i]=acc_real_1[i-1]*(((-1)*mp*alfa*(alfa+3))/(Ep*A*2));

text24[i]=text21[i]+text22[i];

text25[i]=text24[i]+text23[i];
gama_real_1[i]=d_real_1[i]/(Ep*A)+text25[i];

}

{

text5[i]=w1_real_2[i-1]*(-1*K*exp(-(k[1]*delta_t)/c[1]))+w2_real_2[i-1]*(-
1*K*exp(-(k[2]*delta_t)/c[2]));
text6[i]=w3_real_2[i-1]*(-1*K*exp(-(k[3]*delta_t)/c[3]))+p_real_2[i-1]*(-1*K*Hn);
d_real_2[i]=text5[i]+text6[i];

text31[i]=w_real_2[i-1]*(((-1)*mp*(alfa+1)*(alfa+2))/(Ep*A*delta_t*delta_t));
text32[i]=vel_real_2[i-1]*(((-1)*mp*(alfa+1)*(alfa+2))/(Ep*A*delta_t));
text33[i]=acc_real_2[i-1]*(((-1)*mp*alfa*(alfa+3))/(Ep*A*2));

text34[i]=text31[i]+text32[i];
text35[i]=text34[i]+text33[i];

```

```

gama_real_2[i]=d_real_2[i]/(Ep*A)+text35[i];

}

{

text7[i]=w1_real_3[i-1]*(-1*K*exp(-(k[1]*delta_t)/c[1]))+w2_real_3[i-1]*(-
1*K*exp(-(k[2]*delta_t)/c[2]));
text8[i]=w3_real_3[i-1]*(-1*K*exp(-(k[3]*delta_t)/c[3]))+p_real_3[i-1]*(-1*K*Hn);

d_real_3[i]=text7[i]+text8[i];

text41[i]=w_real_3[i-1]*((-1)*mp*(alfa+1)*(alfa+2))/(Ep*A*delta_t*delta_t);
text42[i]=vel_real_3[i-1]*((-1)*mp*(alfa+1)*(alfa+2))/(Ep*A*delta_t);
text43[i]=acc_real_3[i-1]*((-1)*mp*alfa*(alfa+3))/(Ep*A*2);

text44[i]=text41[i]+text42[i];
text45[i]=text44[i]+text43[i];
gama_real_3[i]=d_real_3[i]/(Ep*A)+text45[i];

}

{

text110[i]=P_real_0[i]*((-1)*B4/A4)+gama_real_0[i]*((-1)*M41/A4);

text120[i]=gama_real_1[i]*((-1)*(X41+M42)/A4)+gama_real_2[i]*(-1*(X42+M43)/A4);

text130[i]=gama_real_3[i]*(-1*(X43+Q14)/A4);

text140[i]=text110[i]+text120[i];

w_real_0[i]=text140[i]+text130[i];

w_0[i]=      w_real_0[i]/fact[i];
w_mag_0[i] = w_real_0[i].mag();
//w_mag1_0[i] = w_0[i].mag();

```

```

text150[i]=w_real_0[i]*C4+P_real_0[i]*D4;
text160[i]=gama_real_0[i]*Y41+gama_real_1[i]*(Z41+Y42);
text170[i]=gama_real_2[i]*(Z42+Y43)+gama_real_3[i]*(Z43+Q34);
text180[i]=text150[i]+text160[i];
P_real_4[i]=text180[i]+text170[i];

```

```

p_real_0[i]=w_real_0[i]*K+d_real_0[i];

```

```

text1110[i]=w1_real_0[i-1]*exp(-(k[1]*delta_t)/c[1])+p_real_0[i-1]*H1;
text1120[i]=w2_real_0[i-1]*exp(-(k[2]*delta_t)/c[2])+p_real_0[i-1]*H2;
text1130[i]=w3_real_0[i-1]*exp(-(k[3]*delta_t)/c[3])+p_real_0[i-1]*H3;

```

```

w1_real_0[i]=text1110[i]+p_real_0[i]*I1;
w2_real_0[i]=text1120[i]+p_real_0[i]*I2;
w3_real_0[i]=text1130[i]+p_real_0[i]*I3;

```

```

text1140[i]=w_real_0[i]*((alfa+2)/delta_t)+w_real_0[i-1]*((-1*(alfa+2))/delta_t);
text1150[i]=vel_real_0[i-1]*((-1)*(alfa+1))+acc_real_0[i-1]*((-1)*alfa*delta_t*0.5);

```

```

vel_real_0[i]=text1140[i]+text1150[i];

```

```

text1160[i]=w_real_0[i]*(((alfa+1)*(alfa+2))/(delta_t*delta_t))+ w_real_0[i-1]*((-1*(alfa+1)*(alfa+2))/(delta_t*delta_t));
text1170[i]=vel_real_0[i-1]*((-1*(alfa+1)*(alfa+2))/delta_t)+acc_real_0[i-1]*(-1*alfa*(alfa+3)*0.5);
acc_real_0[i]=text1160[i]+text1170[i];
}

```

```

{
text111[i]=w_real_0[i]*T11+P_real_0[i]*T21;
text121[i]=gama_real_0[i]*Q11+gama_real_1[i]*Q21;
w_real_1[i]=text111[i]+text121[i];

```

```

text131[i]=w_real_0[i]*T31+P_real_0[i]*T41;
text141[i]=gama_real_0[i]*Q31+gama_real_1[i]*Q41;
//P_real_1[i]=text131[i]+text141[i];

```

```

p_real_1[i]=w_real_1[i]*KL+d_real_1[i];

```

$p_1[i]=p_real_1[i]/fact[i];$

```

text1111[i]=w1_real_1[i-1]*exp(-(kL[1]*delta_t)/cL[1])+p_real_1[i-1]*H1L;
text1121[i]=w2_real_1[i-1]*exp(-(kL[2]*delta_t)/cL[2])+p_real_1[i-1]*H2L;
text1131[i]=w3_real_1[i-1]*exp(-(kL[3]*delta_t)/cL[3])+p_real_1[i-1]*H3L;
w1_real_1[i]=text1111[i]+p_real_1[i]*I1L;

```

$w2_real_1[i]=text1121[i]+p_real_1[i]*I2L;$

$w3_real_1[i]=text1131[i]+p_real_1[i]*I3L;$

```

text1141[i]=w_real_1[i]*((alfa+2)/delta_t)+w_real_1[i-1]*((-1*(alfa+2))/delta_t);
text1151[i]=vel_real_1[i-1]*(-1*(alfa+1))+acc_real_1[i-1]*(-1*alfa*delta_t*0.5);

```

$vel_real_1[i]=text1141[i]+text1151[i];$

```

text1161[i]=w_real_1[i]*(((alfa+1)*(alfa+2))/(delta_t*delta_t))+ w_real_1[i-1]*((-1*(alfa+1)*(alfa+2))/(delta_t*delta_t));
text1171[i]=vel_real_1[i-1]*((-1*(alfa+1)*(alfa+2))/delta_t)+acc_real_1[i-1]*(-1*alfa*(alfa+3)*0.5);
acc_real_1[i]=text1161[i]+text1171[i];
}

```

```

{
text112[i]=w_real_0[i]*A2+P_real_0[i]*B2;
text113[i]=gama_real_0[i]*M2+gama_real_1[i]*(X2+Q12);
text114[i]=text112[i]+text113[i];
w_real_2[i]=text114[i]+gama_real_2[i]*Q22;
text115[i]=w_real_0[i]*C2+P_real_0[i]*D2;
text116[i]=gama_real_0[i]*Y2+gama_real_1[i]*(Z2+Q32);
text117[i]=text115[i]+text116[i];

```

$P_real_2[i]=text117[i]+gama_real_2[i]*Q42;$

$p_real_2[i]=w_real_2[i]*K+d_real_2[i];$

```

p_2[i]=p_real_2[i]/fact[i];
//cout<<"\n:::p_2::"<<endl;
//p_2[i].show();

```

```

text1112[i]=w1_real_2[i-1]*exp(-(k[1]*delta_t)/c[1])+p_real_2[i-1]*H1;
text1122[i]=w2_real_2[i-1]*exp(-(k[2]*delta_t)/c[2])+p_real_2[i-1]*H2;
text1132[i]=w3_real_2[i-1]*exp(-(k[3]*delta_t)/c[3])+p_real_2[i-1]*H3;
w1_real_2[i]=text1112[i]+p_real_2[i]*I1;

w2_real_2[i]=text1122[i]+p_real_2[i]*I2;

w3_real_2[i]=text1132[i]+p_real_2[i]*I3;

text1142[i]=w_real_2[i]*((alfa+2)/delta_t)+w_real_2[i-1]*((-1*(alfa+2))/delta_t);
text1152[i]=vel_real_2[i-1]*(-1*(alfa+1))+acc_real_2[i-1]*(-1*alfa*delta_t*0.5);

vel_real_2[i]=text1142[i]+text1152[i];

text1162[i]=w_real_2[i]*(((alfa+1)*(alfa+2))/(delta_t*delta_t))+ w_real_2[i-1]*((-1*(alfa+1)*(alfa+2))/(delta_t*delta_t));
text1172[i]=vel_real_2[i-1]*((-1*(alfa+1)*(alfa+2))/delta_t)+acc_real_2[i-1]*(-1*alfa*(alfa+3)*0.5);
acc_real_2[i]=text1162[i]+text1172[i];
    }

{

text1003[i]=w_real_0[i]*A3+P_real_0[i]*B3;
text1023[i]=gama_real_0[i]*M31+gama_real_1[i]*(M32+X31);
text1033[i]=gama_real_2[i]*(X32+Q13)+gama_real_3[i]*Q23;
text1043[i]=text1003[i]+text1023[i];

w_real_3[i]=text1043[i]+text1033[i];

text1053[i]=w_real_0[i]*C3+P_real_0[i]*D3;
text1063[i]=gama_real_0[i]*Y31+gama_real_1[i]*(Z31+Y32);
text1073[i]=gama_real_2[i]*(Z32+Q33)+gama_real_3[i]*Q43;
text1083[i]=text1053[i]+text1063[i];
P_real_3[i]=text1083[i]+text1073[i];

p_real_3[i]=w_real_3[i]*K+d_real_3[i];

p_3[i]=p_real_3[i]/fact[i];

text1113[i]=w1_real_3[i-1]*exp(-(k[1]*delta_t)/c[1])+p_real_3[i-1]*H1;
text1123[i]=w2_real_3[i-1]*exp(-(k[2]*delta_t)/c[2])+p_real_3[i-1]*H2;
text1133[i]=w3_real_3[i-1]*exp(-(k[3]*delta_t)/c[3])+p_real_3[i-1]*H3;

```


w1_real_3[i]=text1113[i]+p_real_3[i]*I1;

w2_real_3[i]=text1123[i]+p_real_3[i]*I2;

w3_real_3[i]=text1133[i]+p_real_3[i]*I3;

text1143[i]=w_real_3[i]*((alfa+2)/delta_t)+w_real_3[i-1]*((-1*(alfa+2))/delta_t);
text1153[i]=vel_real_3[i-1]*(-1*(alfa+1))+acc_real_3[i-1]*(-1*alfa*delta_t*0.5);

vel_real_3[i]=text1143[i]+text1153[i];

text1163[i]=w_real_3[i]*(((alfa+1)*(alfa+2))/(delta_t*delta_t))+ w_real_3[i-1]*((-1*(alfa+1)*(alfa+2))/(delta_t*delta_t));
text1173[i]=vel_real_3[i-1]*((-1*(alfa+1)*(alfa+2))/delta_t)+acc_real_3[i-1]*(-1*alfa*(alfa+3)*0.5);
acc_real_3[i]=text1163[i]+text1173[i];
}

if(i>150)

```

outf<<i<<"\t"<<w_mag_0[i]<<"\t"<<P_real_0[i].rshow()<<"\t"<<P_real_0[i].ishow()<<"\t"
<<w_real_0[i].rshow()<<"\t"<<w_real_0[i].ishow()<<"\t"<<p_real_0[i].rshow()<<"\t"<<p_r
real_0[i].ishow()<<"\t"<<w_real_1[i].rshow()<<"\t"<<w_real_1[i].ishow()<<"\t"<<p_real_1[i
].rshow()<<"\t"<<p_real_1[i].ishow()<<"\t"<<w_real_2[i].rshow()<<"\t"<<w_real_2[i].isho
w()<<"\t"<<p_real_2[i].rshow()<<"\t"<<p_real_2[i].ishow()<<"\t"<<w_real_3[i].rshow()<<"
\t"<<w_real_3[i].ishow()<<"\t"<<p_real_3[i].rshow()<<"\t"<<p_real_3[i].ishow()<<endl;

```

```

//outf<<i<<"\t"<<t[i]<<"\t"<<p_real_0[i]<<"\t"<<P_real_0[i]<<"\t"<<w_real_0[i]<<"\t"<<p
_real_1[i]<<"\t"<<P_real_1[i]<<"\t"<<w_real_1[i]<<"\t"<<p_real_2[i]<<"\t"<<P_real_2[i]<
<"\t"<<w_real_2[i]<<"\t"<<p_real_3[i]<<"\t"<<P_real_3[i]<<"\t"<<w_real_3[i]<<"\t"<<P_r
real_4[i]<<endl;

```

```

//outf<<i<<"\t"<<t[i]<<"\t"<<p_real_0[i].show()<<"\t"<<P_real_0[i].show()<<"\t"<<w_real
_0[i].show()<<"\t"<<p_real_1[i].show()<<"\t"<<P_real_1[i].show()<<"\t"<<w_real_1[i].sho
w()<<"\t"<<p_real_2[i].show()<<"\t"<<P_real_3[i].show()<<"\t"<<w_real_3[i].show()<<"\t"
<<P_real_4[i].show()<<"\t"<<gama_real_0[i].show()<<"\t"<<d_real_0[i].show()<<"\t"<<ga
ma_real_1[i].show()<<"\t"<<d_real_1[i].show()<<"\t"<<gama_real_2[i].show()<<"\t"<<d_re
al_2[i].show()<<"\t"<<gama_real_3[i].show()<<"\t"<<d_real_3[i].show()<<endl;

```

}

}

